WIDEBAND SIGNAL DETECTION USING A DOWN-CONVERTING CHANNELIZED RECEIVER

THESIS

Willie H. Mims, Second Lieutenant, USAF

AFIT/GE/ENG/06-42

DEPARTMENT OF THE AIR FORCE
AIR UNIVERSITY

AIR FORCE INSTITUTE OF TECHNOLOGY

Wright-Patterson Air Force Base, Ohio

The views expressed in this thesis are those of the author and do not reflect the official policy or position of the United States Air Force, Department of Defense, or the U.S. Government.

AFIT/GE/ENG/06-42

WIDEBAND SIGNAL DETECTION USING A DOWN-CONVERTING CHANNELIZED RECEIVER

THESIS

Presented to the Faculty

Department of Electrical and Computer Engineering

Graduate School of Engineering and Management

Air Force Institute of Technology

Air University

Air Education and Training Command

In Partial Fulfillment of the Requirements for the

Degree of Master of Science in Electrical Engineering

Willie H. Mims, BSEE

Second Lieutenant, USAF

March 2006

AFIT/GE/ENG/06-42

WIDEBAND SIGNAL DETECTION USING A DOWN-CONVERTING CHANNELIZED RECEIVER

Willie H. Mims, BSEE

Second Lieutenant, USAF

Approved:

_____/Signed/_____	_____
Michael A. Temple, Ph. D. (Chairman)	Date
_____/Signed/_____	_____
Steven C. Gustafson, Ph. D. (Member)	Date
_____/Signed/_____	_____
Robert F. Mills, Ph. D. (Member)	Date

Abstract

Ultra wideband (UWB) signals typically occupy a very large spectral bandwidth resulting from extremely short duration pulses. Direct sequence spread spectrum (DSSS) signals typically occupy a large spectral bandwidth resulting from spreading methods. Both signals can be difficult to detect without having prior knowledge of their structure and/or existence.

This research develops and evaluates techniques for the non-cooperative (non-matched filter) detection of such signals. Impulse-like UWB and DSSS signals are received in an Additive White Gaussian Noise (AWGN) channel and are assessed using a bandpass filtered, down-converting (BPF-D/C) channelized receiver architecture.

Modeling and simulation is conducted to characterize BPF-D/C channelized receiver detection performance, which is compared with the performance of two other non-cooperative detection receivers: a previously-introduced down-converting (D/C) channelized receiver and a conventional radiometer.

The BPF-D/C channelized receiver detection performance for both signals of interest is shown to depend on the initial phase of the down-conversion mixers. There are usually some combinations of signal-to-noise ratio (SNR) and channel bandwidth where the BPF-D/C channelized receiver outperforms the radiometer and D/C channelized receiver for a UWB pulse. For a DSSS waveform, detection performance using the BPF-D/C channelized receiver is consistently poorer than radiometric detection.

Table of Contents

Page

List of Figures

Figure Page

Figure Page

Figure Page

Figure Page

Figure Page

Figure Page

Figure Page

List of Tables

WIDEBAND SIGNAL DETECTION USING A DOWN-CONVERTING CHANNELIZED RECEIVER

I. Introduction

1.1 Introduction

Non-cooperative communication channel assessment is perhaps the most challenging signal detection task. The ability to monitor and characterize channel activity via non-cooperative and non-intrusive means has potential for a wide range of communication applications, which could prove especially significant for 4G (4^{th} generation) deployment.

1.2 Problem Statement

Ultra wideband (UWB) signals typically occupy a very large spectral bandwidth resulting from extremely short duration pulses. Direct sequence spread spectrum (DSSS) signals typically occupy a large spectral bandwidth resulting from spreading methods. Both signals are difficult to detect without prior knowledge of their structure and/or existence, and at times they may reside below the noise floor. This research focuses upon developing techniques for the non-cooperative detection of UWB signals and WB signals using channelized receiver architecture techniques. The ability to monitor and characterize channel activity using non-cooperative, non-synchronized mechanisms could greatly simplify network design by minimizing the amount of coordination and/or information exchange between users.

1.3 Research Assumption

The following assumptions are made:

- The channel of interest is modeled as Additive White Gaussian Noise (AWGN).
- All Signal-to-Noise Ratio (SNR) measurements are made at the RF filter output.
- All RF frequency responses are centered at the center frequency of the signal of interest.
- Only one signal of interest is present at a given time in the RF environment. The signal present is either the ultra wideband pulse or the direct sequence spread spectrum waveform. Coexistence is not addressed.
- The propagation path from transmitter to receiver is considered to be line-of-sight. Thus, multi-path signals and multi-path propagation are not present.
- All signal detection is performed using test statistics generated under Constant False Alarm Rate (CFAR) conditions. Thus, the detection threshold varies as a function of signal-to-noise ratio (SNR) to maintain a constant probability of false alarm of $P_{FA} = 10^{-2}$.

1.4 Research Scope

Channelized receiver processing techniques are initially investigated for the purpose of detecting UWB signals. Four distinct processing techniques are presented and modeled. Detection performance simulations are conducted to (1) verify previously published results for a down-converting (D/C) channelized receiver and to (2) introduce new results for a bandpass filtered, down-converting (BPF-D/C) channelized receiver which incorporates additional bandpass filters relative to the original D/C channelized

receiver architecture. The performance of each channelized receiver architecture is compared with radiometric detection in the presence of AWGN.

1.5 Research Approach

Initial research into the UWB signal provides temporal and power spectral density expressions for a uniform pulse train (UPT). Research into the DSSS waveform provides temporal and power spectral density expressions for a signal employing Gold-coding spreading techniques. The analytic results for both signals of interest are plotted to show structural characteristics of both signals.

Three non-cooperative receiver models are considered, including (1) a conventional radiometer (energy detector), (2) a D/C channelized receiver and (3) a BPF-D/C channelized receiver. Simulated detection results for the radiometer provide baseline detection performance, which is compared with detection results obtained for both channelized methods.

The research concludes with detection performance and filter characterization of the D/C channelized receiver models. Both receivers spectrally separate (channelize) the received signal and employ mixers and low-pass filters to downconvert each channelized signal to baseband. However, the BPF-D/C channelized receiver uses a set of additional bandpass filters to isolate spectral bands prior to mixing and low-pass filtering. For both channelized receiver architectures considered, the final channelized signals are digitized following down-conversion for signal processing. The digital processor uses data obtained over an observation interval which is stored in an $M \times S$ matrix where M is the number of receiver channel filters and S is the number of time samples within the

observation interval. The detection performance of each processing technique for both receivers is determined by simulation and compared with radiometric results.

1.6 Materials and Equipment

All work presented is simulated using MATLAB® Version 7.1. Simulations are run on a 2.8 GHz Precision Workstation x86 Intel XP personal computer and an AFIT mainframe UNIX based system.

1.7 Thesis Organization

Chapter 2 provides background information on the UWB and DSSS signals. Also provided are overviews of channelized receiver detection and down-converting channelized receiver detection and overviews of four channelized receiver processing techniques which are implemented using Fourier transformation and cross correlation. Chapter 3 presents the methodology, which focuses on BPF channelization with down-conversion. Chapter 4 provides simulated detection results and analysis for the D/C channelized receiver and the BPF-D/C channelized receiver, and filter characterization of both D/C receivers is also presented. Chapter 5 presents conclusions and provides recommendations for possible future research. Additional data is provided in the appendices: Appendix A contains simulated detection results for the BPF-D/C ChRx not included in Chapter 4; Appendix B contains MATLAB® code used in simulations.

II. Background

2.1 Chapter Overview

This chapter introduces the characteristics of the ultra wideband (UWB) pulse and direct sequence spread spectrum (DSSS) signals as used for this research. A discussion on the channelized receiver architecture and channelized receiver processing techniques is provided as well. Section 2.2 describes the uniform pulse train (UPT) UWB signal and its power spectral density, and also the Gold-coded DSSS waveform and its power spectral density. Section 2.3 describes detection techniques, including matched filter, radiometric, and channelized receiver detection. Section 2.4 further describes non-cooperative detection techniques, and it presents down-converting (D/C) channelized receiver detection. Section 2.5 presents the channelized receiver processing matrices, Section 2.6 describes threshold detection using the processing matrices, and Section 2.7 provides concluding remarks.

2.2 Received Signals Overview

This section introduces the temporal and spectral characteristics of the UWB and the DSSS signals used here.

2.2.1 Ultra Wideband Signal. Impulse based UWB systems transmit data over a very large bandwidth using extremely short duration pulses. The FCC First Report and Order was released in April 2002 [1], and it places strict emission limitations on UWB signaling for various applications, including radar, imaging and communication devices. The restrictions are imposed (1) to limit potential interference with narrow band systems coexisting in the same spectral region, and (2) to minimize collateral interference to

systems operating outside assigned spectral regions. Indoor UWB system operation is limited to the unlicensed spectrum of 3.1 to 10.6 GHz (measured at -10 dB bandwidth points). The FCC also specifies a maximum allowable Effective Isotropic Radiated Power (EIRP) of –41.4 dBm/MHz within the specified frequency range.

As defined by the FCC [1], a system is considered UWB if it either has (1) a bandwidth greater than or equal to 500 MHz, or (2) a fractional bandwidth greater than 20%, where fractional bandwidth B_f is

$$B_f = 2 \cdot \left(\frac{f_H - f_L}{f_H + f_L} \right) \tag{2.1}$$

where f_L and f_H are the respective lower and upper –10 dB bandwidth frequencies.

The analytic form chosen to represent the transmitted UWB pulse is the Gaussian monocycle. Due to antenna derivative effects, propagation of the Gaussian monocycle results in a received second derivative Gaussian impulse

$$w(t) = \left[1 - 4\pi \cdot \left(\frac{t}{\tau_m} \right)^2 \right] \cdot \exp\left[-2\pi \cdot \left(\frac{t}{\tau_m} \right)^2 \right] \tag{2.2}$$

where the impulse width τ_m is approximately 0.4 times the pulse width T_w as shown in [2] and discussed in [3]. Fig. 2.1 represents a single UWB pulse in the time domain for $T_w = 0.4ns$. Using the *w(t)* expression of (2.2), the general analytic expression for a UWB signal is:

$$s(t) = \sum_{k=-\infty}^{\infty} A_k \cdot w(t - kT_s - B_k\Delta) \tag{2.3}$$

where A_k and B_k are specified according to modulation type, T_s is the symbol duration, and Δ is the relative position modulation offset. The UWB signal modulation technique considered here is the Uniform Pulse Train (UPT), which is obtained using $A_k = B_k = 1$ in (2.3).

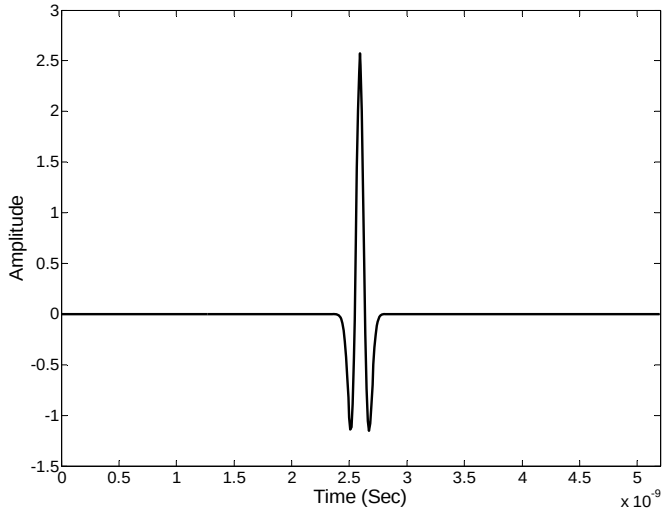

Figure 2.1 A single UWB, second derivative Gaussian impulse

Overall, the parameters defining characteristics of the UWB pulse used in this work are:

- UWB Pulse Width – 0.4 ns
- Total Observation Interval – 5.2 ns
- Time Sample Spacing – 0.01 ns

The general analytic expression for the power spectral density (PSD) of a UWB impulse is derived using methods similar to those presented in [4-7], and is summarized in [8]. The total UWB signal PSD is [8]:

$$S_{UWB}(f) = S_{UPT}(f) \cdot |W(f)|^2 \tag{2.4}$$

where $W(f)$ is the Fourier transform of the received UWB pulse and $w(t)$ is given by (2.2). The PSD for the UPT modulation process, $S_{UPT}(f)$ as in (2.4), is:

$$S_{UPT}(f) = \frac{1}{T_s^2} \sum_{l=-\infty}^{\infty} \delta\left(f - \frac{l}{T_s} \right) \tag{2.5}$$

and the Fourier transform of the received UWB signal is:

$$W(f) = \frac{\pi \tau_m^3 f^2}{\sqrt{2}} \cdot \exp\left(-\frac{\pi \tau_m^2 f^2}{2} \right) \tag{2.6}$$

Fig. 2.2 shows the analytic PSD for a uniform UWB pulse train which was generated using $T_w = 0.4ns$ and $\tau_m = 0.4T_w = 0.16ns$. The pulse repetition interval for the pulse train is $T_s = 2T_w$.

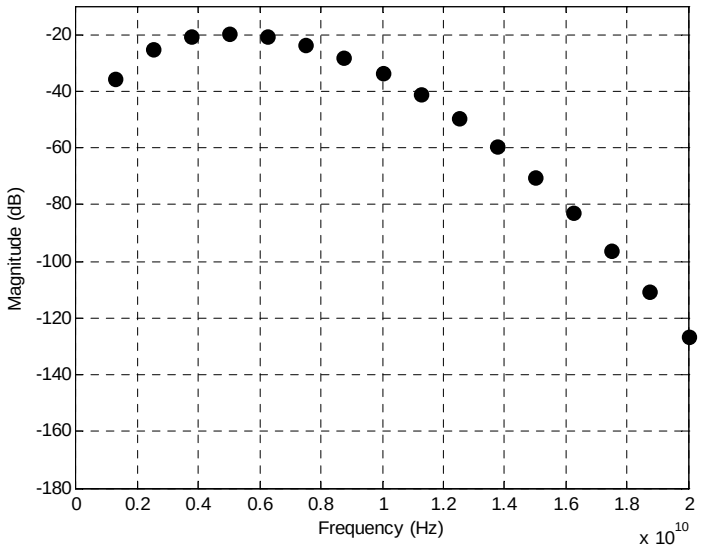

Figure 2.2 Analytical PSD of a uniform UWB pulse train

2.2.2 Direct Sequence Spread Spectrum Signal. Data modulated signals can be spectrally spread by modulating the signal a second time. This spreading can be accomplished using either a very wideband spreading signal, or coding sequence. This bandwidth spreading technique is commonly referred to as direct sequence spread spectrum (DSSS) [9].

The DSSS signal considered here employs binary shift keying (BPSK) for both the data and spreading modulations. This technique features instantaneous phase changes of the carrier by 180 degrees. Streaming bits of information, i.e., a series of 1's and 0's at data rate of R_b, are mapped to antipodal waveforms, respectively, to produce the data modulated waveform $d(t)$. Within the BPSK format, a phase value of $0°$ corresponds to an assigned bit value of +1, whereas a phase value of $180°$ represents an assigned bit value of -1. Here, a Gold-coded spreading waveform $c(t)$ is used to spectrally spread the data modulated waveform with a chip rate R_c. Typically, Gold-coding is used for multiple-access spread spectrum systems so that as many users as possible can use a band of frequencies with as little mutual interference as possible. The actual coding sequence is further discussed in [9]. Fig. 2.3 is a block diagram of DSSS signal modulation and transmission. The input to the BPSK modulator is the information bit stream {b} at the bit rate R_b, and the output is the data modulated waveform $m(t)$. The Gold-coded spreading waveform $c(t)$ is generated at the chip rate of R_c is applied to the data modulated waveform to produce the spectrally spread transmitted waveform $s(t)$.

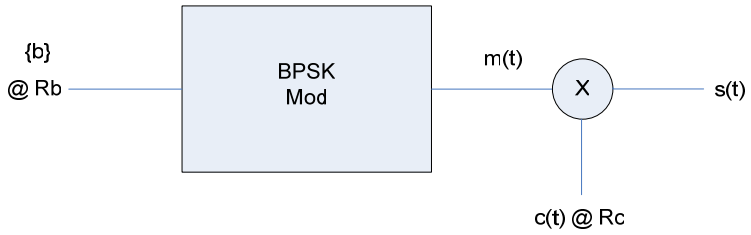

Figure 2.3 Transmitter block diagram for DSSS signaling

The basic signal structure for a DSSS signal is:

$$s(t) = \sqrt{2P} \cdot d(t) \cdot c(t) \cdot \cos\left(2\pi f_0 t - \pi i\right) \tag{2.7}$$

where i is either 1 or 0 for BPSK modulation bits and P and f_0 are the average signal power and center frequency, respectively. Fig. 2.4 shows a representative DSSS waveform in the time domain. Overall, the parameters that define the DSSS signal used in this work include:

- Data Rate (R_b) – 12.5 kHz
- Chip Rate (R_c) – 1 GHz
- Time Sample Spacing – 0.01 ns

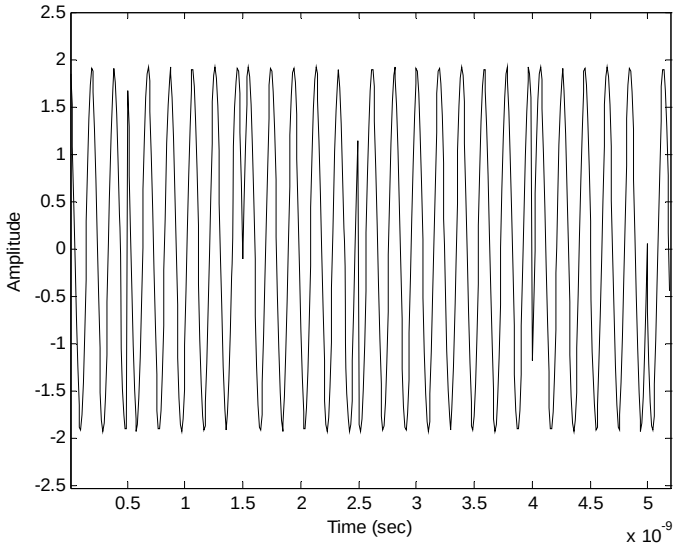

Figure 2.4 Representative DSSS waveform in the time domain
(A symbol boundary / phase change is evident near 2.5 ns)

The two-sided general analytic expression for the power spectral density (PSD) of a DSSS signal is derived using methods similar to those presented in [10-13]. As summarized in [9], the approximate DSSS signal PSD is:

$$S_t(f) = \tfrac{1}{2} P T_c \left\{ \mathrm{sinc}^2 \left[(f - f_0) T_c \right] + \mathrm{sinc}^2 \left[(f + f_0) T_c \right] \right\} \tag{2.8}$$

where the *sinc*^{2} function emerges from the Fourier transform of the spreading code autocorrelation function. Fig. 2.5 shows the PSD for the simulated DSSS waveform.

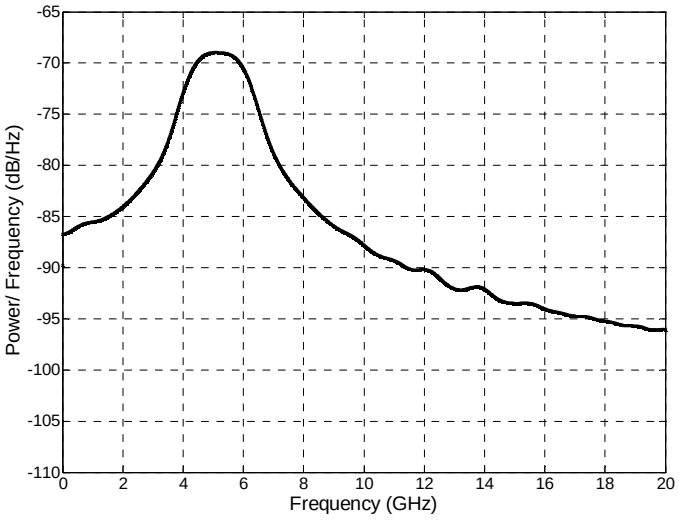

Figure 2.5 PSD of simulated DSSS waveform

2.3 Channelized Receiver Detection

To understand the channelized receiver architecture and detection, a brief overview of detection techniques is provided. Receiver detection can be classified as either cooperative or non-cooperative detection. In cooperative detection, the form and arrival time of a received signal are known. With these known parameters, a correlation implementation of a matched filter (MF) receiver [14] can be used to detect and estimate the presence of a particular signal of interest (SOI). The block diagram for a MF with correlation is shown in Fig. 2.6. In this figure the received signal is:

$$r(t) = s(t) + n(t) \tag{2.9}$$

where $s(t)$ is the signal of interest (SOI) and $n(t)$ is AWGN. For all detection methods considered here, a test statistic Z is produced and compared with a threshold Z_T, which

is established using various detection criteria [15]. For a matched filter detector signal "presence" is declared when $Z > Z_T$.

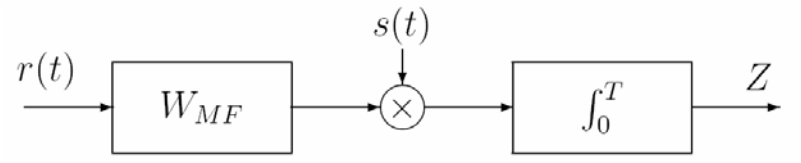

Figure 2.6 Matched filter detector with correlation implementation [3]

Non-matched filter detection may be employed if the form and arrival time of received signals are unknown. As with the MF detection method, non-cooperative detection methods produce a test statistic Z for comparison with threshold Z_T. A signal is declared present if $Z \geq Z_T$ and not present if $Z < Z_T$. Two conditional probabilities exist when a signal is present, including:

P_D = P[$Z >$ Z_T | Signal Present] (Probability of Detection)

P_M = P[$Z <$ Z_T | Signal Present] (Probability of a Miss)

When the signal is not present, only channel noise is present, which may or may not trigger signal declaration. Two conditional probabilities exist when a signal is not present, including:

P_{FA} = P[$Z >$ Z_T | Signal Absent] (Probability of False Alarm)

P_{ND} = P[$Z <$ Z_T | Signal Absent] (Probability of No Detection)

Constant false alarm rate (CFAR) processing occurs when the threshold Z_T adapts to changing channel conditions. In this case, a constant P_{FA} is maintained [16].

The radiometer is one form of non-cooperative detector which detects signal energy in bandwidth W_{RAD} by processing the received signal over time interval T [17]. The resultant test statistic Z is compared with threshold γ and a detection decision is made. As with previous detectors, if $Z > Z_T$ a signal is declared present and if $Z < Z_T$ no signal is declared. Fig. 2.7 is a block diagram of radiometric detection.

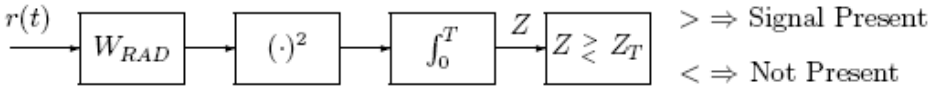

Figure 2.7 Block diagram of radiometric detection process [3]

"A channelized receiver architecture provides wide instantaneous bandwidth so that all signals present are received simultaneously without the necessity of tuning a receiver to a specified signal or band of interest." [18]. According to Tsui in [18], the only practical implementation of a wideband receiver is channelization, involving parallel processing of outputs from a series of smaller bandwidth filters which span the larger desired bandwidth of interest. As shown in Fig. 2.8 and further discussed in [2, 8], a channelized receiver consists of a bank of M filters spanning the total bandwidth of interest. The output of each bandpass filter is sent to a respective analog-to-digital (A/D) converter, and all outputs are processed collectively to exploit the power of channelization.

Implementing this receiver architecture in hardware may not be practical, given that A/D converters must sample at least twice as fast as the highest frequency component appearing in the bandpass filters (Nyquist sampling criteria). The frequency

range for signals of interest here (especially the UWB signals) extends much higher than current A/D technology can feasibly support.

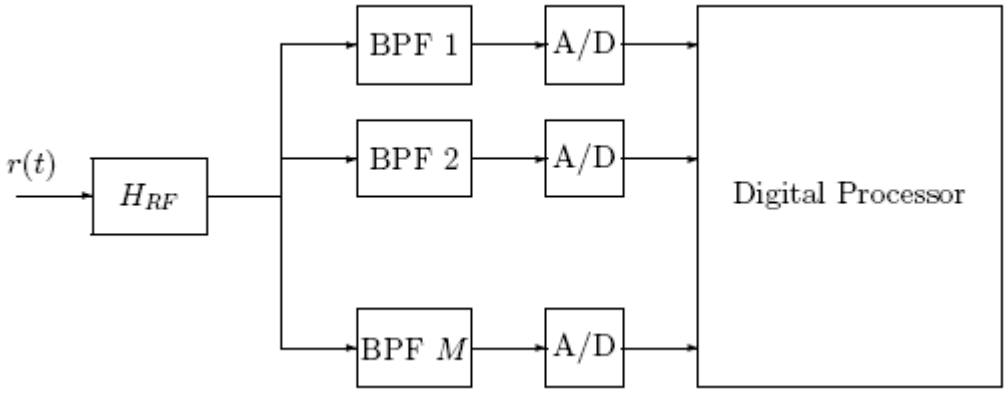

Figure 2.8 Channelized receiver block diagram [8]

2.4 Down-Converting Channelized Receiver Detection

One possible solution to the A/D limitation of the wideband channelized receiver, as presented in [8, 19], is to implement signal down-conversion prior to A/D conversion [20]. Fig. 2.9 illustrates one possible implementation for a down-converting channelized receiver. In this case, M mixers at equally spaced local oscillator frequencies and initial phase values are employed for down-conversion. Each mixer essentially takes the input signal (the spectral response of which spans H_{RF}) and translates it to a lower intermediate frequency. This frequency translation reduces the A/D sampling rate necessary to reliably recreate a signal of interest. The mixers are followed by M low-pass filters. Each down-converted low-pass filtered signal is sent to an A/D converter, and the M outputs are processed collectively.

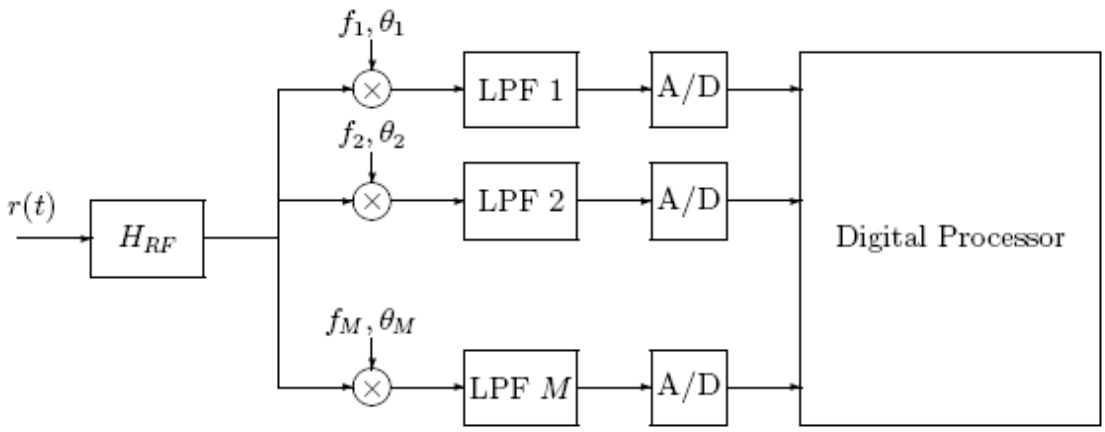

Figure 2.9 D/C channelized receiver block diagram [8]

2.5 Channelized Receiver Processing

The four detection methods for channelized receiver processing, as discussed in [2, 8, 19], are introduced in this section. These processing techniques include the temporal-temporal matrix (TTM), cross-temporal matrix (CTM), spectral-spectral matrix (SSM), and cross-spectral matrix (CSM) methods.

The A/D converted signals from both the channelized and down-converting channelized receiver architectures may be used to form the Channelized Data Matrix (CDM). As illustrated in Fig. 2.10, the CDM is a $M \times S$ matrix, where M is the number of receiver channels and S is the number of time samples spanning the observation interval. Thus, each row in the matrix is time-sampled data from a specific channel of the receiver being evaluated.

$$\begin{bmatrix} X_{11} & X_{12} & \cdots & X_{1S} \\ X_{21} & X_{22} & \cdots & X_{2S} \\ \vdots & \vdots & \ddots & \vdots \\ X_{M1} & X_{M2} & \cdots & X_{MS} \end{bmatrix}$$

Figure 2.10 Channelized data matrix (CDM) structure

2.5.1 Temporal-Temporal Matrix (TTM). The TTM is formed by performing an inverse Fast Fourier Transform (IFFT) on each column of the CDM and taking the absolute value of each element in the resulting matrix. Zero-padding is used if the number of IFFT points N_{ifft} is greater than the number of receiver channels M. Truncation of higher frequency samples occurs if $N_{ifft} < M$.

Fig. 2.11 and Fig. 2.12 show plots of representative TTM data for a received UWB pulse input to the channelized and down-converting channelized receivers, respectively. Data for these TTM matrices are formed by applying a 64-point IFFT on the columns of the CDM.

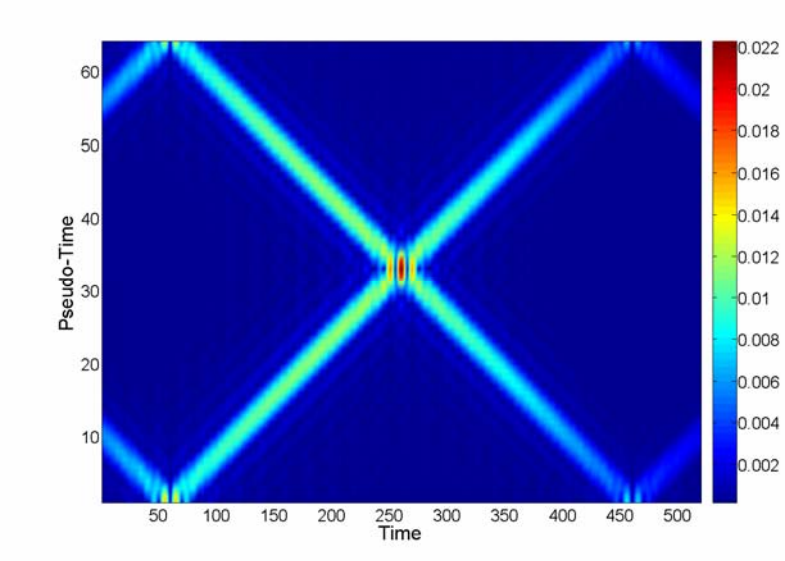

Figure 2.11 UWB: Temporal-temporal matrix (TTM) from channelized receiver

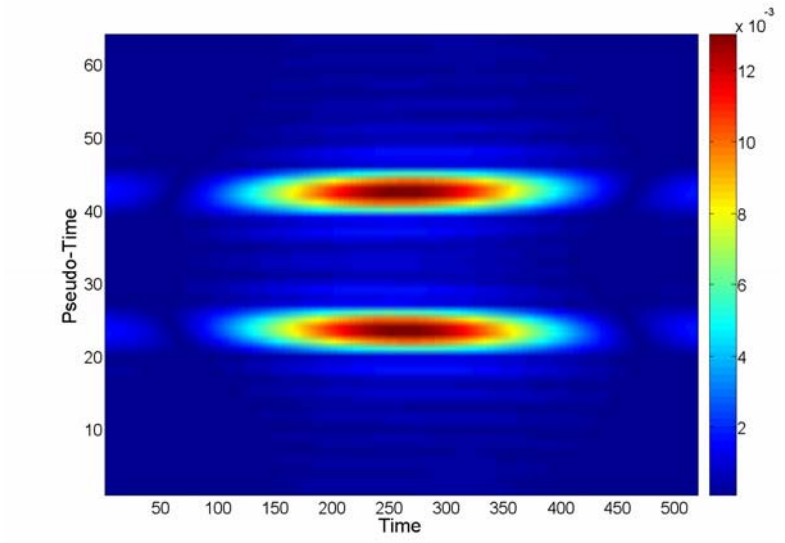

Figure 2.12 UWB: Temporal-temporal matrix (TTM) from D/C channelized receiver

2.5.2 Cross Temporal Matrix (CTM). The CTM is formed by taking the absolute value of the correlation between all combinations of TTM columns. CTM elements are:

$$CTM = \frac{1}{N_{ifft}} \left| TTM^{H} \cdot TTM \right| \tag{2.10}$$

where N_{ifft} is the number of IFFT points used to form the TTM and the $(\cdot)^{H}$ operation is the Hermitian or complex transpose. Representative CTM data for the channelized and down-converting channelized receivers for a received UWB pulse are shown in Fig. 2.13 and Fig. 2.14, respectively. The data in these plots are formed using (2.10) with the TTM data from Fig. 2.11 and Fig. 2.12.

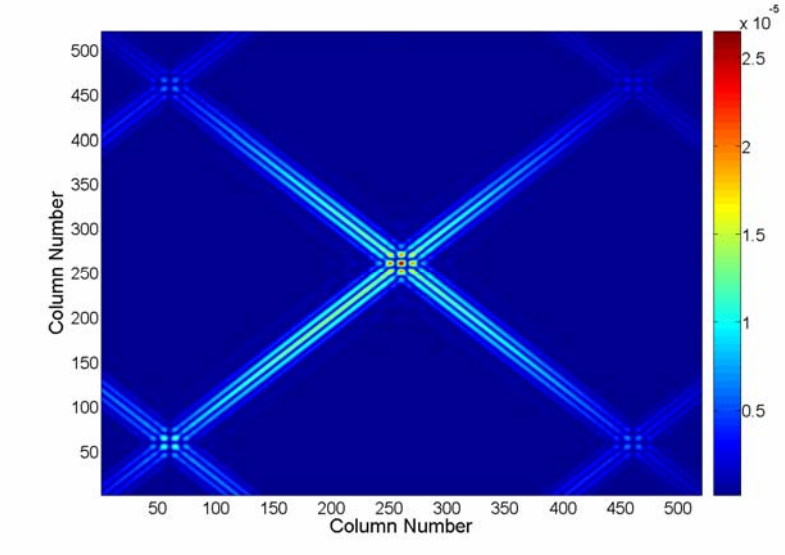

Figure 2.13 UWB: Cross temporal matrix (CTM) from channelized receiver

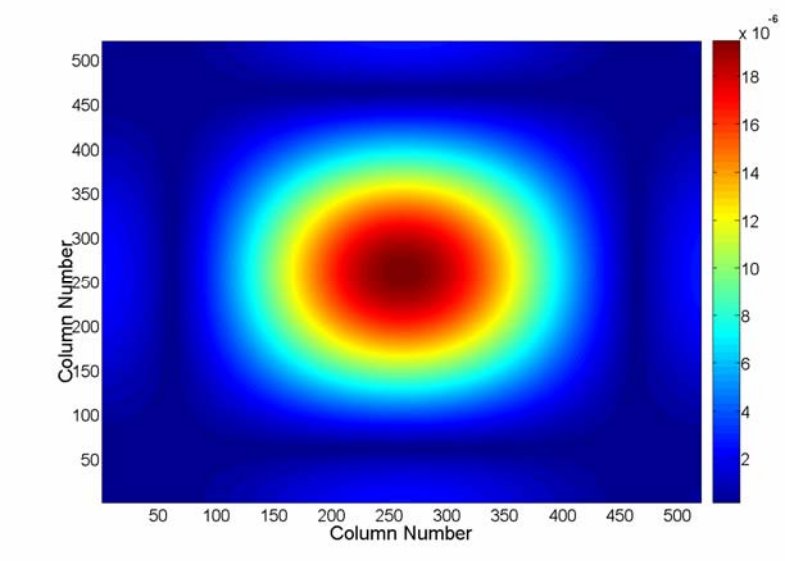

Figure 2.14 UWB: Cross temporal matrix (CTM) from D/C channelized receiver

2.5.3 Spectral-Spectral Matrix (SSM). The SSM is formed by performing a Fast Fourier Transform (FFT) on each row of the CDM and taking the absolute value of each element in the resulting matrix. The number of FFT points N_{fft} must be greater than the number of samples S in the observation interval so that no time samples are truncated in the FFT process. Zero-padding is used if N_{fft} is greater than the number of samples in the observation interval. Representative SSM data from the channelized and down-converting channelized receivers for a received UWB pulse are shown in Fig. 2.15 and Fig. 2.16, respectively. These matrices are formed by applying a 512-point FFT on the rows of the CDM.

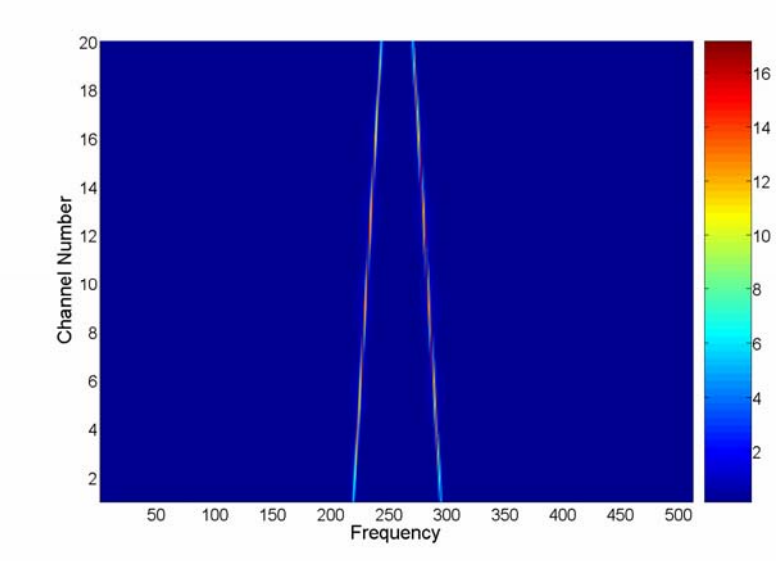

Figure 2.15 UWB: Spectral-spectral matrix (SSM) from channelized receiver

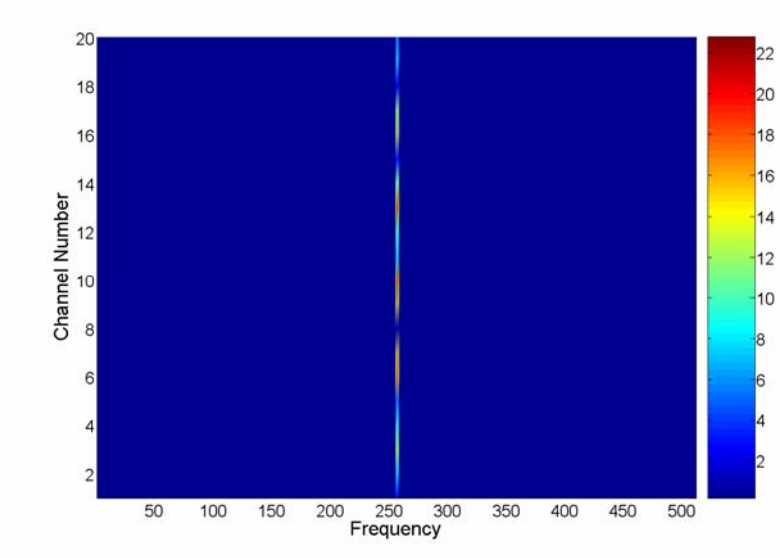

Figure 2.16 UWB: Spectral-spectral matrix (SSM) from D/C channelized receiver

2.5.4 Cross Spectral Matrix (CSM). The CSM is formed by taking the absolute value of the correlation between all combinations of SSM columns, and is simplified as:

$$CSM = \frac{1}{M}\left|SSM^{H} \cdot SSM\right| \tag{2.11}$$

where M is the number of receiver channels and the $(\cdot)^H$ operation is the Hermitian complex transpose. Representative CSM data from the channelized receiver and the down-converting channelized receiver for a received UWB pulse are shown in Fig. 2.17 and Fig. 2.18, respectively. The data in these plots are formed using (2.11) with the SSM data from Fig. 2.15 and Fig. 2.16.

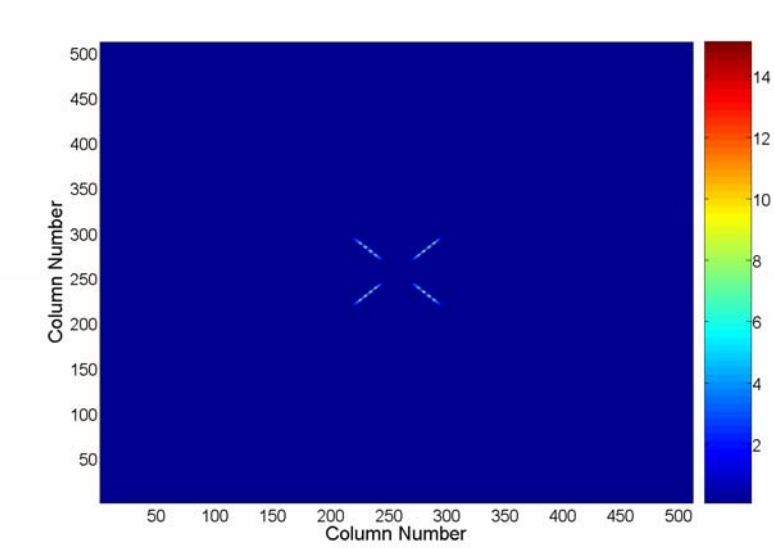

Figure 2.17 UWB: Cross spectral matrix (CSM) from channelized receiver

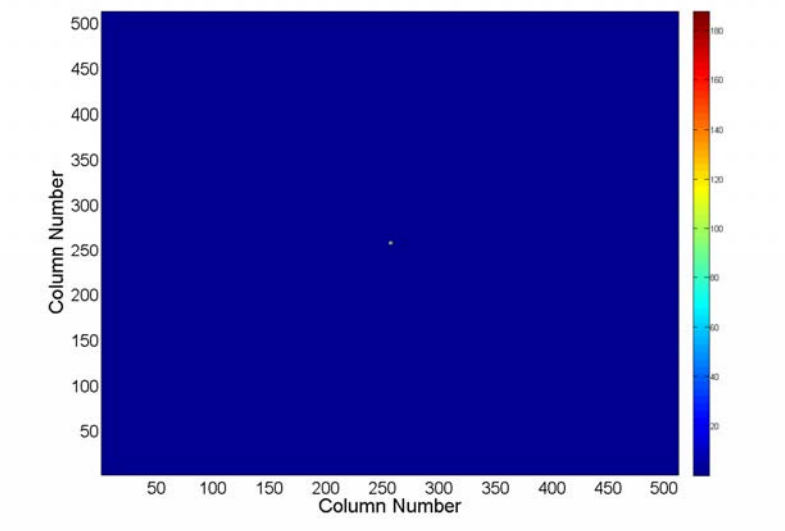

Figure 2.18 UWB: Cross spectral matrix (CSM) from D/C channelized receiver

2.6 Threshold Detection

Two-dimensional threshold detection is performed using each of the four processing methods to characterize P_D performance for each method.

Once a given matrix of data is generated, the maximum value of the processed matrix is chosen as the test statistic Z_N for comparison with the threshold Z_T. The threshold value is determined by processing a number of matrices created using R noise realizations for a given signal-to-noise ratio (SNR). These R noise realizations are set to achieve the desired probability of false alarm. The threshold value Z_T is set as the lower bound of the 10 largest Z_N test statistics. The number of R realizations required is:

$$R = \frac{10}{P_{FA}} \tag{2.12}$$

where P_{FA} is the desired probability of false alarm, which is maintained constant (CFAR conditions) as SNR is varied [16]. To achieve a $P_{FA} = 10^{-2}$ the number of R realizations must equal 1000.

The R matrices are regenerated with the R noise realizations and signal of interest present. The Z test statistics from these signal present conditions are compared to threshold Z_T and P_D determined by

$$P_D = \frac{\#Z > Z_T}{R} \tag{2.13}$$

The procedure of threshold determination by noise realization and P_D determination is repeated for each desired SNR value. Fig. 2.19 illustrates the overall process and data flow used for detection performance characterization.

2.7 Summary

This chapter introduces the UWB and DSSS waveforms considered here. Channelized and down-converting channelized receiver architectures are introduced along with various detection techniques. Four processing techniques are addressed, including the temporal-temporal matrix (TTM), cross temporal matrix (CTM), spectral-spectral matrix (SSM), and the cross spectral matrix (CSM). Threshold detection for determining probability of detection (P_D) under constant false alarm rate (CFAR) conditions is also discussed.

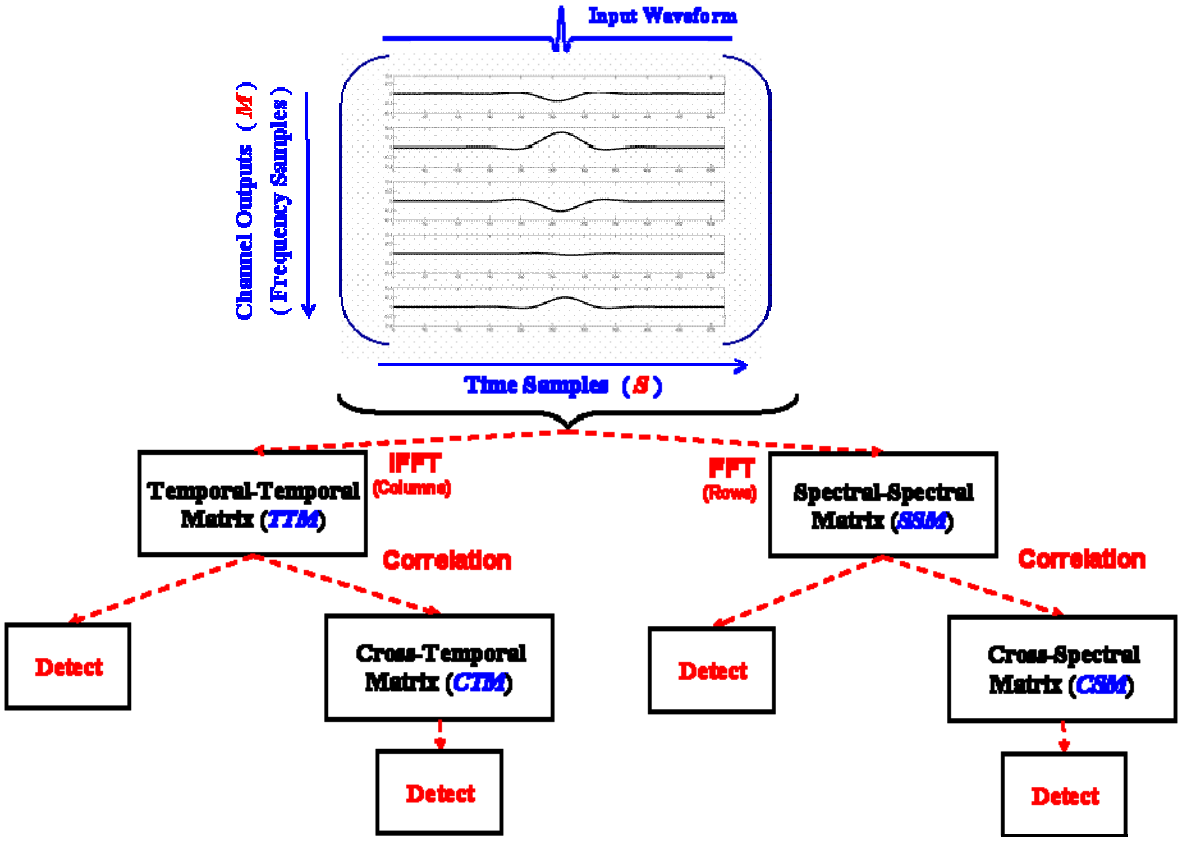

Figure 2.19 Process flow for channelized receiver detection

III. Methodology

3.1 Chapter Overview

This chapter introduces the bandpass filtered down-converting channelized receiver (BPF-D/C ChRx) architecture considered for this research. Section 3.2 examines the BPF-D/C channelized receiver as one alternative to the D/C channelized receiver presented in [8, 19] and described in Chapter 2, and Section 3.3 provides conclusions.

3.2 Bandpass Filtered, Down-Converting Channelized Receiver Architecture

One alternative to the down-converting channelized receiver (D/C ChRx) presented in [8, 19] and described in Section 2.4 is the bandpass filtered down-converting channelized receiver (BPF-D/C ChRx) evaluated here. One issue that may arise when using a down-converting channelized receiver architecture without bandpass filtering is aliasing.

In the D/C ChRx architecture of [8, 19], the signal of interest is first filtered with a single RF bandpass filter and combined using M mixer frequencies which span the spectrum of interest. This process produces a higher frequency and a lower frequency component in both the positive and negative frequency domains. The low-pass filtering which follows the conversion process suppresses the high frequency components and passes the lower frequency components for subsequent processing. For the first mixer frequency no aliasing is apparent. However, for the second and all remaining mixer frequencies aliasing may occur as negative spectral responses are translated to positive frequency locations and vice versa.

One possible solution to minimizing aliasing effects involves modifying the D/C ChRx architecture to incorporate bandpass filters. In this case bandpass filters are employed *before* the down-conversion process to isolate each spectral band of interest. Fig. 3.1 shows the BPF-D/C ChRx architecture, which includes a bank of M bandpass filters spanning the total bandwidth of interest. The BPFs are followed by M mixers operating at equally spaced frequencies with initial phase values. Each mixer is followed by one of M identical low-pass filters. The bandpass filtered down-converted output of each low-pass filter is sent to a respective A/D converter, and all outputs are processed collectively.

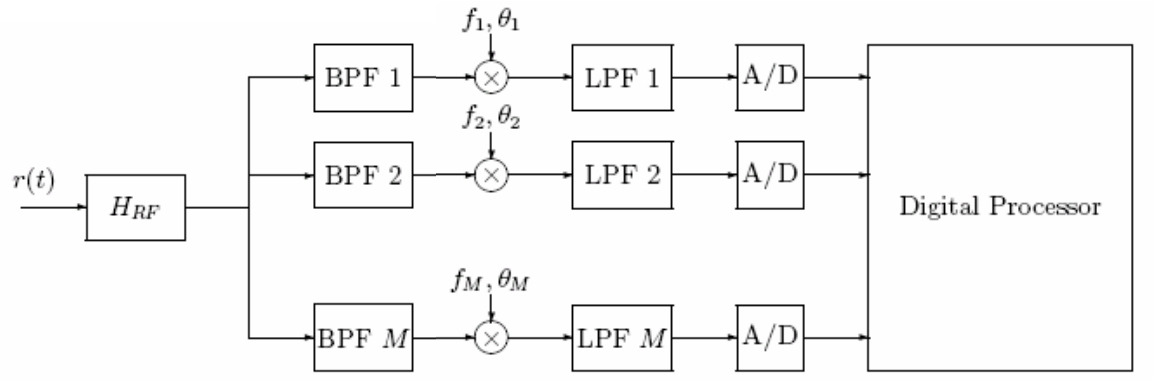

Figure 3.1 Bandpass filtered, D/C channelized receiver (BPF-D/C ChRx)

The A/D converted signals are used to form the Channelized Data Matrix (CDM), as in the channelized [3, 4] and D/C ChRx [8, 19] architectures described in Section 2.3 and Section 2.4, respectively. The four detection techniques introduced in Section 2.5 are used for signal processing. Fig. 3.2 shows a plot of representative temporal-temporal matrix data for a received UWB pulse input to the BPF-D/C ChRx. Fig. 3.3 shows TTM data for a received DSSS waveform input to the BPF-D/C ChRx. Data for both TTM matrices are formed by applying a 64-point IFFT on the columns of the CDM.

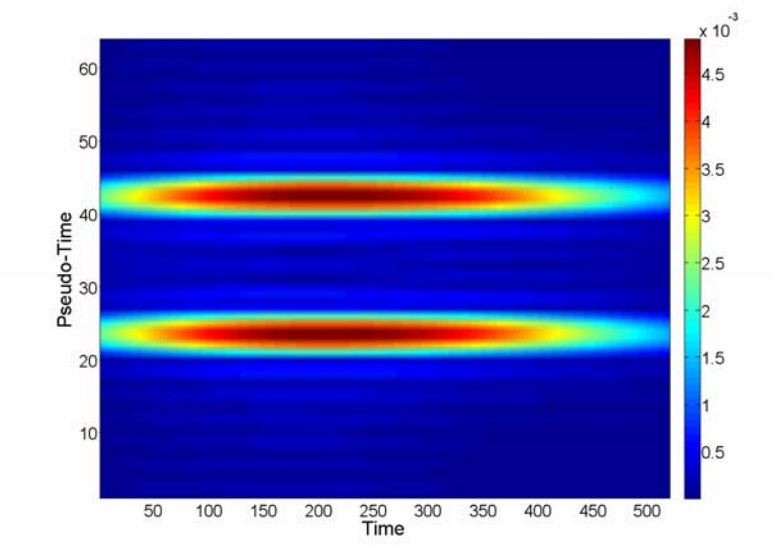

Figure 3.2 UWB temporal-temporal matrix (TTM) from a bandpass filtered, down-converting channelized receiver (BPF-D/C ChRx)

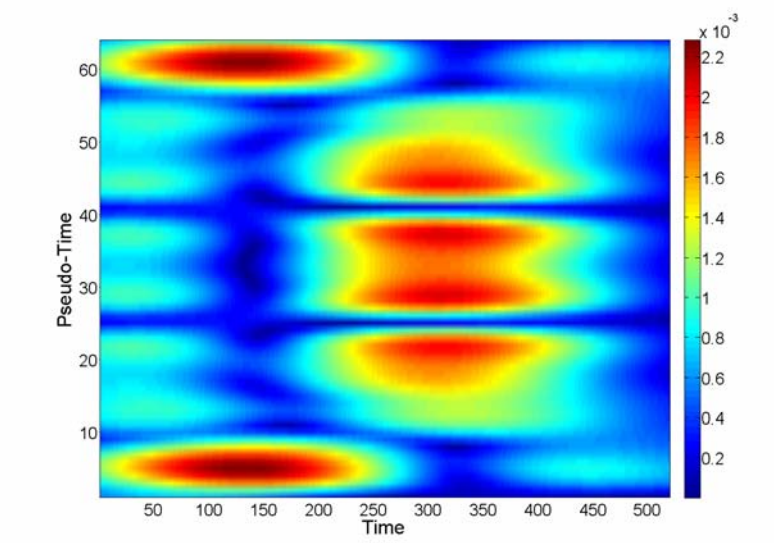

Figure 3.3 DSSS temporal-temporal matrix (TTM) from a bandpass filtered, down-converting channelized receiver (BPF-D/C ChRx)

A plot of representative cross temporal matrix data for a received UWB pulse input to the BPF-D/C ChRx is shown in Fig. 3.4. The plot is formed using (2.10) with the TTM data from Fig. 3.2. Likewise, Fig. 3.5 shows CTM data for a received DSSS

waveform input to the BPF-D/C ChRx, formed using (2.10) with the TTM data from Fig. 3.3. The CDM yields the spectral-spectral matrix from a UWB received pulse as shown in Fig. 3.6, which is formed by applying a 512-point FFT on the rows of the CDM. Fig. 3.7 shows data for a received DSSS waveform input to the BPF-D/C ChRx, which is formed using the same number of FFT points as in Fig. 3.6. Fig. 3.8 shows representative cross spectral matrix data from the BPF-D/C ChRx for a received UWB pulse. Fig. 3.9 shows data from a received DSSS waveform input to the BPF-D/C ChRx. The data in Figs. 3.8 and 3.9 are formed using (2.11) with the SSM data from Figs. 3.6 and 3.7, respectively.

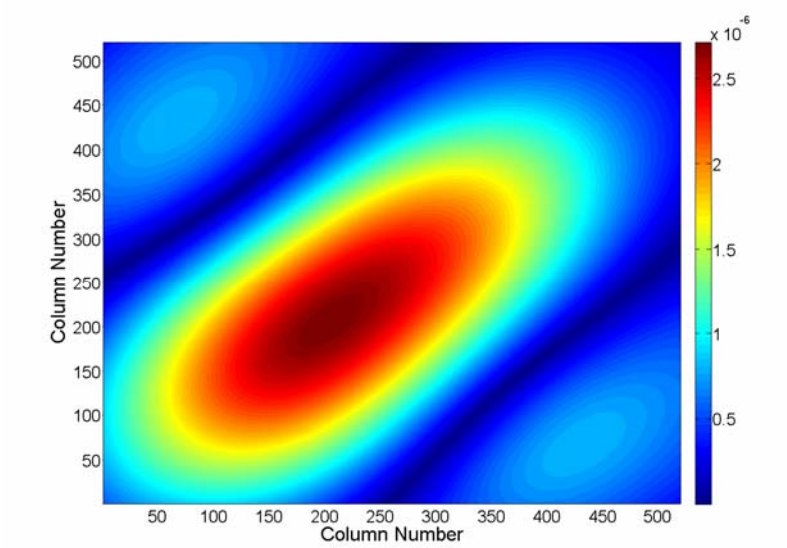

Figure 3.4 UWB cross temporal matrix (CTM) from a bandpass filtered, down-converting channelized receiver (BPF-D/C ChRx)

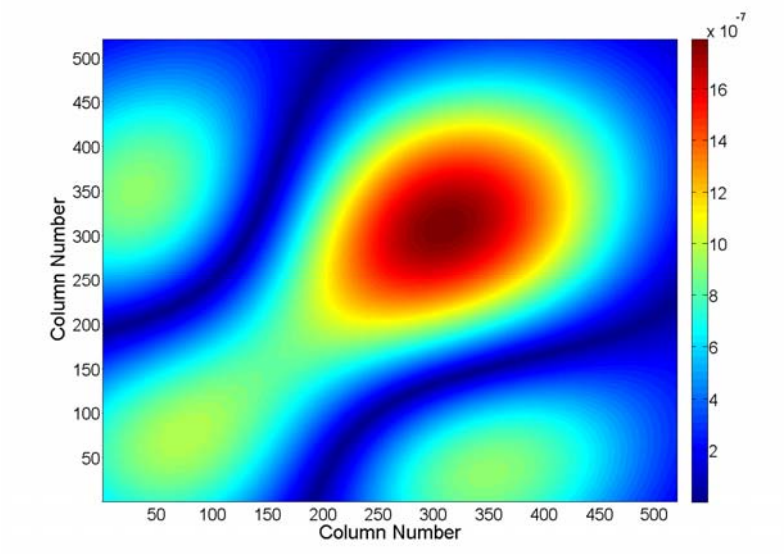

Figure 3.5 DSSS cross temporal matrix (CTM) from a bandpass filtered, down-converting channelized receiver (BPF-D/C ChRx)

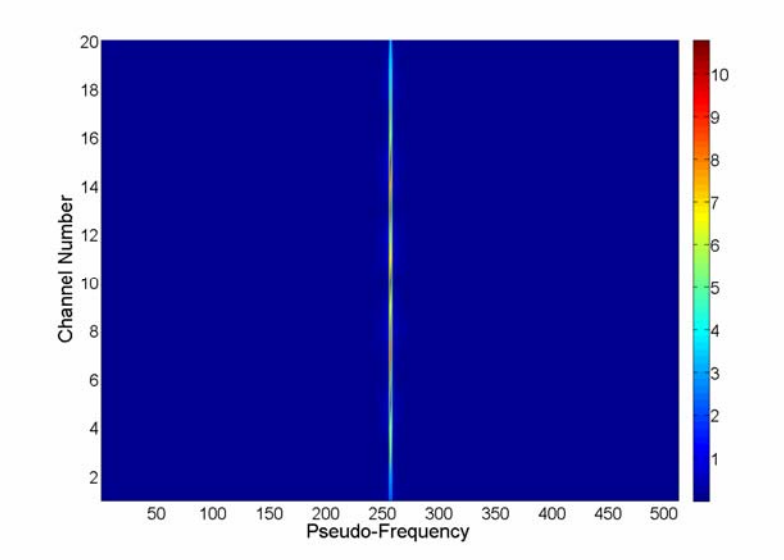

Figure 3.6 UWB spectral-spectral matrix (SSM) from a bandpass filtered, down-converting channelized receiver (BPF-D/C ChRx)

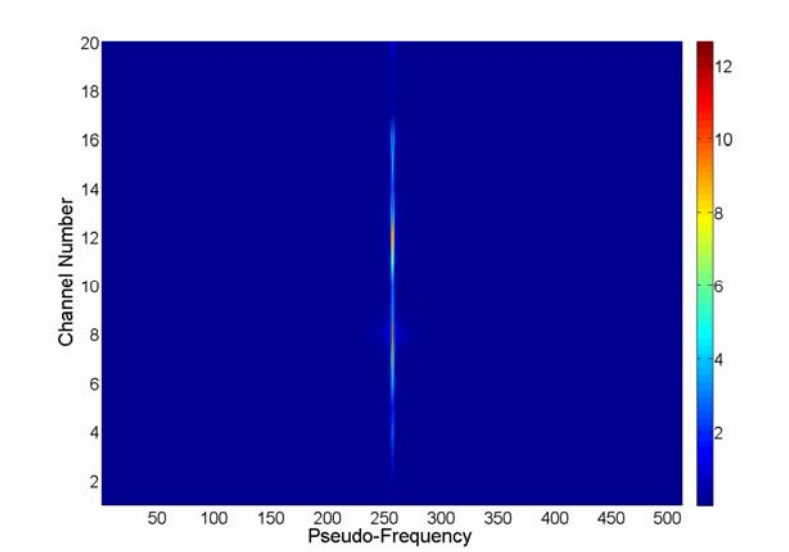

Figure 3.7 DSSS spectral-spectral matrix (SSM) from a bandpass filtered, down-converting channelized receiver (BPF-D/C ChRx)

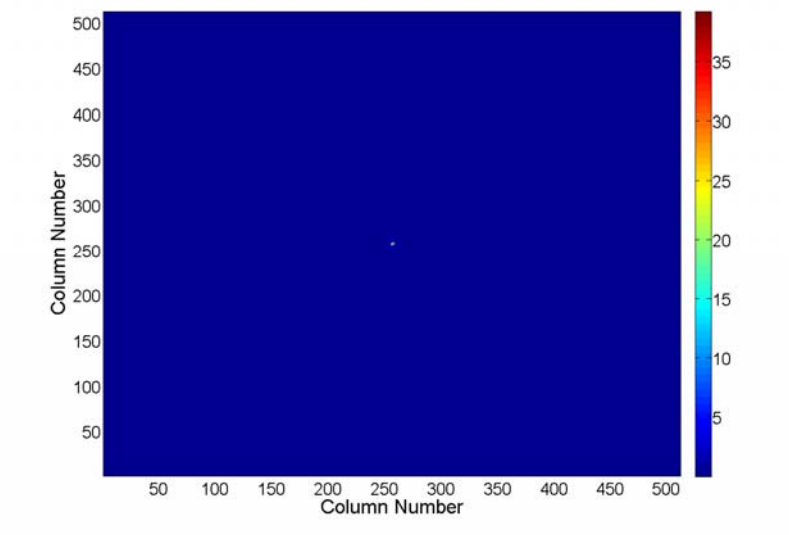

Figure 3.8 UWB cross spectral matrix (CSM) from a bandpass filtered, down-converting channelized receiver (BPF-D/C ChRx)

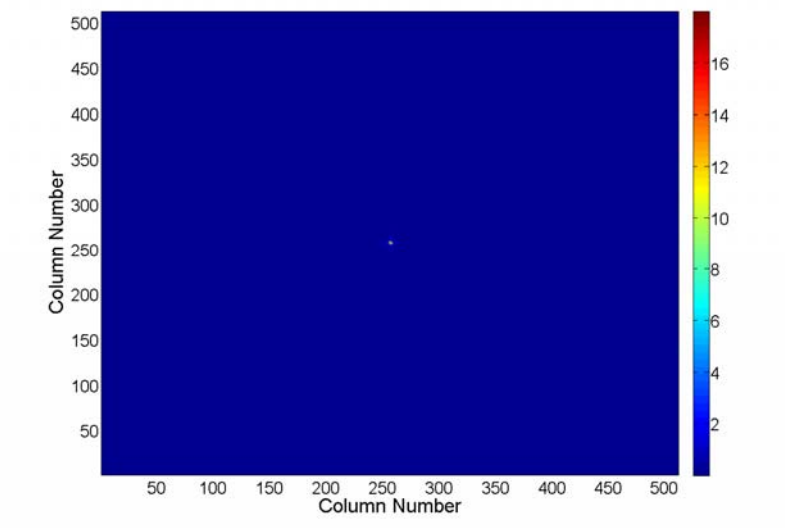

Figure 3.9 DSSS cross spectral matrix (CSM) from a bandpass filtered, down-converting channelized receiver (BPF-D/C ChRx)

The method for determining the probability of detection (P_D) from the processing techniques shown in Fig. 3.2 through Fig. 3.5 is the same as the threshold detection method discussed in Section 2.6.

As in [8], various parameters are changed to generate results for different detection scenarios and arrangements, including

- Received Signal-to-Noise (SNR), measured at the RF filter output
- Number of IFFT (N_{ifft}) and FFT (N_{fft}) points to create the four processing matrices (TTM, CTM, SSM, CSM)
- Bandpass filtered, down-converting channelized receiver channel bandwidths
- Down-conversion mixer starting phase

3.3 Summary

This chapter introduces the bandpass filtered down-converting channelized receiver as one alternative to the architectures presented in Chapter 2. Results for the threshold detection process with each of the four detection matrices generated for both the D/C ChRx and the BPF-D/C ChRx are presented in Chapter 4.

IV. Results and Analysis

4.1 Chapter Overview

This chapter provides filter characterization and detection performance results for the receivers and processing techniques introduced in Chapters 2 and 3. First, Section 4.2 characterizes the filter responses of both the down-converting channelized receiver (D/C ChRx) and the bandpass filtered down-converting channelized receiver (BPF-D/C ChRx). Next, Section 4.3 presents D/C ChRx detection performance results using the channelized matrix data and techniques introduced in Chapter 2, where the signal of interest is the UWB pulse. Section 4.4 provides the BPF-D/C ChRx detection performance results using the channelized matrix data and techniques introduced in Chapter 2, where the signal of interest is the UWB pulse. Finally, Section 4.5 presents the BPF-D/C ChRx detection performance results for the case where a DSSS waveform is introduced as the signal of interest. Section 4.6 concludes the chapter.

4.2 Filter Characterization

This section provides characterization of the Butterworth filters used for both the D/C ChRx and BPF-D/C ChRx. Channelized data using the ultra wideband signal shown in Fig. 2.1 is also presented.

4.2.1 Down-Converting Channelized Receiver. The D/C ChRx presented in [8, 19] and described in Section 2.4 consists of RF filter H_{RF}, M mixers, and M low-pass filters (LPF), followed by M analog-to-digital converters and digital signal processing. The filters employed in this work are 4^{th}-order Butterworth filters. The Butterworth filter is chosen because of its specific filtering characteristics; the Butterworth filter has a

magnitude response that is maximally flat without ripples in the passband [21]. A 4th-order filter is chosen because the roll-off is steeper than for a lower order filter. Ultimately, roll-off steepness is sacrificed for smoothness in the band of interest.

The received signal is first filtered by H_{RF}, which spans 2.5 GHz to 7.5 GHz as measured between the -3 dB points. The magnitude and phase responses of the Butterworth H_{RF} are shown in Fig. 4.1.

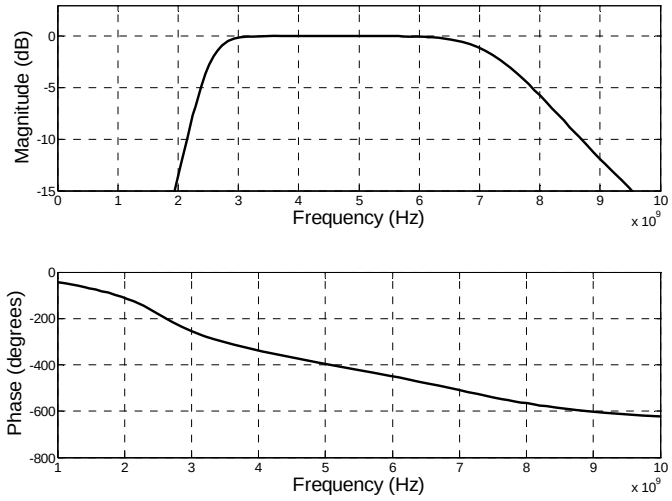

Figure 4.1 Magnitude and phase response of H_{RF} spanning 2.5 to 7.5 GHz

The filtered signal output (S_{RF}) is passed to a bank of M mixers spanning the total bandwidth of interest. The down-converted signal output of each mixer is then passed to a Butterworth LPF. Figure 4.2 shows the magnitude and phase response of a 250 MHz Butterworth LPF.

The output of each LPF is passed to its respective A/D converter, and all outputs are processed collectively. Figure. 4.3 illustrates five channelized ultra wideband signal

responses sampled over an observation interval at the D/C ChRx output. The data are shown for channel bandwidths of 1 GHz that span 5.0 GHz.

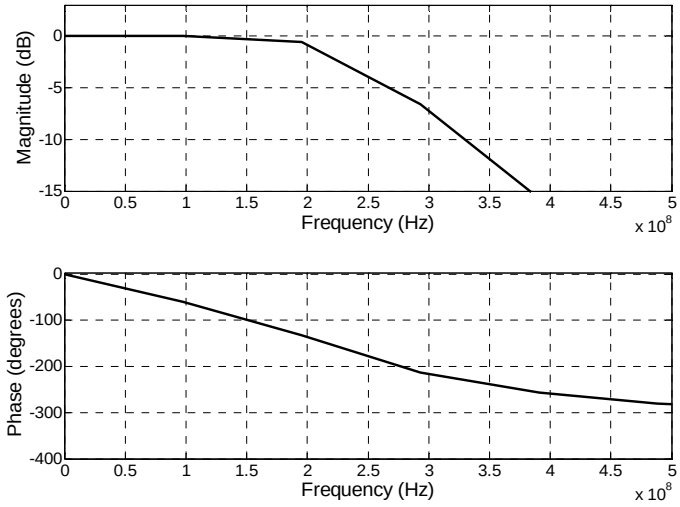

Figure 4.2 Magnitude and phase response of a 250 MHz LPF channel

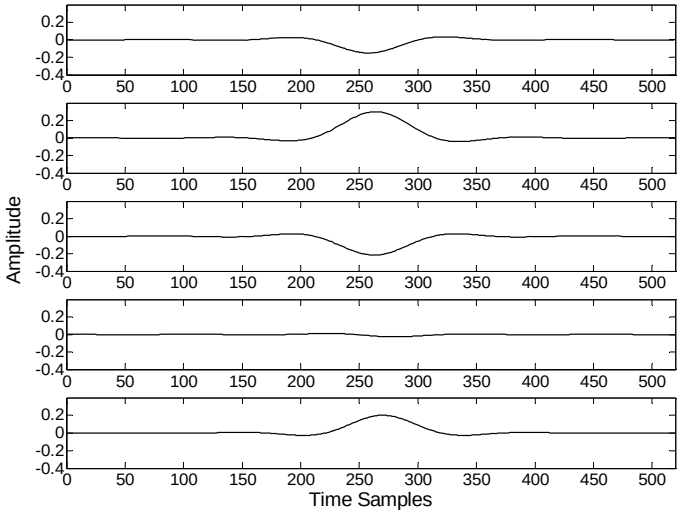

Figure 4.3 Channelized data matrix (CDM) for a D/C channelized receiver with a channel bandwidth of 1 GHz and a received UWB signal

4.2.2 Bandpass Filtered, Down-Converting Channelized Receiver. As presented in Section 3.2, the BPF-D/C ChRx is one alternative to the D/C ChRx architecture. A bank of M bandpass filters spanning the total bandwidth of interest is employed before the down-conversion process. The H_{RF} and LPF filter responses of the BPF-D/C ChRx are identical to those illustrated in Fig. 4.1 and Fig. 4.2 for the D/C ChRx, respectively. Figure 4.4 shows the magnitude and phase response of a representative 250 MHz BPF channel. The signal characteristics of the ultra wideband signal at the output of the BPFs are illustrated in Fig. 4.5, where the bandwidth of each channel is 1 GHz.

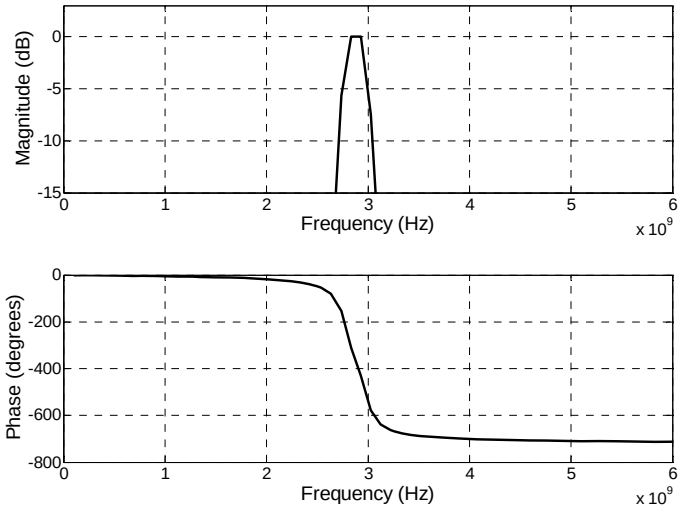

Figure 4.4 Magnitude and phase response of a 250 MHz BPF channel

The output of each LPF is passed to its respective A/D converter and all outputs are processed collectively. Fig. 4.6 illustrates the channelized signal sampled over an observation interval at the D/C ChRx output. Channel bandwidths of 1 GHz that span the total bandwidth of interest are shown.

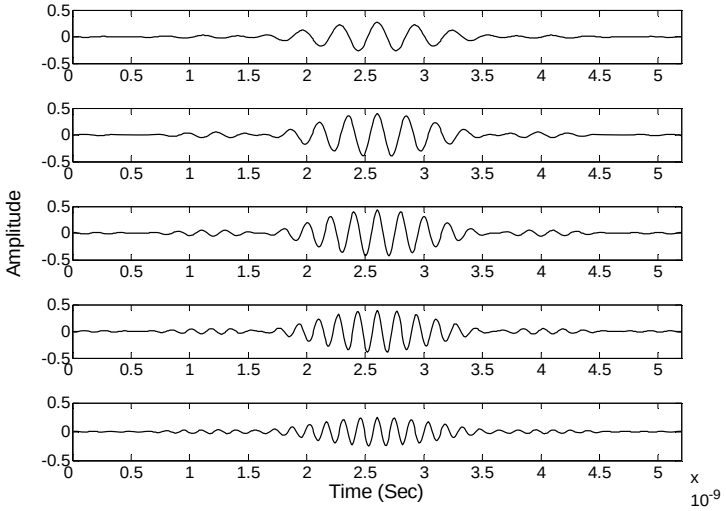

Figure 4.5 Channelized data for BPF-D/C channelized receiver with a channel bandwidth of 1 GHz and a received UWB signal

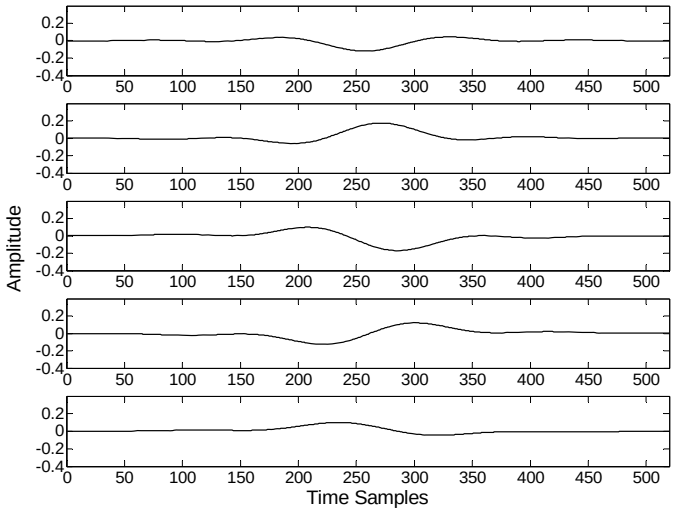

Figure 4.6 Channelized data matrix (CDM) for a BPF-D/C channelized receiver with a channel bandwidth of 1 GHz and a received UWB signal

4.3 Down-Converting Channelized Receiver Detection Performance

As stated in Chapter 2, D/C ChRx threshold detection is performed using each of the four processed channelized data matrices (TTM, CTM, SSM, and CSM) examined in Section 2.5. In this section, detection results of each processed data matrix are set for $P_{FA} = 10^{-2}$ using the received UWB signal shown in Fig. 2.1. These results are compared with probability of detection results from a radiometer. Results observed in [8] were supported in [19] and are extended in this work.

4.3.1 Down-Converting Temporal-Temporal Matrix (TTM) Detection. Probability of detection (P_D) results are shown in Fig. 4.7 for a D/C ChRx with $M = 20$, 250 MHz channels, and two different numbers of IFFT points (N_{ifft}) used to form the TTM. The initial mixer phase value is held constant at 0 degrees for these results. As shown, detection performance remains approximately the same for all N_{ifft} values. A limit for best performance is given in [8, 19] and supported by additional TTM D/C ChRx results in Appendix A. Best performance is achieved when N_{ifft} is greater than twice the number of channelized receiver channels, or $N_{ifft} > 2M$.

Detection performance response due to variation in the initial down-conversion mixer phase value is considered next. As in [8, 19], the initial phase values of all mixers are set equal at the start of the observation interval and are subsequently varied to generate the results in Fig. 4.8, where the signal-to-noise ratio (SNR) is held constant at $SNR = 0\ dB$. Radiometric performance for the UWB pulse at $SNR = 0\ dB$ is approximately $P_D = 0.9$ as shown in Fig. 4.7. Data shown in Fig. 4.8 suggest that detection using TTM data *can* outperform the radiometer using a 500 MHz channel

bandwidth and a few specific phase values. However, the TTM process outperforms the radiometer across all initial phase values using the 250 MHz channel bandwidth.

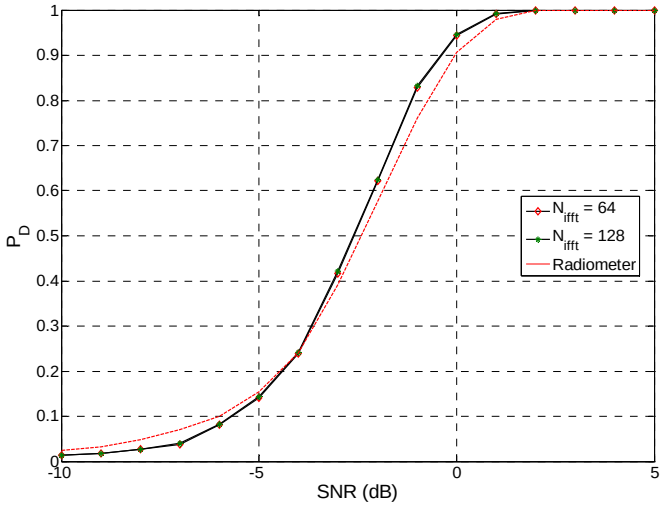

Figure 4.7 TTM detection performance for a down-converting channelized receiver (D/C ChRx) with M = 20, 250 MHz channels and varying number of IFFT points [19]

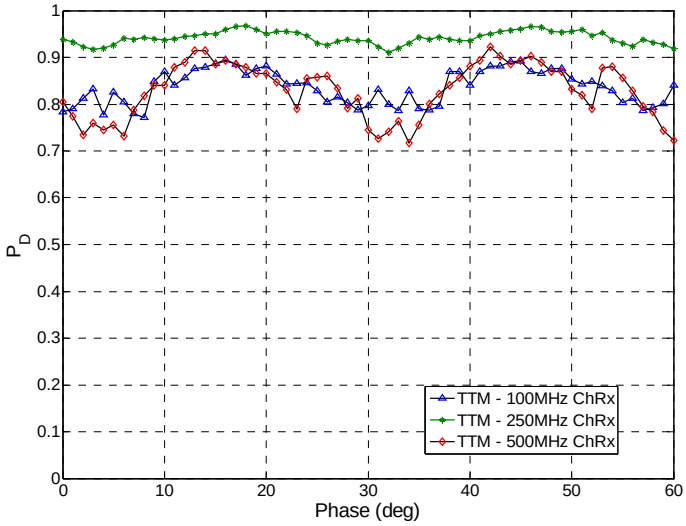

Figure 4.8 TTM detection performance versus mixer phase for a down-converting channelized receiver using *SNR* = 0 dB with varying channel bandwidth [19]

4.3.2 Down-Converting Cross Temporal Matrix (CTM) Detection. Probability of detection (P_D) results are shown in Fig. 4.9 for a D/C ChRx with $M = 20$, 250 MHz channels, and two different number of IFFT points (N_{ifft}) used to form the CTM from the corresponding TTM. The initial mixer phase value was held constant at 0 degrees for these results. As shown, detection performance remains approximately the same for all N_{ifft} values considered. As in the TTM, a limit for best performance is given in [8, 19] and supported by additional CTM D/C ChRx results in Appendix A. Best performance is achieved when N_{ifft} is greater than twice the number of channelized receiver channels, or $N_{ifft} > 2M$.

Detection performance response due to variation in the initial down-conversion mixer phase value is considered next. As in [8, 19], the initial phase values of all mixers are set equal at the start of the observation interval and subsequently varied to generate results shown in Fig. 4.10, and the signal-to-noise ratio (SNR) is held constant at $SNR = 0\ dB$. The radiometric detection performance of the UWB pulse at $SNR = 0\ dB$ is approximately $P_D = 0.9$ as shown in Fig. 4.9. Data in Fig. 4.10 suggest that detection using CTM data outperforms the radiometer using both the 500 MHz and 250 MHz channel bandwidths across all initial phase values.

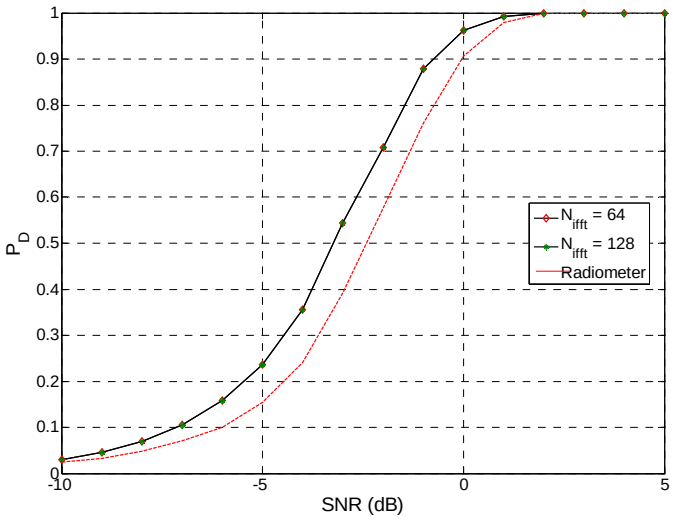

Figure 4.9 CTM detection performance for a down-converting channelized receiver (D/C ChRx) with $M = 20$, 250 MHz channels and varying number of IFFT points [19]

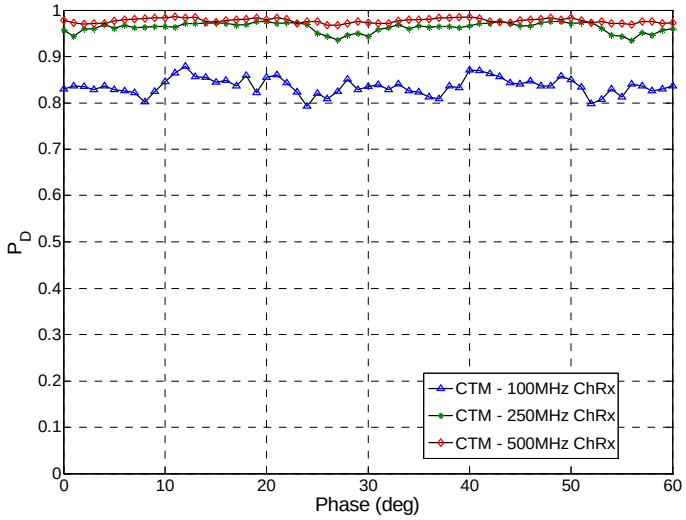

Figure 4.10 CTM detection performance versus mixer phase for a D/C channelized receiver using SNR = 0 dB with varying channel bandwidth [19]

4.3.3 Down-Converting Spectral-Spectral Matrix (SSM) Detection. Probability of detection (P_D) results are shown in Fig. 4.11 for a D/C ChRx with $M = 20$, 250 MHz channels, and two different number of FFT points (N_{fft}) used to form the SSM. The initial mixer phase value is held constant at 0 degrees for these results. As shown, detection performance remains approximately the same for all N_{fft} values considered. This conclusion is supported by results in Fig. 4.11 and additional SSM D/C ChRx results presented in Appendix A.

Detection performance response due to variation in the initial down-conversion mixer phase value is considered next. As in [8, 19], the initial phase values of all mixers are set equal at the start of the observation interval and are subsequently varied to generate results in Fig. 4.12, where the signal-to-noise ratio (SNR) is held constant at $SNR = 0\ dB$. For the same SNR, radiometric performance is approximately $P_D = 0.9$ as

shown in Fig. 4.11. Data in Fig. 4.12 show that D/C SSM detection performance is much poorer than radiometric detection for all channel bandwidths considered.

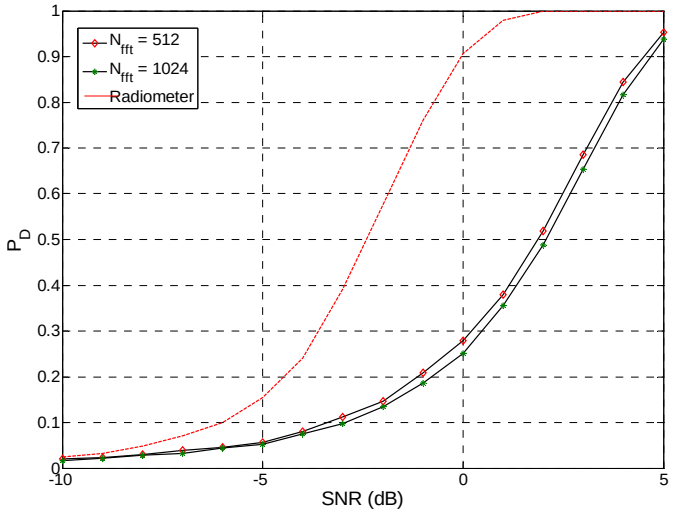

Figure 4.11 SSM detection performance for a D/C channelized receiver (D/C ChRx) with $M = 20$, 250 MHz channels and varying number of FFT points [19]

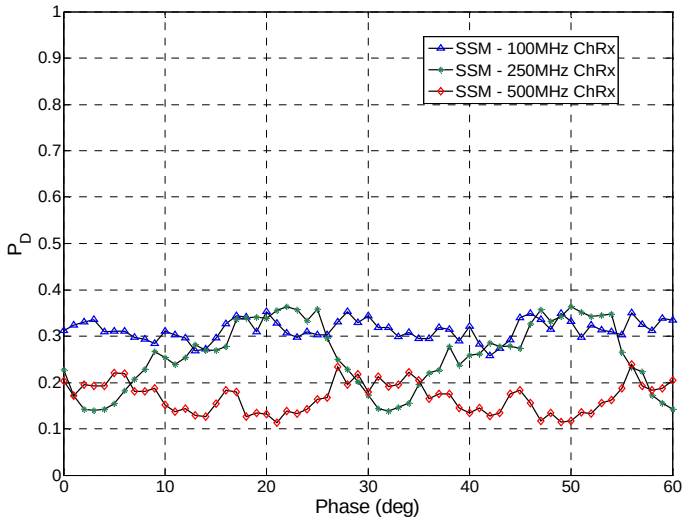

Figure 4.12 SSM detection performance versus mixer phase for a D/C channelized receiver using $SNR = 0$ dB with varying channel bandwidth [19]

4.3.4 Down-Converting Cross Spectral Matrix (CSM) Detection. Probability of detection (P_D) results are shown in Fig. 4.13 for a D/C ChRx with $M = 20$, 250 MHz channels, and two different number of FFT points (N_{fft}) used to form the CSM from the corresponding SSM. The initial mixer phase value is held constant at 0 degrees for these results. As shown, detection performance remains approximately the same for all N_{fft} values considered. This conclusion is supported by results in Fig. 4.13 and additional CSM D/C ChRx results presented in Appendix A.

Detection performance response due to variation in the initial down-conversion mixer phase value is considered next. As in [8, 19], the initial phase values of all mixers are set equal at the start of the observation interval and subsequently varied to generate results in Fig. 4.14, and the signal-to-noise ratio (SNR) is held constant at $SNR = 0\ dB$. Radiometric performance at $SNR = 0\ dB$ is approximately $P_D = 0.9$ as shown in Fig. 4.13. Data in Fig. 4.14 show that D/C SSM detection performance is poorer than radiometric detection for all channel bandwidths considered.

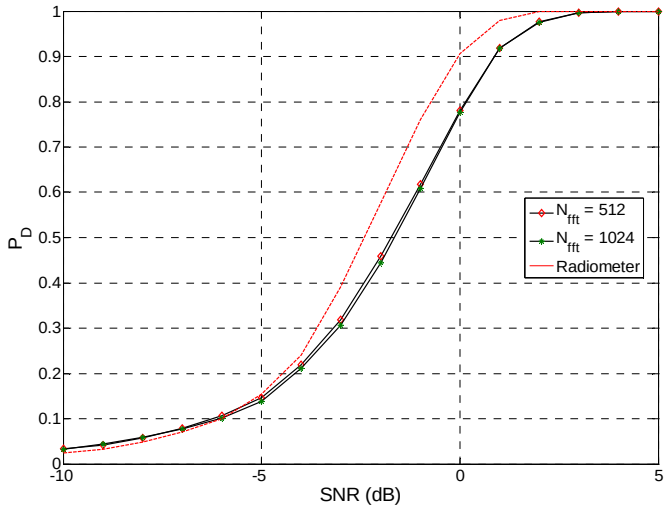

Figure 4.13 CSM detection performance for a D/C channelized receiver (D/C ChRx) with $M = 20$, 250 MHz channels and varying number of FFT points [19]

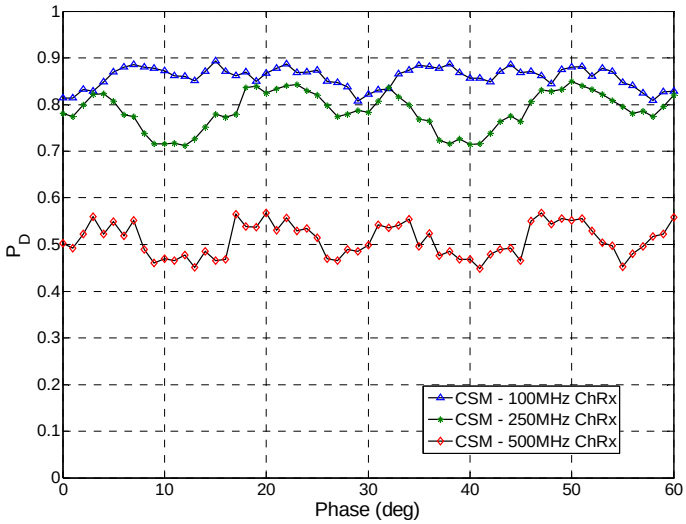

Figure 4.14 CSM detection performance versus mixer phase for a D/C channelized receiver using $SNR = 0$ dB with varying channel bandwidth [19]

4.4 Bandpass Filtered, Down-Converting Channelized Receiver Detection Performance – UWB Results

As stated in Chapter 3, BPF-D/C ChRx threshold detection is performed using each of the four processed channelized data matrices (TTM, CTM, SSM, and CSM) examined in Section 2.5. For comparison between receiver architectures, the total observation interval (T_{obs}) used for processing in the BPF-D/C ChRx is the same as that employed in D/C ChRx processing. In this section, detection results of each processed data matrix are set for $P_{FA} = 10^{-2}$ using the received UWB signal shown in Fig. 2.1. These results are compared with probability of detection results for a radiometer.

4.4.1 BPF Down-Converting Temporal-Temporal Matrix (TTM) Detection. Probability of detection (P_D) results are shown in Fig. 4.15 for a BPF-D/C ChRx with $M = 20$, 250 MHz channels, and a varying number of IFFT points (N_{ifft}) used to form the TTM. The initial mixer phase value is held constant at 0 degrees. As shown, detection performance remains approximately the same for all N_{ifft} values. A limit for best performance is given in [8, 19] and supported by additional TTM BPF-D/C ChRx results in Appendix A. Best performance is achieved when N_{ifft} becomes greater than twice the number of channelized receiver channels, or $N_{ifft} > 2M$.

Detection performance response due to variation in the initial down-conversion mixer phase value is considered next. As in [8, 19], the initial phase values of all mixers are set equal at the start of the observation interval and subsequently varied to generate the results in Fig. 4.16. The signal-to-noise ratio (SNR) is held constant at $SNR = 0\ dB$

for these results, and the number of IFFT points is set at $N_{ifft} = 64$. For the same SNR, radiometric performance is approximately $P_D = 0.9$, as shown in Fig. 4.15. Data shown in Fig. 4.16 suggest that detection using TTM *can* outperform the radiometer when using the 250 MHz channel bandwidth. The 100 MHz channel bandwidth performs much poorer than other channel bandwidths, which may be due to a 'spreading effect' found in TTM processing that is more evident in the BPF-D/C ChRx than in the D/C ChRx. This 'spreading effect' reduces the maximum value of the processed matrix, which may not be detected when compared with the threshold set for a constant false alarm rate (CFAR) of 10^{-2}.

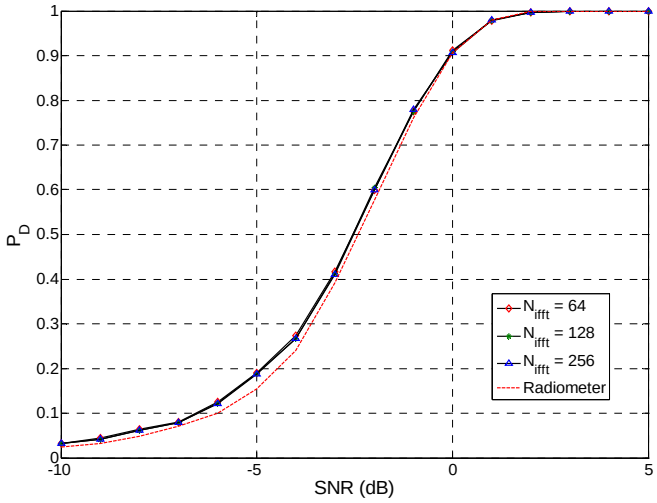

Figure 4.15 TTM detection performance for a BPF-D/C channelized receiver with M = 20, 250 MHz channels and varying number of IFFT points

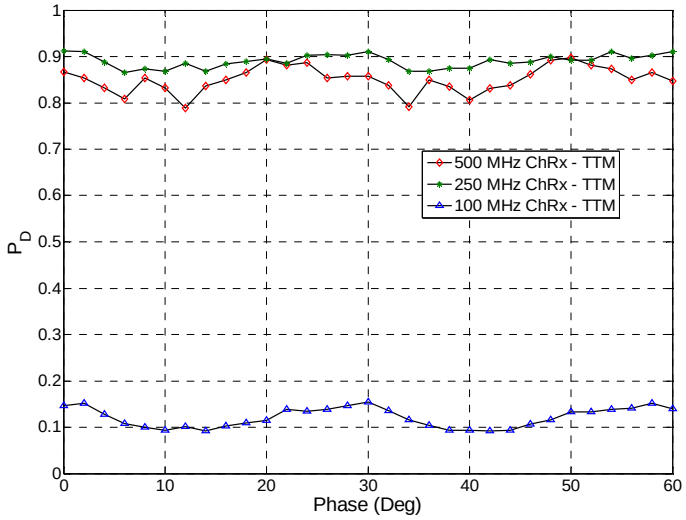

Figure 4.16 TTM detection performance versus mixer phase for a BPF-D/C channelized receiver using *SNR* = 0 dB with varying channel bandwidth

4.4.2 BPF Down-Converting Cross Temporal Matrix (CTM) Detection. Probability of detection (P_D) results are shown in Fig. 4.17 for a BPF-D/C ChRx with $M = 20$, 250 MHz channels, and a varying number of IFFT points (N_{ifft}) used to form the CTM from the corresponding TTM. The initial mixer phase value was held constant at 0 degrees for these results. As shown, detection performance remains approximately the same for all N_{ifft} values considered. A limit for best performance is given in [8, 19] and supported by additional CTM BPF-D/C ChRx results presented in Appendix A. Best performance is achieved when N_{ifft} is greater than twice the number of channelized receiver channels, or $N_{ifft} > 2M$.

Detection performance response due to variation in the initial down-conversion mixer phase value is considered next. As in [8, 19], the initial phase values of all mixers are set equal at the start of the observation interval and subsequently varied to generate

results in Fig. 4.18. The signal-to-noise ratio (SNR) is held constant at $SNR = 0\ dB$ for these results, and the number of IFFT points is set at $N_{ifft} = 64$. Radiometric performance at $SNR = 0\ dB$ is approximately $P_D = 0.9$ as shown in Fig. 4.17. Data in Fig. 4.18 suggest that detection using CTM processing outperforms the radiometer when employing the 500 MHz channel bandwidth. The 100 MHz channel bandwidth performs much poorer than other channel bandwidths due to the 'spreading effect' in the observation interval briefly discussed in Section 4.4.1.

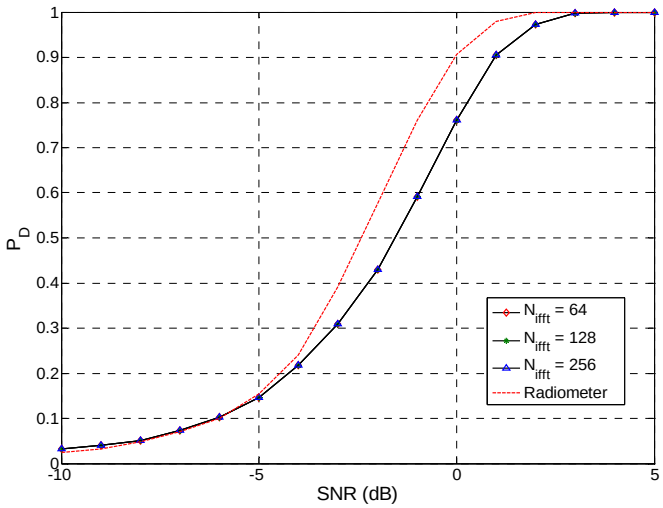

Figure 4.17 CTM detection performance for a BPF-D/C channelized receiver with $M = 20$, 250 MHz channels and varying number of IFFT points

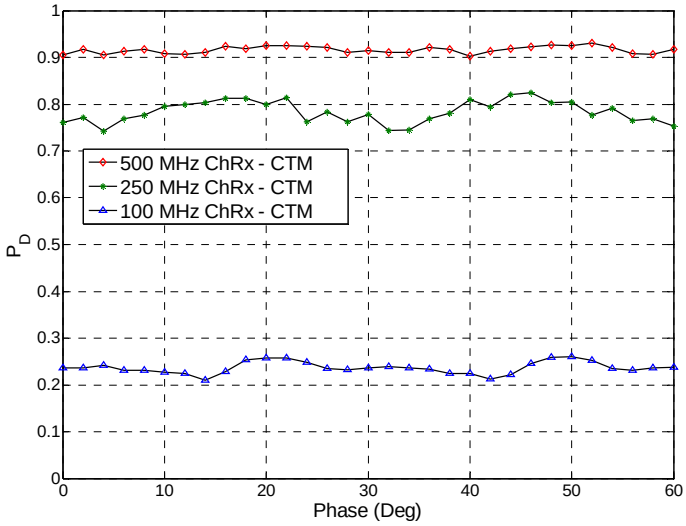

Figure 4.18 CTM detection performance versus mixer phase for a BPF-D/C channelized receiver using SNR = 0 dB with varying channel bandwidth

4.4.3 BPF Down-Converting Spectral-Spectral Matrix (SSM) Detection. Probability of detection (P_D) results are shown in Fig. 4.19 for a BPF-D/C ChRx with $M = 20$, 250 MHz channels, and two different number of FFT points (N_{fft}) used to form the SSM. The initial mixer phase value is held constant at 0 degrees for these results. As shown, detection performance remains approximately the same for all N_{fft} values. This conclusion is supported by results in Fig. 4.19 and additional SSM BPF-D/C ChRx results presented in Appendix A.

Detection performance response due to variation in the initial down-conversion mixer phase value is considered next. As in [8, 19], the initial phase values of all mixers are set equal at the start of the observation interval and subsequently varied to generate results in Fig. 4.20. The signal-to-noise ratio (SNR) is held constant at $SNR = 0\ dB$ for these results, and the number of FFT points is set at $N_{fft} = 512$. Radiometric

performance at $SNR = 0\ dB$ is approximately $P_D = 0.9$ as shown in Fig. 4.19. Data in Fig. 4.20 show that BPF-D/C SSM detection performance is much poorer than radiometric detection for all channel bandwidths considered. The 100 MHz channel bandwidth performs even poorer than the 250 and 500 MHz bandwidths due to the spreaded overall energy in the observation interval over 50 channels. With a decrease in energy per channel, the maximum value of the processed matrix may not be detected when compared with the threshold set for a constant false alarm rate (CFAR) of 10^{-2}.

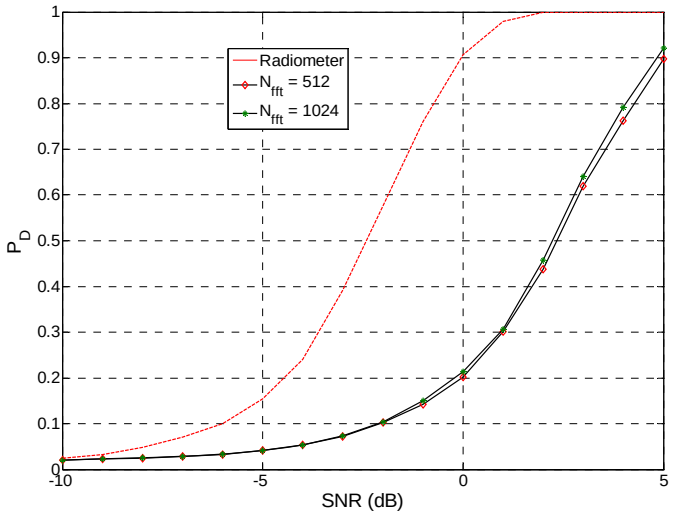

Figure 4.19 SSM detection performance for a BPF-D/C channelized receiver with $M = 20$, 250 MHz channels and varying number of FFT points

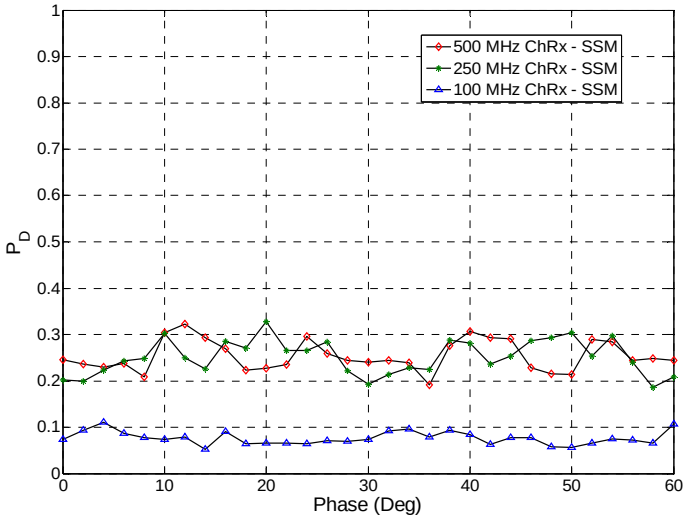

Figure 4.20 SSM detection performance versus mixer phase for a BPF-D/C channelized receiver using $SNR = 0$ dB with varying channel bandwidth

4.4.4 BPF Down-Converting Cross Spectral Matrix (CSM) Detection. Probability of detection (P_D) results are shown in Fig. 4.21 for a BPF-D/C ChRx with $M = 20$, 250 MHz channels, and two different number of FFT points (N_{fft}) used to form the CSM from the corresponding SSM. The initial mixer phase value is held constant at 0 degrees for these results. As shown, detection performance improves slightly with an increase in N_{fft} values. This conclusion is supported by results in Fig. 4.21 and additional CSM BPF-D/C ChRx results presented in Appendix A.

Detection performance response due to variation in the initial down-conversion mixer phase value is considered next. As in [8, 19], the initial phase values of all mixers are set equal at the start of the observation interval and subsequently varied to generate results in Fig. 4.22. The signal-to-noise ratio (SNR) is held constant at $SNR = 0\ dB$ for these results, and the number of FFT points is set at $N_{fft} = 512$. Radiometric

performance at $SNR = 0\ dB$ is approximately $P_D = 0.9$ as shown in Fig. 4.21. Data in Fig. 4.22 shows that D/C SSM detection performance is poorer than radiometric detection for all channel bandwidths considered. The 100 MHz channel bandwidth performs much poorer than other channel bandwidths, as explained briefly in Section 4.4.3.

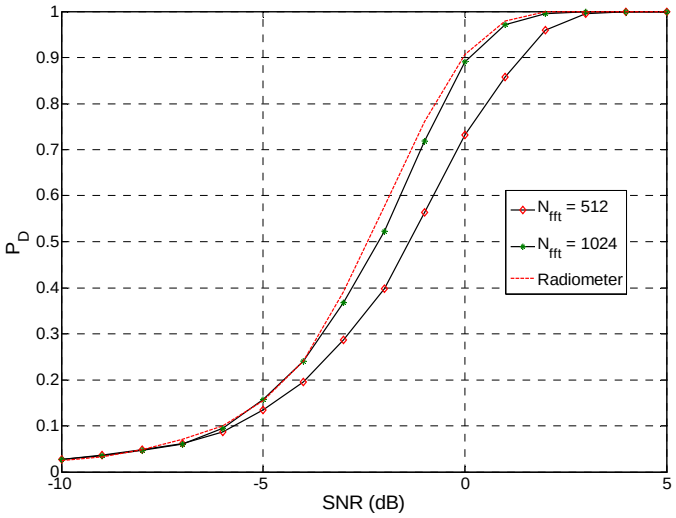

Figure 4.21 CSM detection performance for a BPF-D/C channelized receiver with $M = 20$, 250 MHz channels and varying number of FFT points

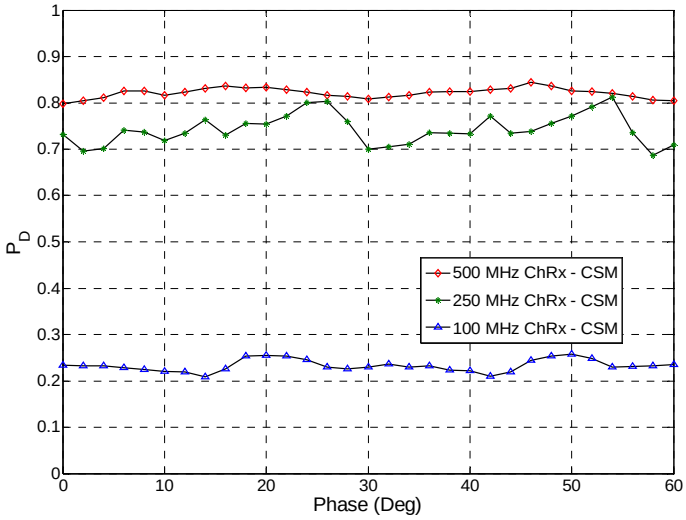

Figure 4.22 CSM detection performance versus mixer phase for a BPF-D/C channelized receiver using SNR = 0 dB with varying channel bandwidth

4.5 Comparative Performance Summary – UWB Results

The detection performance results of the down-converting (D/C) and bandpass filtered down-converting (BPF-D/C) channelized receivers are now compared with a received UWB pulse. Parameters compared for the different detection processes (TTM, CTM, SSM and CSM) include:

- Number of IFFT (N_{ifft}) and FFT (N_{fft}) points used to generate data
- Channel bandwidth selection
- Mixer initial phase value

4.5.1 Temporal-Temporal matrix (TTM) Processing Results

- N_{fft} / N_{ifft} variation – Performance detection results are approximately the same for both receivers and all values of N_{ifft} considered.
- Channel bandwidth – Results in Fig. 4.8 (D/C) and Fig. 4.16 (BPF-D/C) indicate that the 250 MHz channel bandwidth outperforms the 500 and 100 MHz channel

bandwidths for both receivers. The 250 MHz channel bandwidth for the D/C ChRx outperforms the radiometric detector for all phase values. In addition, the D/C ChRx outperforms the BPF-D/C ChRx for both the 100 and 250 MHz channel bandwidths.

- Mixer initial phase values – Results in Fig. 4.8 (D/C) show that the 250 MHz channel bandwidth case exceeds radiometric detection performance for *all* initial phase values considered. By contrast, results in Fig. 4.16 (BPF-D/C) show that the 250 MHz channel bandwidth only outperforms radiometric detection at a few phase values. Depending on mixer phase, the BPF-D/C ChRx *can* outperform the D/C ChRx when employing the 500 MHz bandwidth.

4.5 2 Cross Temporal Matrix (CTM) Processing Results

- N_{fft} / N_{ifft} variation – Performance detection results are approximately the same for both receivers and all values of N_{ifft} considered.
- Channel bandwidth – Results in Fig. 4.10 (D/C) show that both the 250 and 500 MHz channel bandwidths outperform the 100 MHz channel bandwidth. In Fig. 4.18 (BPF-D/C) the 500 MHz channel bandwidth outperforms both the 250 MHz and 100 MHz channel bandwidths. Overall, the D/C ChRx outperforms the BPF-D/C ChRx for all channel bandwidths considered.
- Mixer initial phase value – Results in Fig. 4.10 (D/C) show that both the 250 MHz and 500 MHz channel bandwidths outperform radiometric detection across all initial phase values. Results in Fig. 4.18 (BPF-D/C) show that only the 500 MHz channel bandwidth outperforms radiometric detection for all initial phase

values. Overall, the D/C ChRx outperforms the BPF-D/C ChRx over all initial mixer phase values.

4.5.3 Spectral-Spectral Matrix (SSM) Processing Results

- N_{fft} / N_{ifft} variation – Performance detection results are approximately the same for both receivers and all values of N_{fft} considered.
- Channel bandwidth – Results in Fig. 4.12 (D/C) show that the 100 MHz channel bandwidth outperforms the 500 MHz channel bandwidth. Results in Fig. 4.20 (BPF-D/C) show that both the 250 MHz and 500 MHz channel bandwidths outperform the 100 MHz channel bandwidth. Overall, the BPF-D/C ChRx outperforms the D/C ChRx for the 500 MHz channel bandwidth and performs poorer than the D/C ChRx for the 100 MHz channel bandwidth.
- Mixer initial phase value – Results in Fig. 4.12 (D/C) and Fig. 4.20 (BPF-D/C) show that detection performance is much poorer than radiometric detection across all initial phase values. Depending on mixer phase, the BPF-D/C ChRx *can* outperform the D/C ChRx when employing the 250 MHz channel bandwidth.

4.5.4 Cross Spectral Matrix (CSM) Processing Results

- N_{fft} / N_{ifft} variation – Performance detection results for the D/C ChRx are approximately the same for all values of N_{fft} considered. For the BPF-D/C ChRx, performance detection improves slightly with an increase in N_{fft}.
- Channel bandwidth – Results in Fig. 4.14 (D/C) show that both the 100 MHz and 250 MHz channel bandwidths outperform the 500 MHz channel bandwidth. Results in Fig. 4.22 (BPF-D/C) show that the 250 MHz and 500 MHz channel bandwidths outperform the 100 MHz channel bandwidth. Overall, the BPF-D/C

ChRx outperforms the D/C ChRx for the 500 MHz channel bandwidth and performs poorer than the D/C ChRx when employing the 100 MHz channel bandwidth.

- Mixer initial phase value – Results in Fig. 4.14 and Fig. 4.22 show that detection performance is much poorer than radiometric detection across all initial phase values. Depending on mixer phase, the BPF-D/C ChRx *can* outperform the D/C ChRx when employing the 250 MHz channel bandwidth.

4.6 Bandpass Filtered, Down-Converting Channelized Receiver Detection Performance – DSSS Waveform Results

As stated in Chapter 3, BPF-D/C ChRx detection is implemented by performing threshold detection on the processed channelized data matrices (TTM, CTM, SSM, and CSM) examined in Section 2.5. In this section, detection results of each processed data matrix are set for $P_{FA} = 10^{-2}$ using the received DSSS signal shown in Fig. 2.4. These results are compared with probability of detection results for a radiometer.

4.6.1 BPF Down-Converting Temporal-Temporal Matrix (TTM) Detection. Probability of detection (P_D) results are shown in Fig. 4.23 for a BPF-D/C ChRx with $M = 20$, 250 MHz channels, and a varying number of IFFT points (N_{ifft}) used to form the TTM. The initial mixer phase value is held constant at 0 degrees for these results. As shown, detection performance remains approximately the same for all N_{ifft} values. A limit for best performance is given in [8, 19] and supported by additional TTM BPF-D/C

ChRx results presented in Appendix A. Best performance is achieved when N_{ifft} is greater than twice the number of channelized receiver channels, or $N_{ifft} > 2M$.

Detection performance response due to variation in the initial down-conversion mixer phase value is considered next. As in [8, 19], the initial phase values of all mixers are set equal at the start of the observation interval and subsequently varied to generate results in Fig. 4.24. The signal-to-noise ratio (SNR) is held constant at $SNR = 0\ dB$ for these results, and the number of IFFT points is set at $N_{ifft} = 64$. Radiometric performance at $SNR = 0\ dB$ is approximately $P_D = 0.9$ as shown in Fig. 4.23. Data in Fig. 4.24 show that detection using TTM is much poorer than with a radiometer. Detection performance varies most widely when implementing 250 MHz channel bandwidths, and varies minimally with 100 MHz channels.

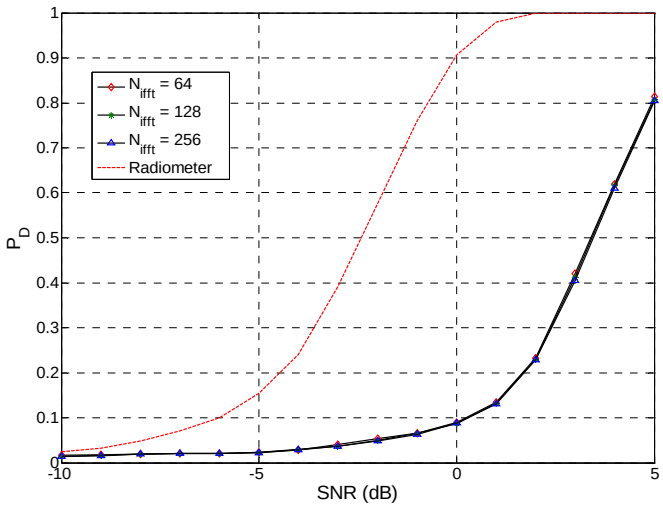

Figure 4.23 DSSS waveform: TTM detection performance for a BPF-D/C channelized receiver with $M = 20$, 250 MHz channels and varying number of IFFT points

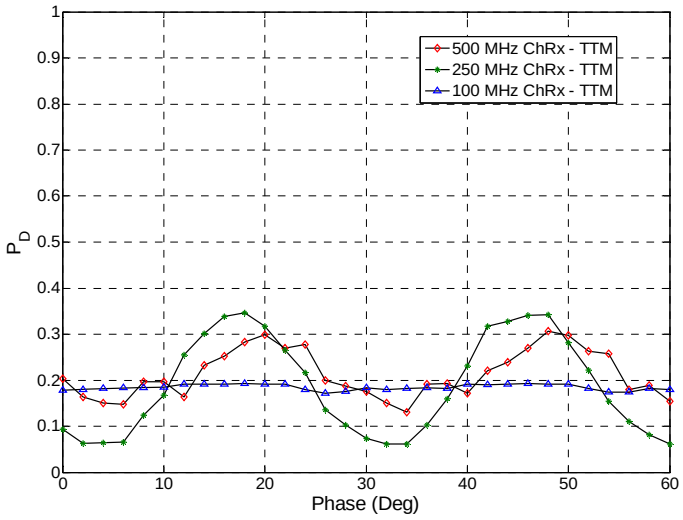

Figure 4.24 DSSS waveform: TTM detection performance versus mixer phase for a BPF-D/C channelized receiver using *SNR* = 0 dB with varying channel bandwidth

4.6.2 BPF Down-Converting Cross Temporal Matrix (CTM) Detection. Probability of detection (P_D) results are shown in Fig. 4.25 for a BPF-D/C ChRx with $M = 20$, 250 MHz channels, and a varying number of IFFT points (N_{ifft}) used to form the CTM from the corresponding TTM. The initial mixer phase value is held constant at 0 degrees for these results. As shown, detection performance remains approximately the same for all N_{ifft} values. A limit for best performance is given in [8, 19] and supported by additional CTM BPF-D/C ChRx results presented in Appendix A. Best performance is achieved when N_{ifft} is greater than twice the number of channelized receiver channels, or $N_{ifft} > 2M$.

Detection performance response due to variation in the initial down-conversion mixer phase value is considered next. As in [8, 19], the initial phase values of all mixers are set equal at the start of the observation interval and subsequently varied to generate

results in Fig. 4.26. The signal-to-noise ratio (SNR) is held constant at $SNR = 0\ dB$ for these results and the number of IFFT points was set at $N_{ifft} = 64$. For the same SNR, radiometric performance is approximately $P_D = 0.9$ as shown in Fig. 4.25. Data in Fig. 4.26 show that detection using CTM is poorer than with a radiometer. Detection performance varies widely in the CTM, with most variation occurring when implementing 250 MHz channel bandwidths. Of the three channel bandwidths considered, the 100 MHz channel has the least variation across initial mixer phases.

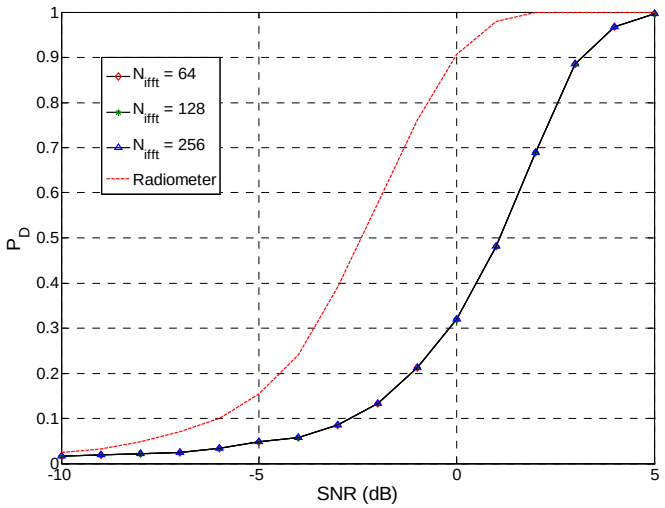

Figure 4.25 DSSS waveform: CTM detection performance for a BPF-D/C channelized receiver with $M = 20$, 250 MHz channels and varying number of IFFT points

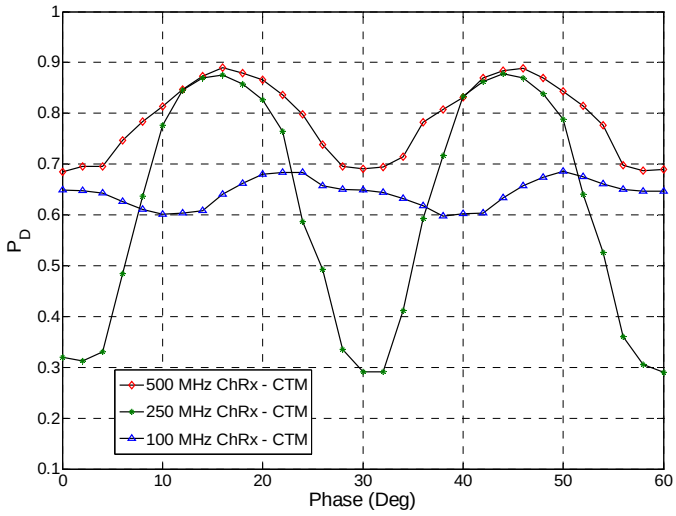

Figure 4.26 DSSS waveform: CTM detection performance versus mixer phase for a BPF-D/C channelized receiver using $SNR = 0$ dB with varying channel bandwidth

4.6.3 BPF Down-Converting Spectral-Spectral Matrix (SSM) Detection. Probability of detection (P_D) results are shown in Fig. 4.19 for a BPF-D/C ChRx with $M = 20$, 250 MHz channels, and two different number of FFT points (N_{fft}) used to form the SSM. The initial mixer phase value is held constant at 0 degrees. As shown, detection performance improves slightly with an increase in N_{fft} values considered. This conclusion is supported by results in Fig. 4.27 and additional SSM BPF-D/C ChRx results presented in Appendix A.

Detection performance response due to variation in the initial down-conversion mixer phase value is considered next. As in [8, 19], the initial phase values of all mixers are set equal at the start of the observation interval and subsequently varied to generate results in Fig. 4.28. The signal-to-noise ratio (SNR) is held constant at $SNR = 0\ dB$ and the number of FFT points is set at $N_{fft} = 512$. Radiometric performance at $SNR = 0\ dB$

is approximately $P_D = 0.9$ as shown in Fig. 4.27. Data in Fig. 4.28 shows that BPF-D/C SSM detection performance is poorer than radiometric detection for all channel bandwidths. Detection performance varies widely in SSM processing, with the most variation occurring in the 250 MHz channel case, followed by the 500 MHz and 100 MHz channel bandwidths, respectively.

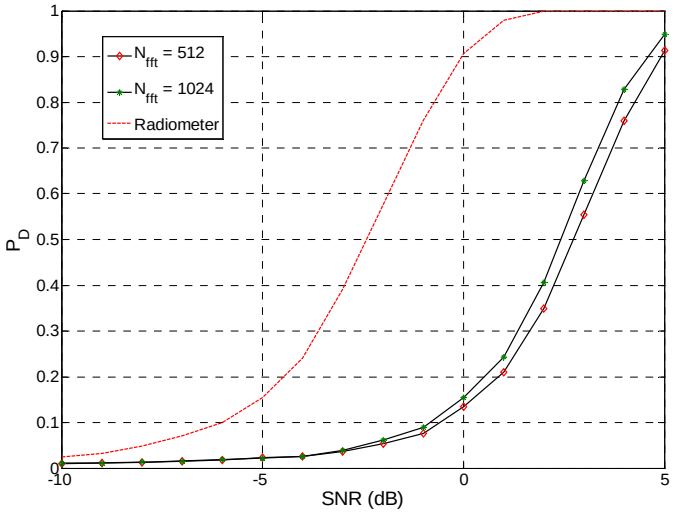

Figure 4.27 DSSS waveform: SSM detection performance for a BPF-D/C channelized receiver with $M = 20$, 250 MHz channels and varying number of FFT points

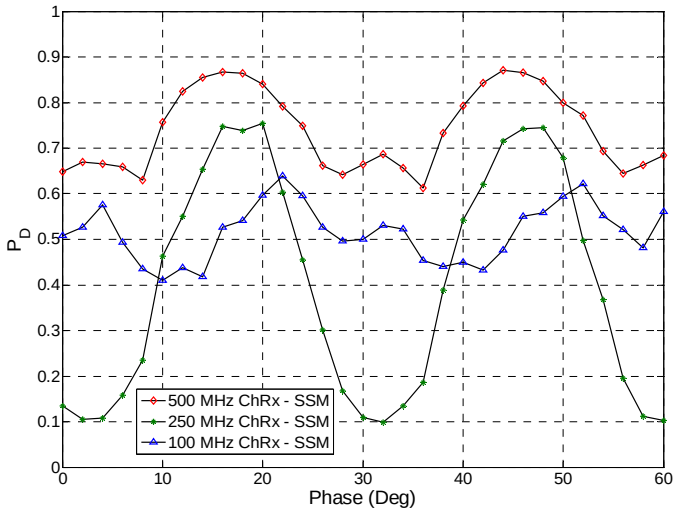

Figure 4.28 DSSS waveform: SSM detection performance versus mixer phase for a BPF-D/C channelized receiver using *SNR* = 0 dB with varying channel bandwidth

4.6.4 BPF Down-Converting Cross Spectral Matrix (CSM) Detection. Probability of detection (P_D) results are shown in Fig. 4.29 for a BPF-D/C ChRx with $M = 20$, 250 MHz channels, and two different number of FFT points (N_{fft}) used to form the CSM from the corresponding SSM. The initial mixer phase value is held constant at 0 degrees for these results. As shown, detection performance improves slightly with an increase in N_{fft}. Other results for the 100 MHz and 500 MHz channel bandwidth cases are presented in Appendix A and show that detection performance remains approximately the same for both N_{fft} values.

Detection performance response due to variation in the initial down-conversion mixer phase value is considered next. As in [8, 19], the initial phase values of all mixers are set equal at the start of the observation interval and subsequently varied to generate results in Fig. 4.30. The signal-to-noise ratio (SNR) is held constant at $SNR = 0\ dB$ for

these results, and the number of FFT points is set at $N_{fft} = 512$. Radiometric performance at $SNR = 0\ dB$ is approximately $P_D = 0.9$ as shown in Fig. 4.29. Data in Fig. 4.30 show that CSM detection performance is poorer than radiometric detection for all channel bandwidths considered. Detection performance varies widely in the 250 MHz channel bandwidth case, with minimal variation in the 100 MHz and 500 MHz channel bandwidth cases.

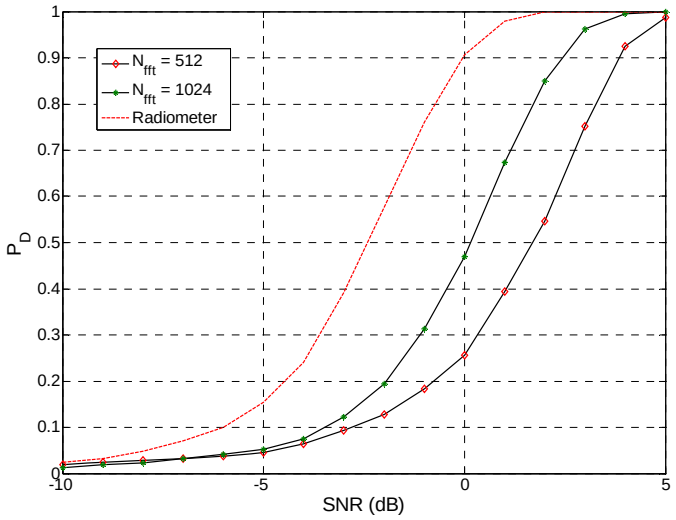

Figure 4.29 DSSS waveform: CSM detection performance for a BPF-D/C channelized receiver with M = 20, 250 MHz channels and varying number of FFT points

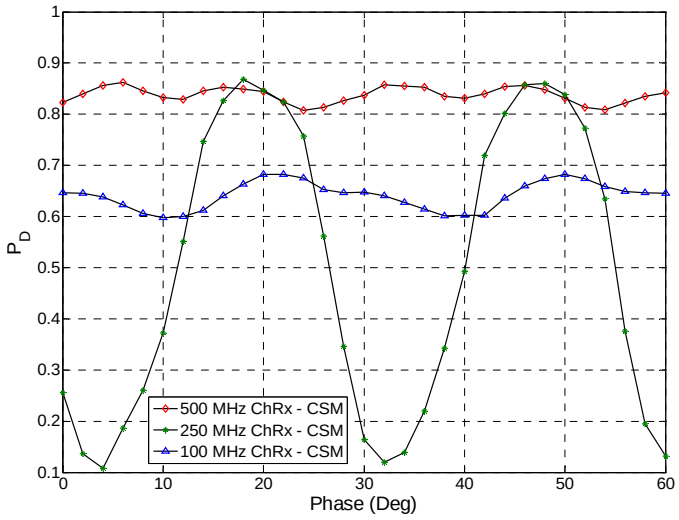

Figure 4.30 DSSS waveform: CSM detection performance versus mixer phase for a BPF-D/C channelized receiver using *SNR* = 0 dB with varying channel bandwidth

4.7 Summary

Filter characterization and detection performance results are provided for the down-converting (D/C) and bandpass filtered down-converting (BPF-D/C) channelized receivers presented in Chapter 2 and Chapter 3. First, the magnitude and phase responses of the Butterworth filters used in the D/C and BPF-D/C ChRx architectures are examined. Then detection performance results using the UWB channelized matrix data (TTM, CTM, SSM, CSM) and techniques introduced in Chapter 2 are presented for both the D/C and BPF-D/C channelized receivers. Finally, detection performance results using the channelized matrix data and processing techniques are presented for the BPF-D/C channelized receiver, where the DSSS waveform is the signal of interest.

V. Conclusions and Recommendations

5.1 Research Summary

The majority of this research involves the introduction and analysis of bandpass filtered down-converting (BPF-D/C) channelized receiver techniques for the detection of ultra wideband (UWB) and direct sequence spread spectrum (DSSS) signals. Detection techniques established in [8] and considered in this work operated on data in the following signal processing matrices: Temporal-Temporal Matrix (TTM), Cross Temporal Matrix (CTM), Spectral-Spectral Matrix (SSM), and Cross Spectral Matrix (CSM). The TTM data is created by implementing an IFFT on columns of the $M \times S$ *Channelized Data Matrix* (CDM), where M is the number of channel filters and S is the number of time samples. The CTM is formed by performing a correlation between all combinations of TTM columns. The SSM is created by implementing an FFT on the rows of the CDM. Finally, the CSM is formed by performing a correlation between all combinations of SSM columns. Threshold detection is performed using each signal processing matrix. Probability of detection (P_D) results are generated for the following varying parameters: received *SNR*, number of IFFT/FFT points used to form the signal processing matrices, receiver channel bandwidth, and initial phase values of down-conversion mixers.

Two other non-cooperative detection receivers, the down-converting (D/C) channelized and the radiometer, are included to permit comparative performance analysis. The performance of the radiometer and D/C channelized receiver are representative of what can be achieved using non-cooperative techniques.

5.2 Research Conclusions

5.2.1 BPF-D/C Channelized Receiver Performance – UWB Results. Detection performance of the BPF-D/C ChRx is compared with that of radiometric and D/C ChRx receiver architectures. Detection performance of the BPF-D/C ChRx using any of the channelized receiver processing techniques is dependent on the initial phase of the down-conversion mixer.

For detection using the TTM, detection performance for the 250 MHz channels outperforms radiometric detection at a few phase values considered. Depending on mixer phase, the BPF-D/C ChRx *can* outperform the D/C ChRx when employing the 500 MHz bandwidth. Detection performance for the CTM generated using 500 MHz channels surpassed radiometric detection for all initial mixer phase values. Detection performance using the SSM is much poorer than radiometric detection across all initial phase values. Depending on initial mixer phase value, the BPF-D/C ChRx outperforms the D/C ChRx when employing the 500 MHz channel bandwidth. The CSM detection performance is much poorer than radiometric detection across all initial phase values. Depending on mixer phase, the BPF-D/C ChRx outperforms the D/C ChRx when employing the 500 MHz channel bandwidth.

Worst case UWB detection results are obtained using the spectrally-based SSM and CSM processing methods, consistent with UWB processing results in [2, 8, 19]. Since UWB pulses are inherently 'featureless' in the spectral domain over a large bandwidth, temporal processing techniques seem to be most promising.

5.2.2 BPF-D/C Channelized Receiver Performance – DSSS Waveform Results. The BPF-D/C ChRx detection performance is compared with radiometric

performance. Detection performance of the down-converting channelized receiver using any of the channelized receiver processing techniques is dependent on the initial phase of the down-conversion mixer.

Using the TTM, detection performance varies most widely when implementing 250 MHz channel bandwidths and varies minimally with 100 MHz channels. Detection performance using TTM is much poorer than with a radiometer across all initial mixer phase values. Detection performance using the CTM is poorer than radiometric detection for all initial mixer phase values. Detection performance varies widely in the CTM, with most variation occurring when implementing 250 MHz channel bandwidths and the least when implementing the 100 MHz channel. For detection using the SSM, detection performance variation varies widely, with the most variation occurring in the 250 MHz channel case, followed by the 500 MHz and 100 MHz channel bandwidths, respectively. Detection performance is poorer with the SSM than in radiometric detection for all initial mixer phase values. Using the CSM, detection performance varies widely in the 250 MHz channel bandwidth case, with minimal variation in the 100 MHz and 500 MHz channel bandwidth cases. Detection performance is poorer in the CSM than in radiometric detection for all initial mixer phase values.

Worst case DSSS detection results are obtained using the TTM processing method. Spectral processing techniques seem to be promising, since spectral variation of the DSSS waveform may be distinguishable. Correlation between columns of the TTM and SSM data matrices (CTM and CSM) also seem to be promising.

Table 1 shows the performance of the D/C ChRx (labeled as D/C) and the BPF-D/C ChRx (labeled as BPF) for each processing technique, both UWB and DSSS signals, and several initial mixer phase values. The D/C ChRx and BPF-D/C ChRx results are compared with the radiometer for $SNR = 0\ dB$. Green values indicate the ChRx outperforming radiometric detection and red values indicate ChRx detection performance poorer than the radiometer.

Table 1. Probability of detection of channelized receivers using 250 MHz channel bandwidths compared to radiometric detection operating at $P_{FA} = 10^{-2}$ and $P_D = 0.9$ (Green = Better, Red = Poorer)

		$\theta_{LO} = 0^o$		$\theta_{LO} = 10^o$		$\theta_{LO} = 20^o$		$\theta_{LO} = 30^o$	
		UWB	**DSSS**	**UWB**	**DSSS**	**UWB**	**DSSS**	**UWB**	**DSSS**
TTM	**D/C**	**0.94**	**N/A**	**0.94**	**N/A**	**0.95**	**N/A**	**0.94**	**N/A**
	BPF	**0.91**	**0.09**	**0.87**	**0.17**	**0.90**	**0.32**	**0.91**	**0.07**
CTM	**D/C**	**0.96**	**N/A**	**0.97**	**N/A**	**0.98**	**N/A**	**0.94**	**N/A**
	BPF	**0.76**	**0.32**	**0.80**	**0.78**	**0.80**	**0.83**	**0.78**	**0.30**
SSM	**D/C**	**0.23**	**N/A**	**0.25**	**N/A**	**0.34**	**N/A**	**0.17**	**N/A**
	BPF	**0.20**	**0.13**	**0.30**	**0.46**	**0.33**	**0.75**	**0.19**	**0.11**
CSM	**D/C**	**0.78**	**N/A**	**0.72**	**N/A**	**0.83**	**N/A**	**0.78**	**N/A**
	BPF	**0.73**	**0.26**	**0.72**	**0.37**	**0.75**	**0.85**	**0.70**	**0.16**

5.3 Recommendations for Future Research

5.3.1 Detection Performance in Spectrally Coexistent Scenarios. This research only considers either a single UWB pulse or DSSS waveform with or without additive white Gaussian noise. As addressed in [2, 19], real-world environments can contain many different signals using different modulation configurations. The down-converting channelized receiver processing techniques presented here could be analyzed in spectrally coexistent scenarios, which could prove to be especially significant as communication technology migrates toward 4G (4^{th} generation) deployment.

5.3.2 Channel Assessment and Pattern Recognition. In some cases, it may be advantageous to perform channel assessment, i.e., identification of type and nature of signals present in an environment. Visual inspection of the processing data matrices (TTM, CTM, SSM and CSM) suggests the possibility of using pattern recognition techniques along with the BPF-D/C channelized receiver processing techniques presented here to make this determination.

Appendix A.

A1. BPF-D/C Channelized Receiver Filter Response

A1.1 Noise Response

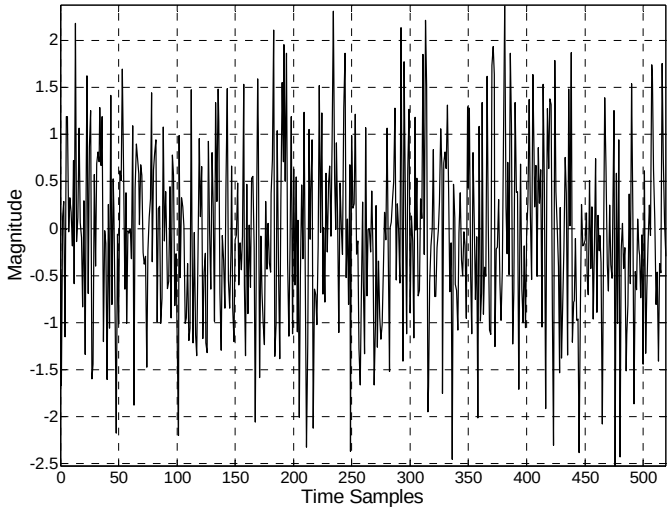

Figure A.1 Received noise realization

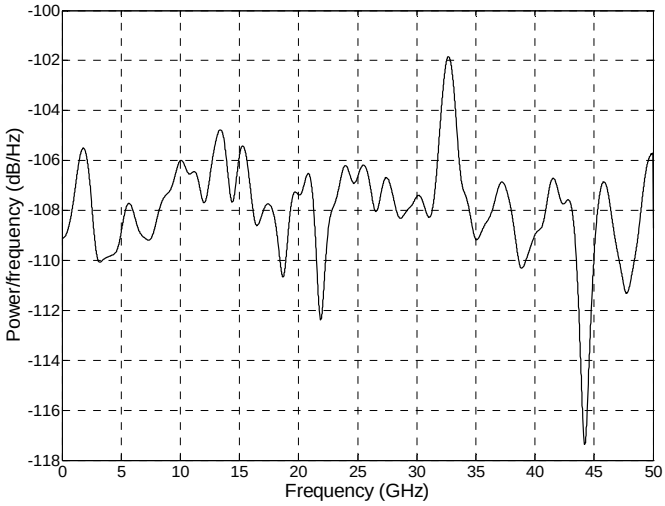

Figure A.2 Received noise realization PSD

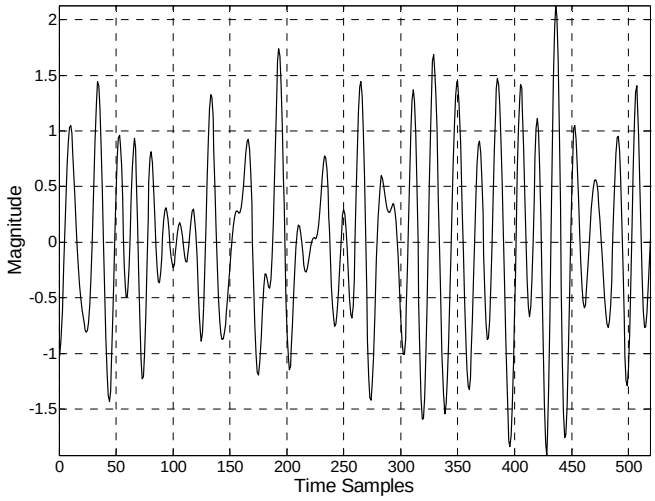

Figure A.3 Received noise realization filtered by H_{RF}

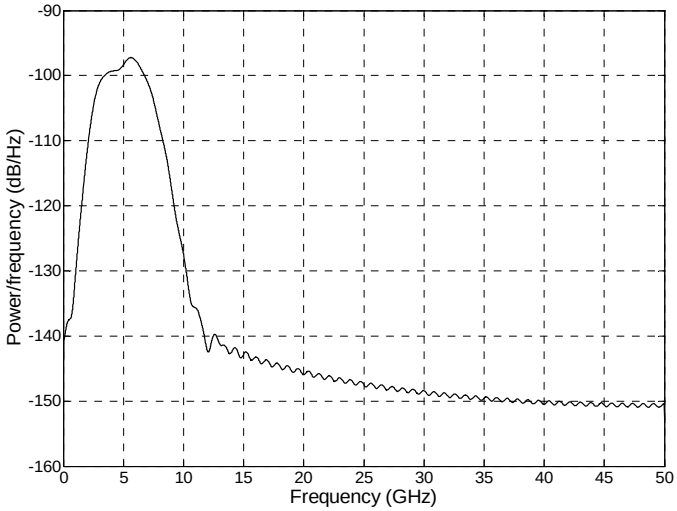

Figure A.4 Received noise realization PSD filtered by H_{RF}

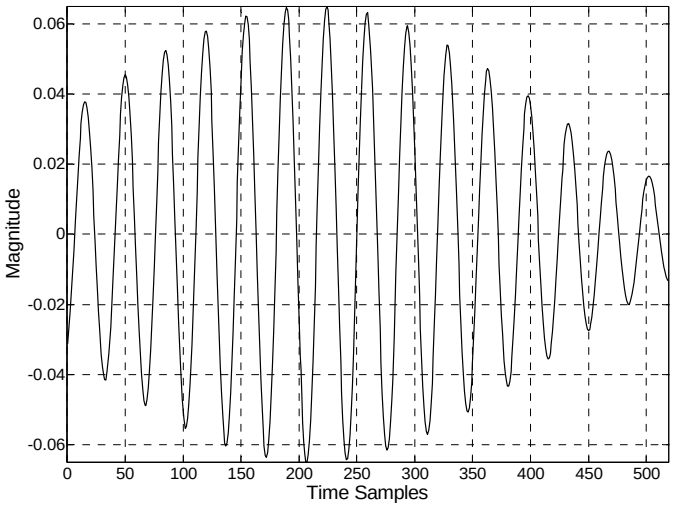

Figure A.5 Received noise realization filtered by a 250 MHz BPF

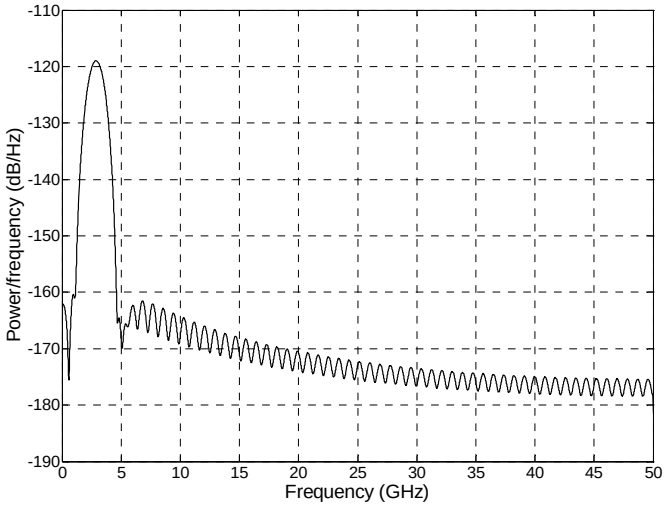

Figure A.6 Received noise realization PSD filtered by a 250 MHz BPF

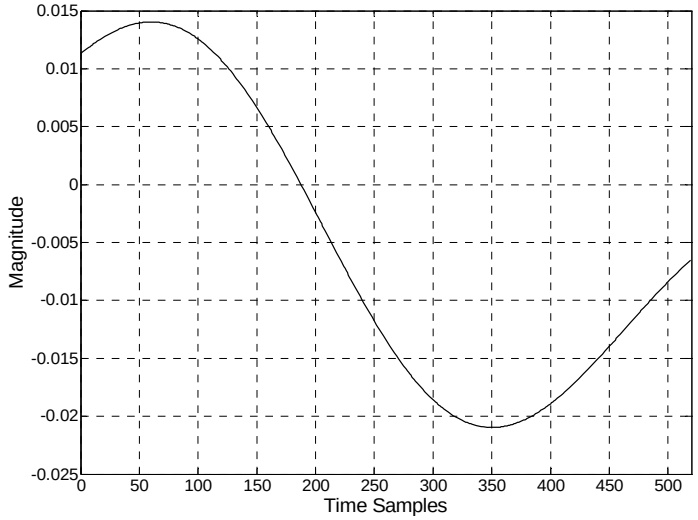

Figure A.7 Down-converted received noise realization

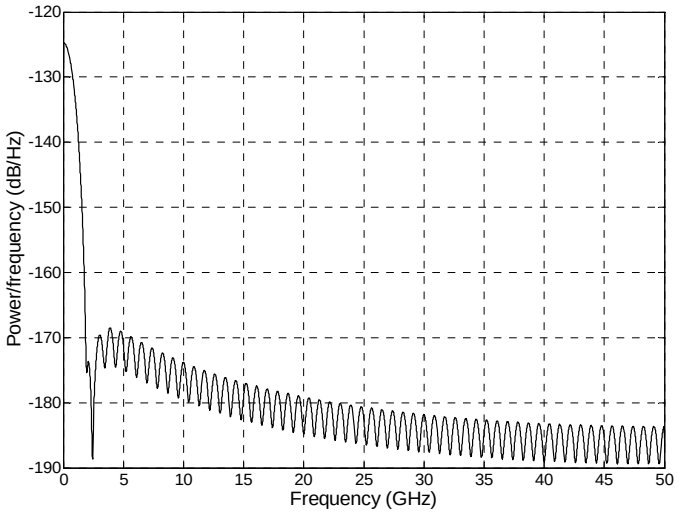

Figure A.8 Down-converted received noise realization PSD

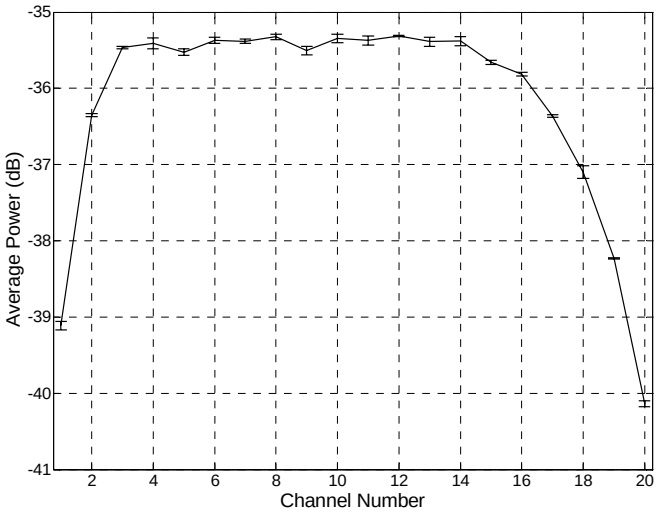

Figure A.9 Noise power deviation over all initial mixer phase values

A1.2 UWB Response

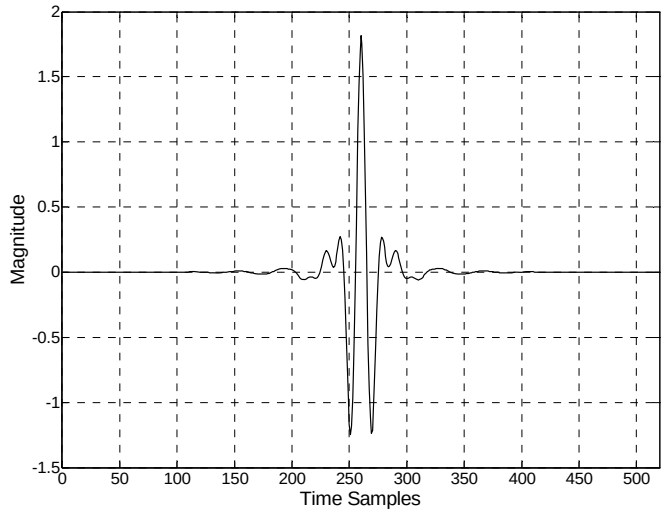

A.10 Received UWB pulse filtered by H_{RF}

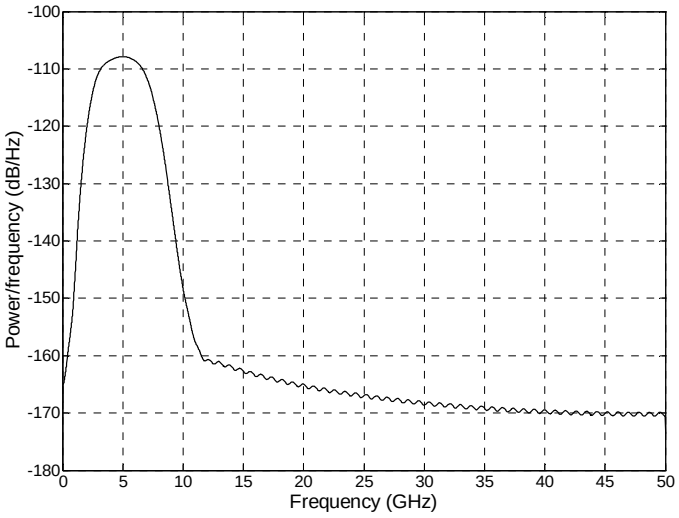

A.11 Received UWB PSD filtered by H_{RF}

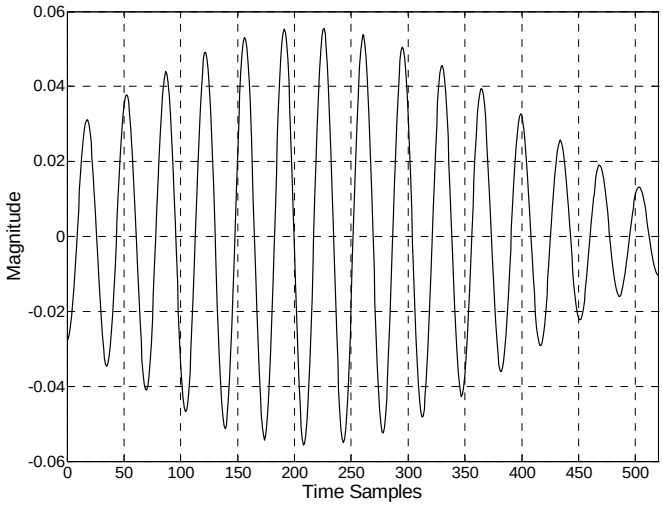

A.12 Received UWB pulse filtered by a 250 MHz BPF

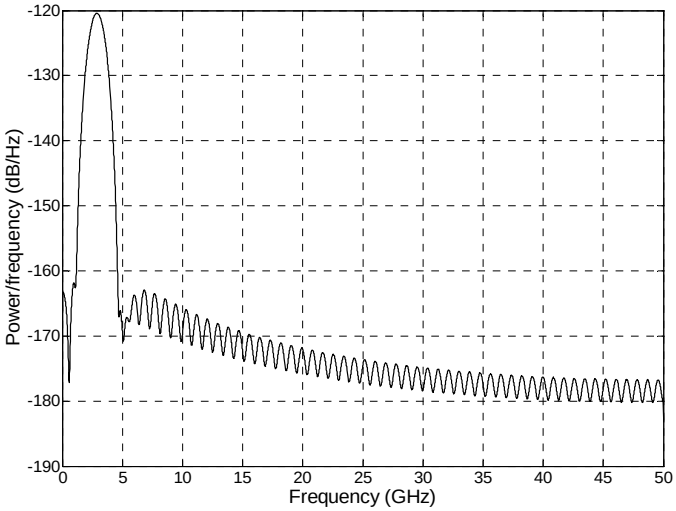

A.13 Received UWB PSD filtered by a 250 MHz BPF

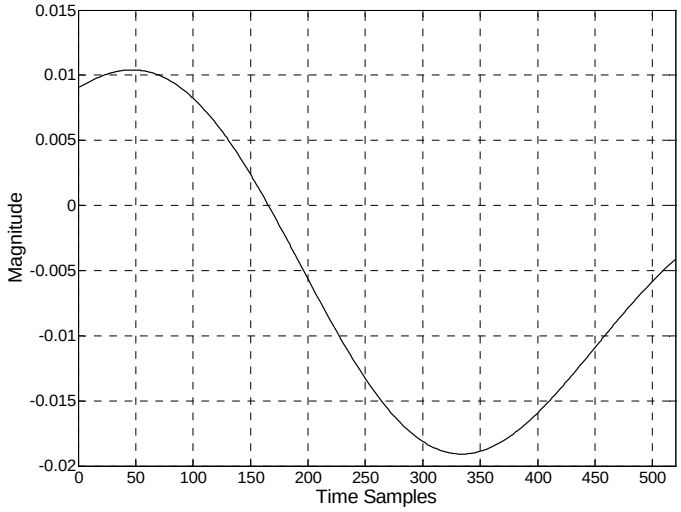

A.14 Down-converted received UWB pulse

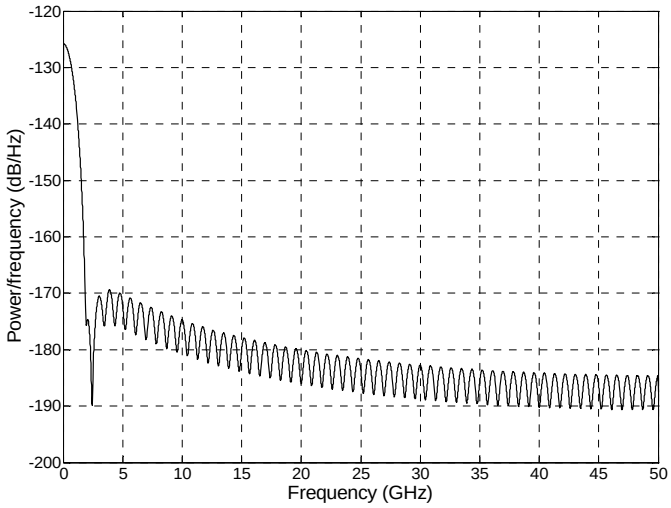

A.15 Down-converted received UWB PSD

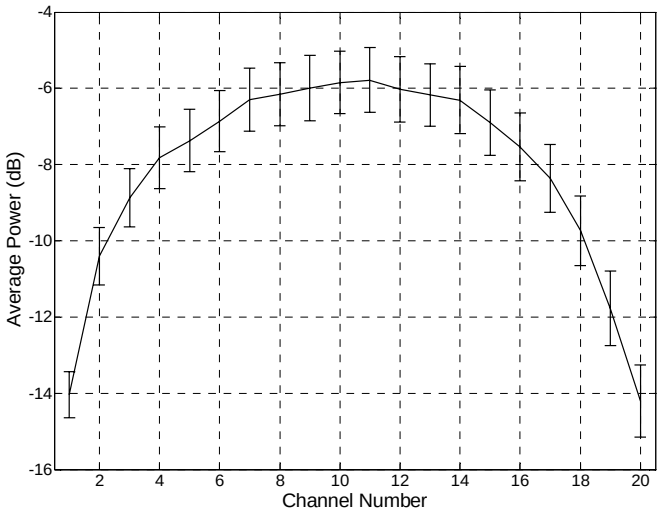

A.16 UWB power deviation over all initial mixer phase values

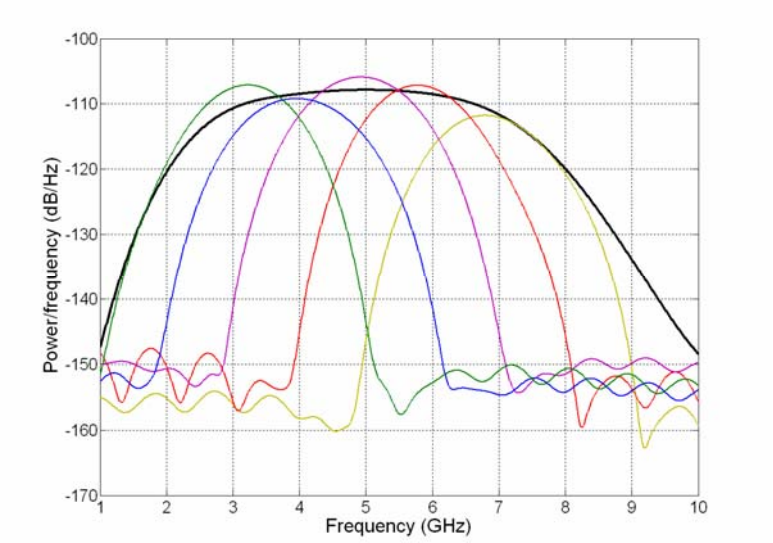

A.17 PSD comparison of H_{RF} and $BPF_{1\text{-}M}$ for UWB using 1 GHz channels

A1.3 DSSS Response

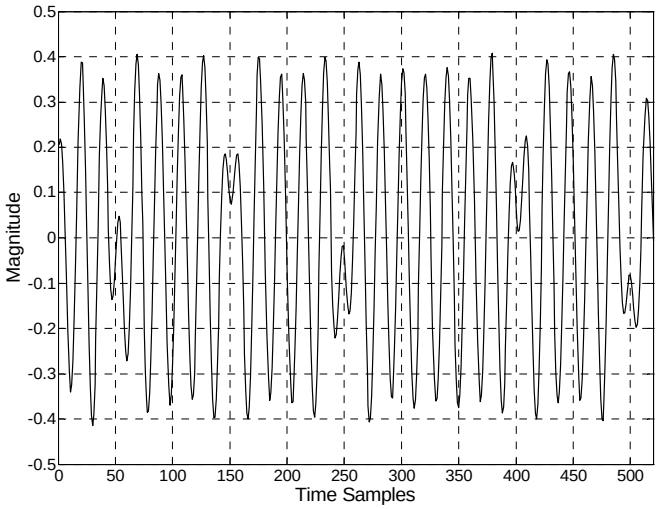

A.18 Received DSSS waveform filtered by H_{RF}

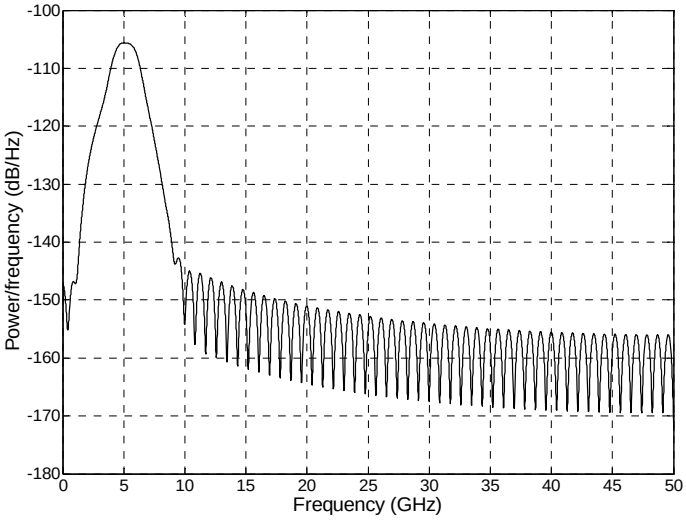

A.19 Received DSSS PSD filtered by H_{RF}

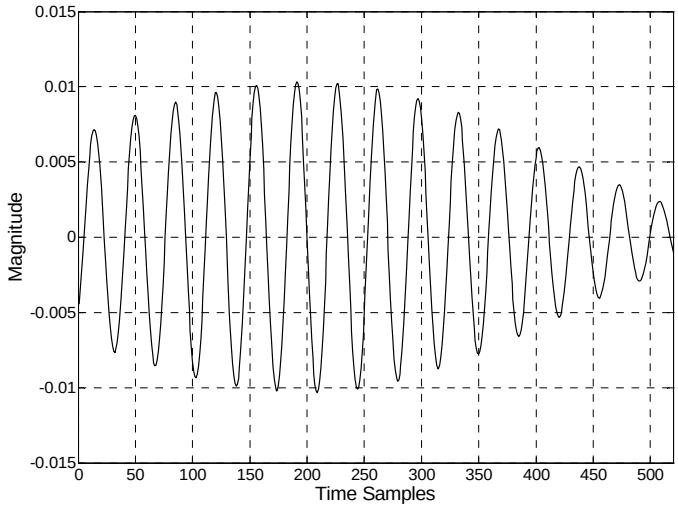

A.20 Received DSSS waveform filtered by a 250 MHz BPF

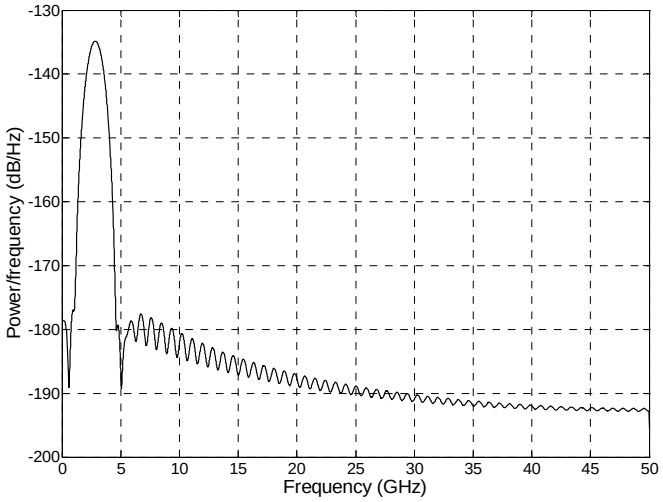

A.21 Received DSSS PSD filtered by a 250 MHz BPF

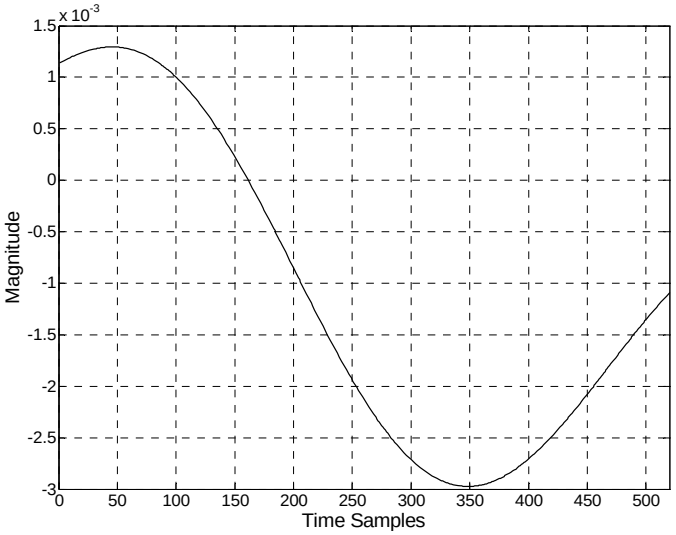

A.22 Down-converted received DSSS waveform

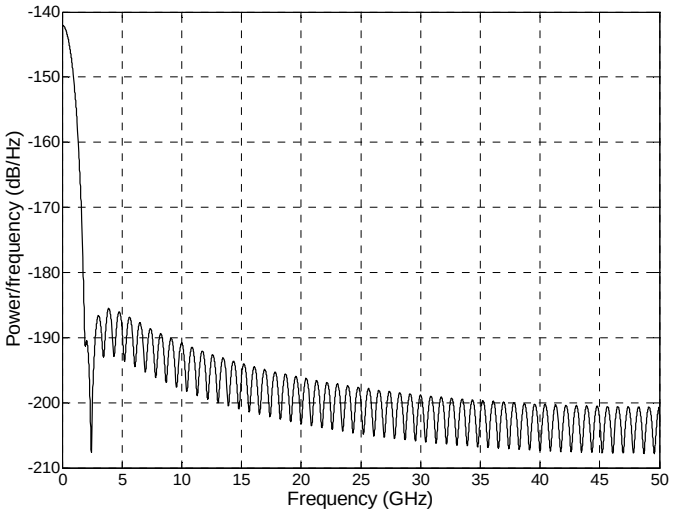

A.23 Down-converted received DSSS PSD

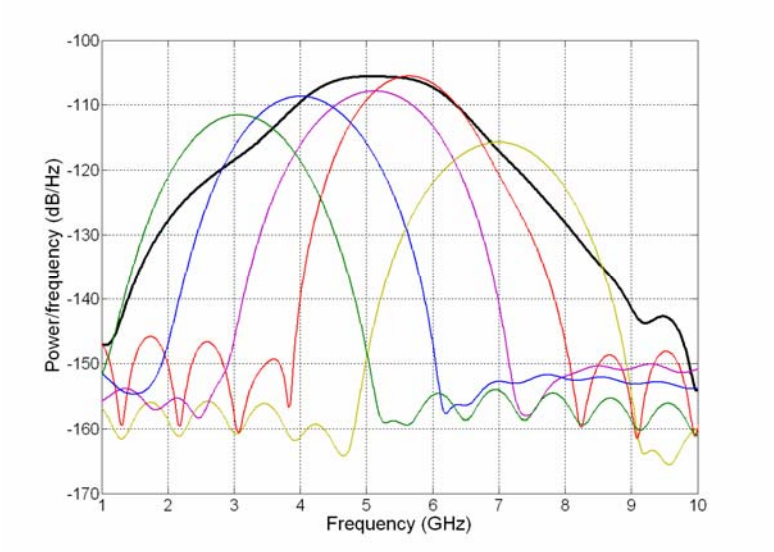

A.24 PSD comparison of H_{RF} and $BPF_{1\text{-}M}$ for DSSS using 1 GHz channels

A2. BPF-D/C Channelized Receiver Performance – UWB Results

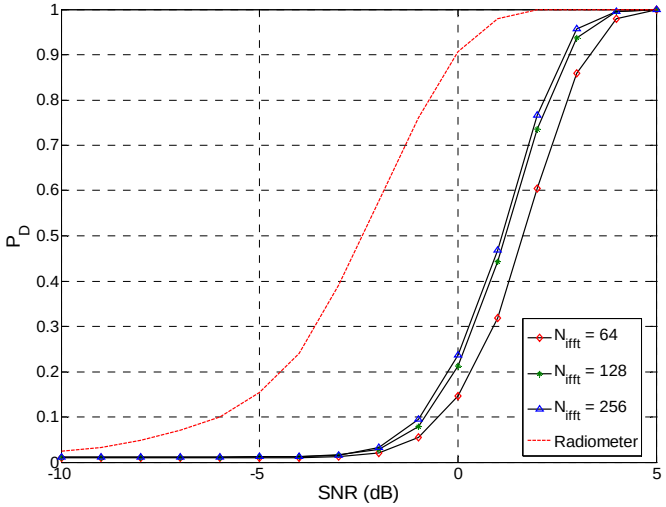

A.25 TTM detection performance for a BPF-D/C channelized receiver with $M = 50$, 100 MHz channels and varying number of IFFT points

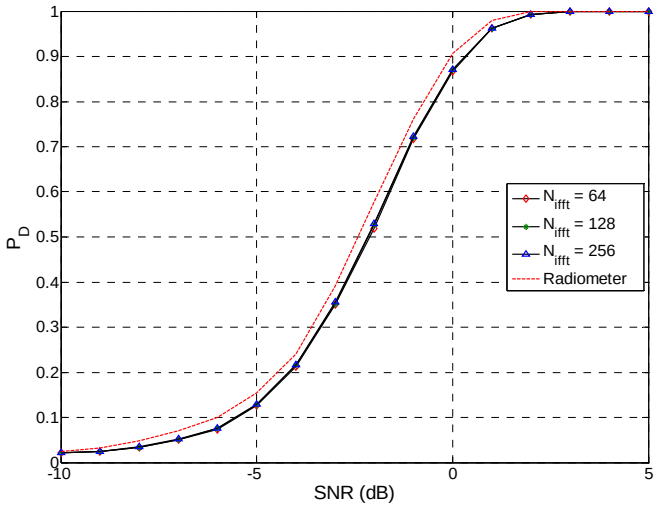

A.26 TTM detection performance for a BPF-D/C channelized receiver with $M = 10$, 500 MHz channels and varying number of IFFT points

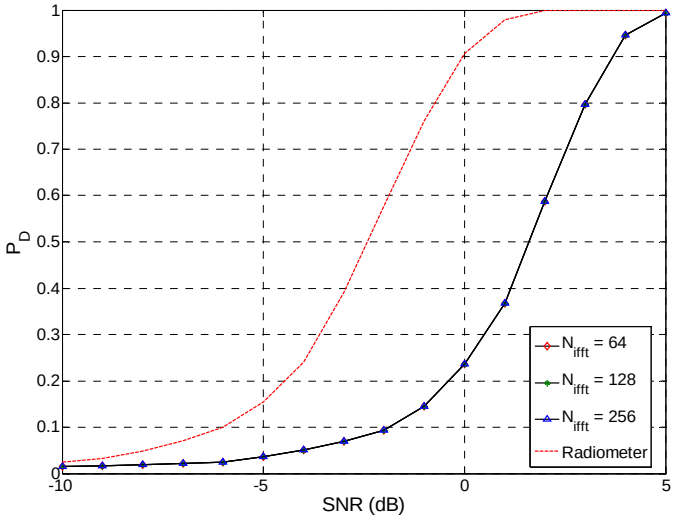

A.27 CTM detection performance for a BPF-D/C channelized receiver with $M = 50$, 100 MHz channels and varying number of IFFT points

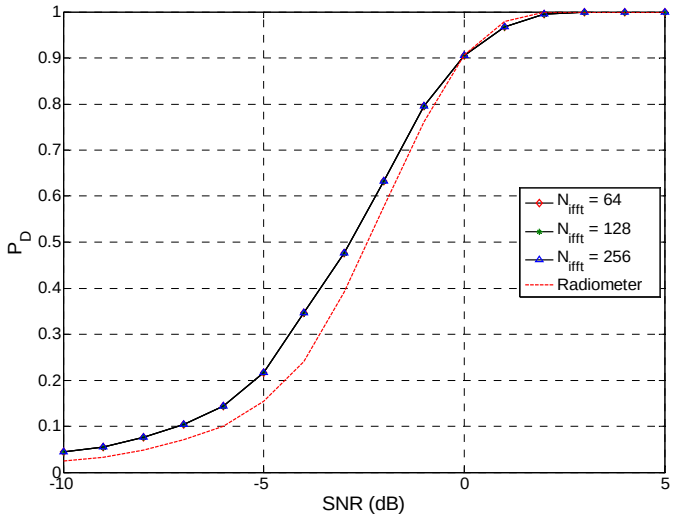

A.28 CTM detection performance for a BPF-D/C channelized receiver with $M = 10$, 500 MHz channels and varying number of IFFT points

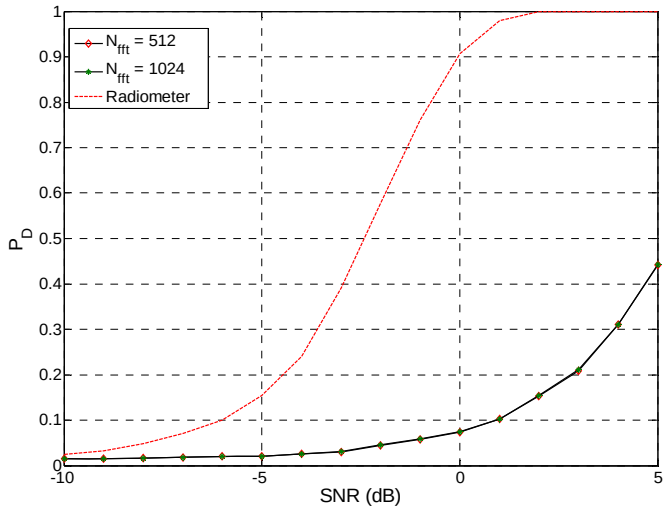

A.29 SSM detection performance for a BPF-D/C channelized receiver with $M = 50$, 100 MHz channels and varying number of FFT points

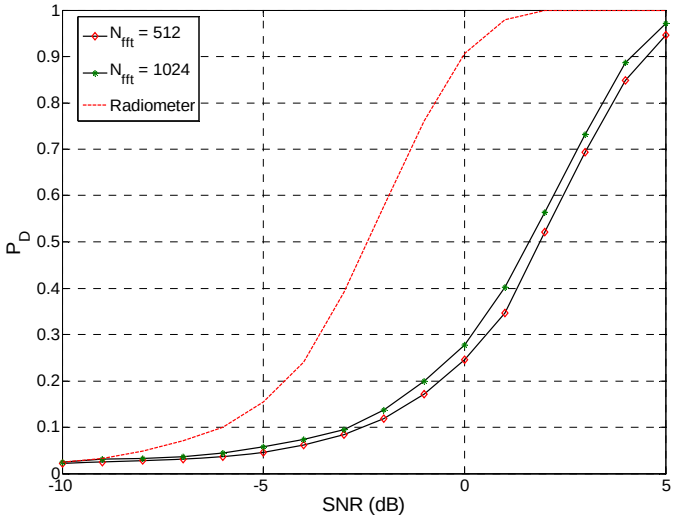

A.30 SSM detection performance for a BPF-D/C channelized receiver with $M = 10$, 500 MHz channels and varying number of FFT points

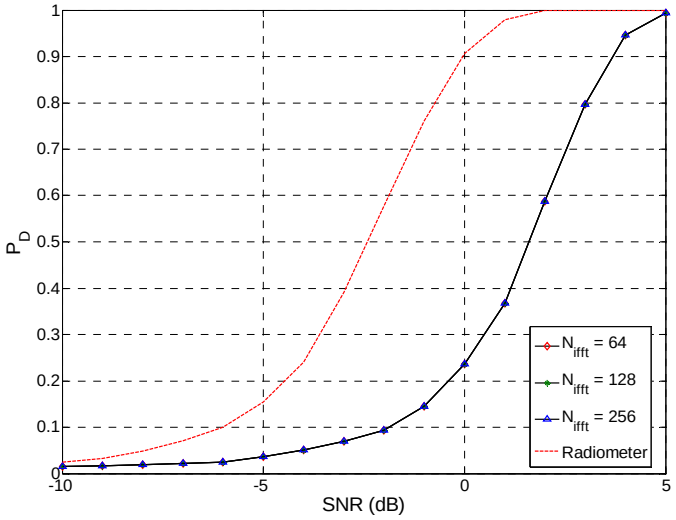

A.31 CSM detection performance for a BPF-D/C channelized receiver with $M = 50$, 100 MHz channels and varying number of FFT points

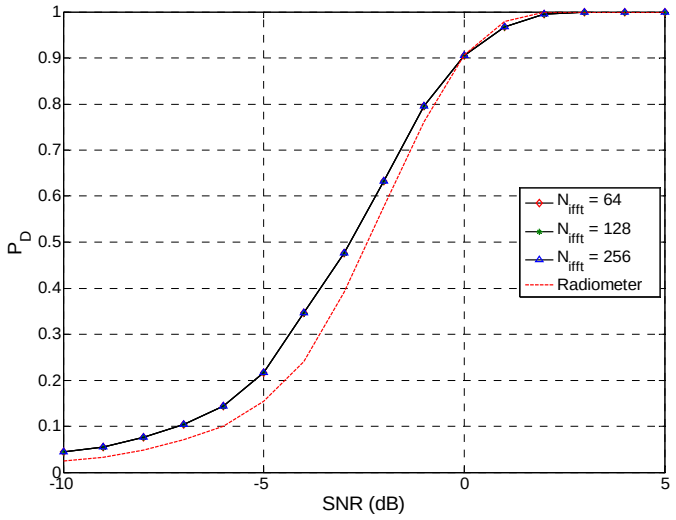

A.32 CSM detection performance for a BPF-D/C channelized receiver with $M = 10$, 500 MHz channels and varying number of FFT points

A3. BPF-D/C Channelized Receiver Performance – DSSS Waveform Results

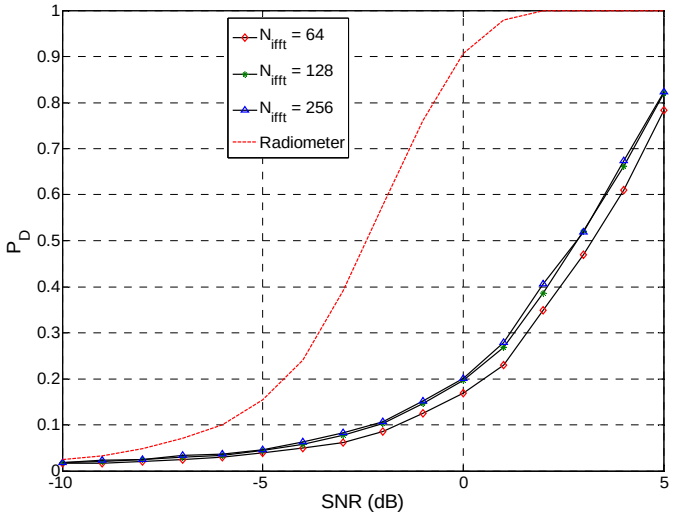

A.33 TTM detection performance for a BPF-D/C channelized receiver with $M = 50$, 100MHz channels and varying number of IFFT points

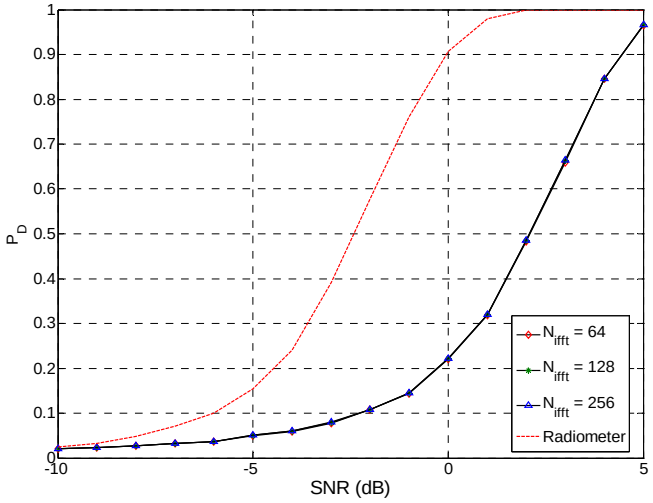

A.34 TTM detection performance for a BPF-D/C channelized receiver with $M = 10$, 500MHz channels and varying number of IFFT points

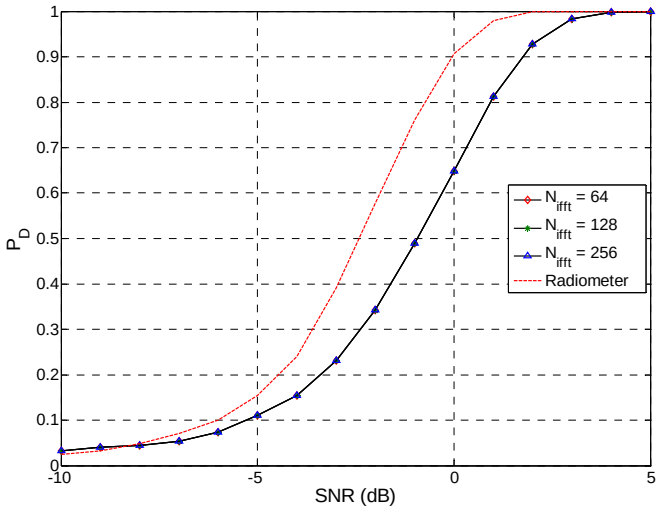

A.35 CTM detection performance for a BPF-D/C channelized receiver with $M = 50$, 100MHz channels and varying number of IFFT points

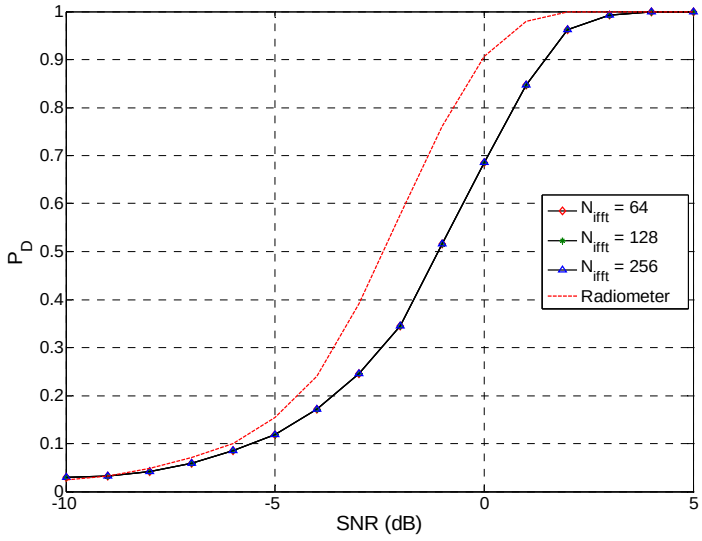

A.36 CTM detection performance for a BPF-D/C channelized receiver with $M = 10$, 500MHz channels and varying number of IFFT points

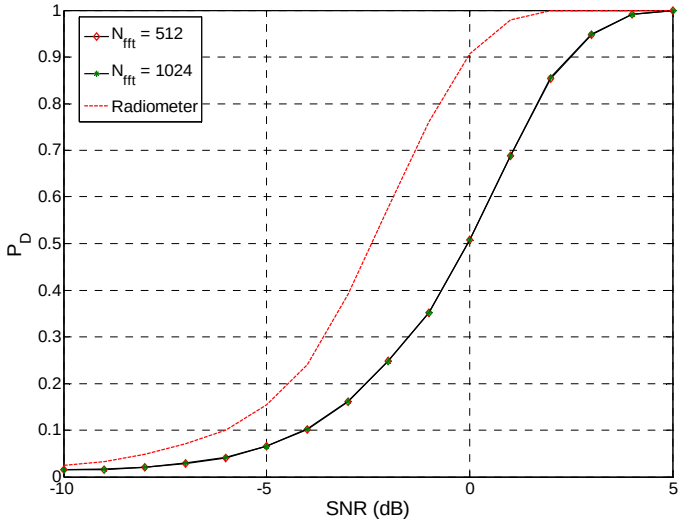

A.37 SSM detection performance for a BPF-D/C channelized receiver with $M = 50$, 100MHz channels and varying number of FFT points

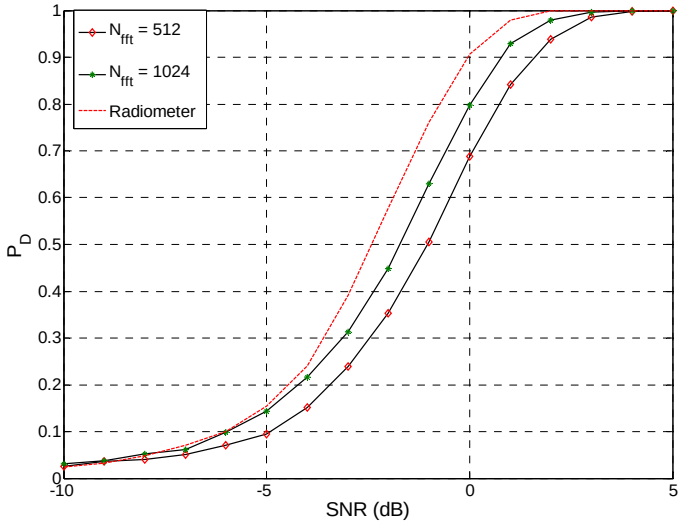

A.38 SSM detection performance for a BPF-D/C channelized receiver with $M = 10$, 500MHz channels and varying number of FFT points

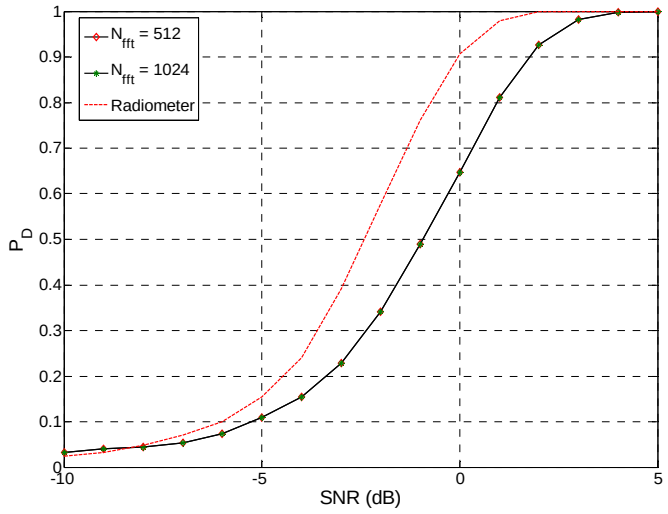

A.39 CSM detection performance for a BPF-D/C channelized receiver with $M = 50$, 100MHz channels and varying number of FFT points

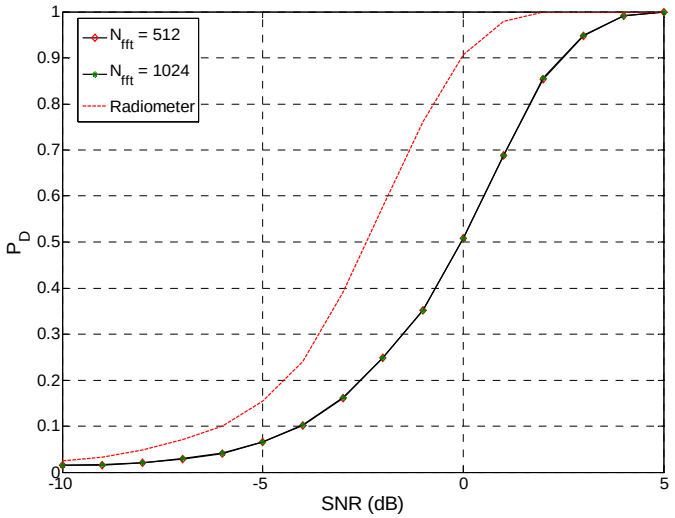

A.40 CSM detection performance for a BPF-D/C channelized receiver with $M = 10$, 500MHz channels and varying number of IFFT points

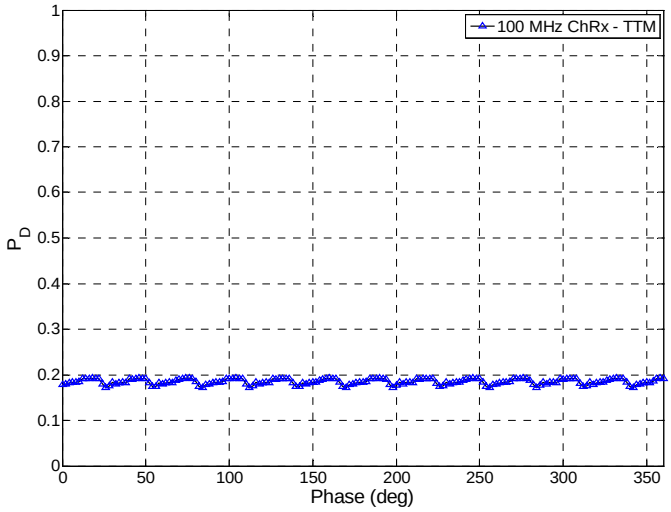

A.41 TTM detection performance versus mixer phase for a BPF-D/C channelized receiver using *SNR* = 0 dB and 100 MHz channels

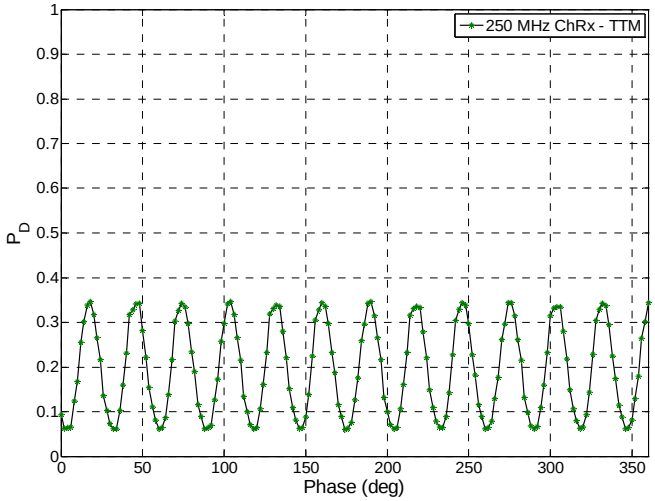

A.42 TTM detection performance versus mixer phase for a BPF-D/C channelized receiver using *SNR* = 0 dB and 250 MHz channels

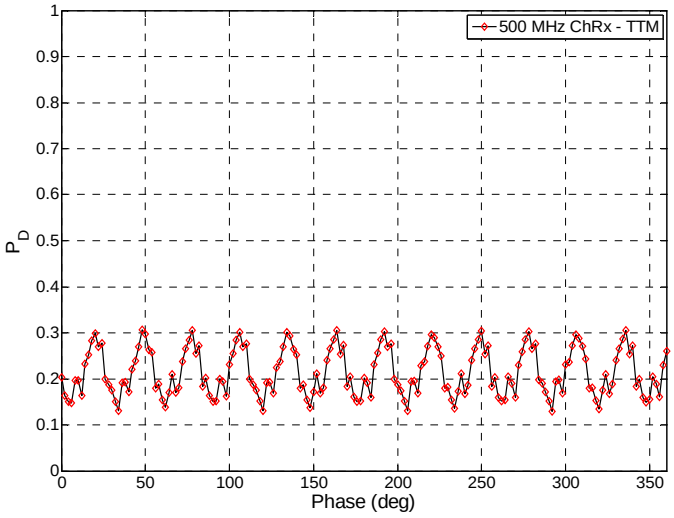

A.43 TTM detection performance versus mixer phase for a BPF-D/C channelized receiver using *SNR* = 0 dB and 500 MHz channels

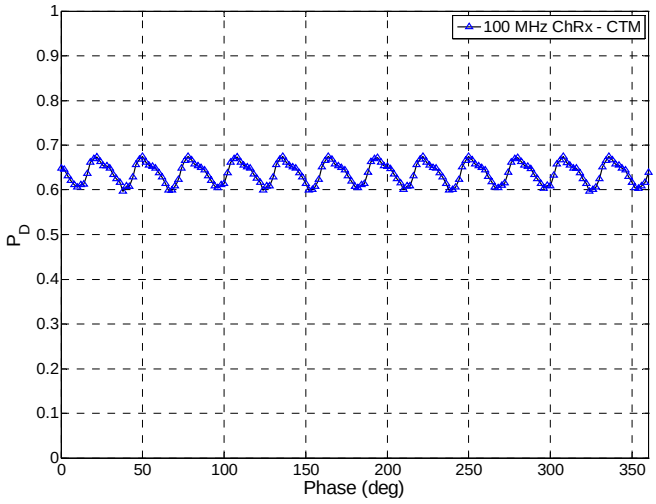

A.44 CTM detection performance versus mixer phase for a BPF-D/C channelized receiver using *SNR* = 0 dB and 100 MHz channels

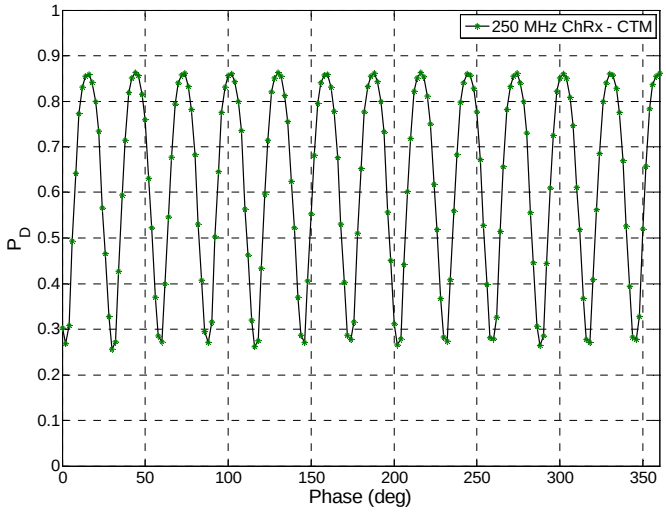

A.45 CTM detection performance versus mixer phase for a BPF-D/C channelized receiver using *SNR* = 0 dB and 250 MHz channels

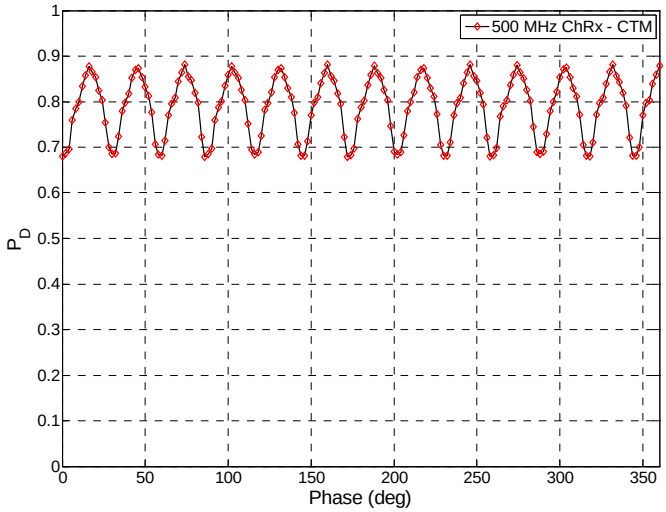

A.46 CTM detection performance versus mixer phase for a BPF-D/C channelized Rreceiver using *SNR* = 0 dB and 500 MHz channels

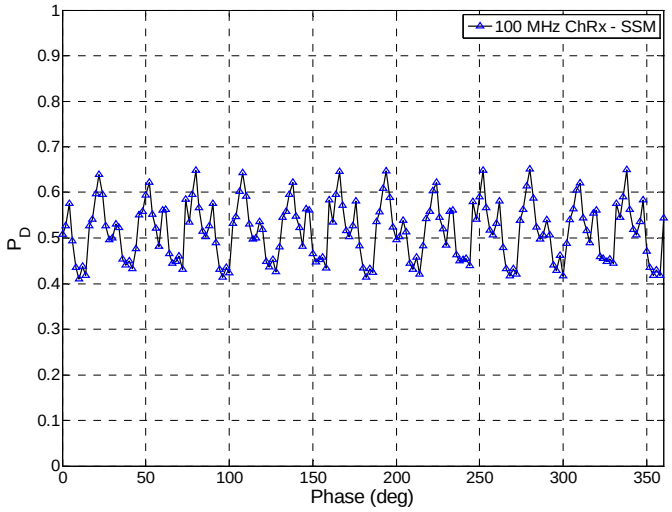

A.47 SSM detection performance versus mixer phase for a BPF-D/C channelized receiver using *SNR* = 0 dB and 100 MHz channels

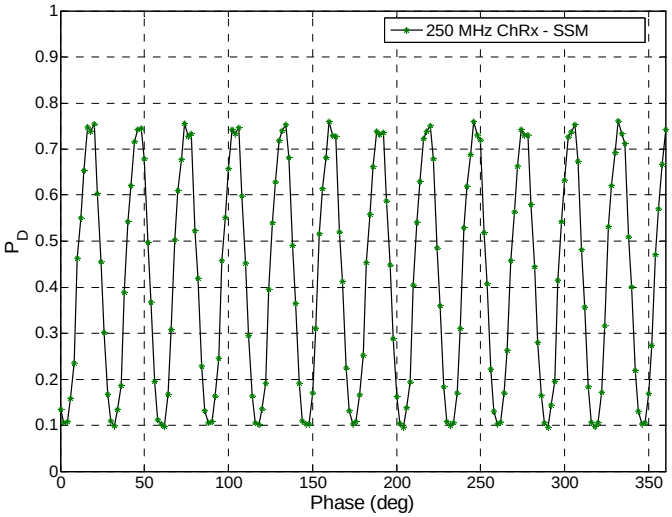

A.48 SSM detection performance versus mixer phase for a BPF-D/C channelized receiver using *SNR* = 0 dB and 250 MHz channels

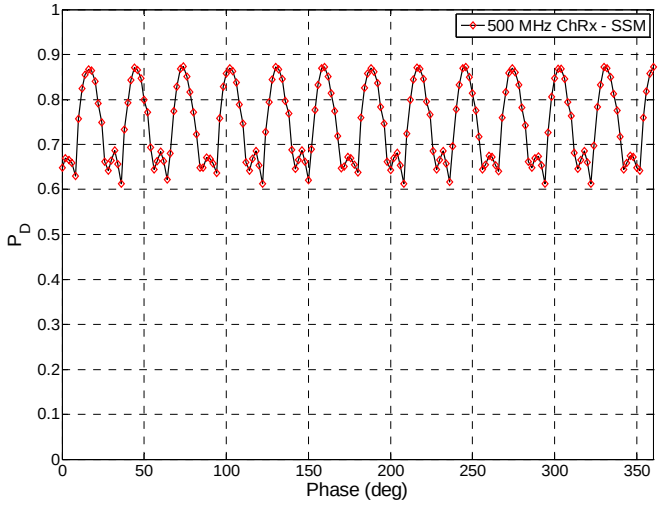

A.49 SSM detection performance versus mixer phase for a BPF-D/C channelized receiver using *SNR* = 0 dB and 500 MHz channels

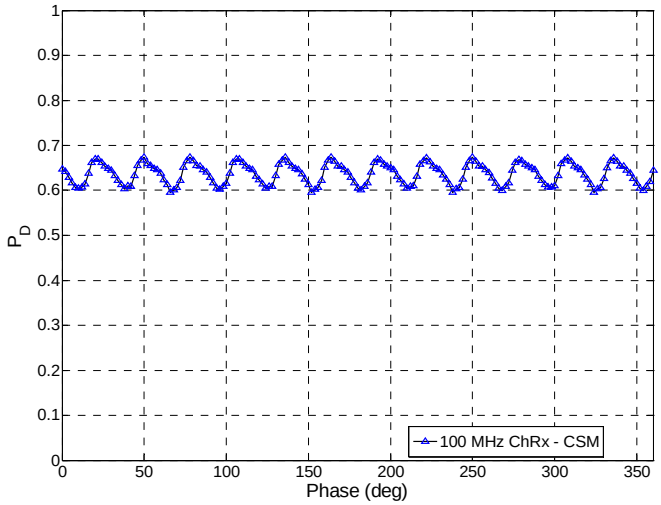

A.50 CSM detection performance versus mixer phase for a BPF-D/C channelized receiver using *SNR* = 0 dB and 100 MHz channels

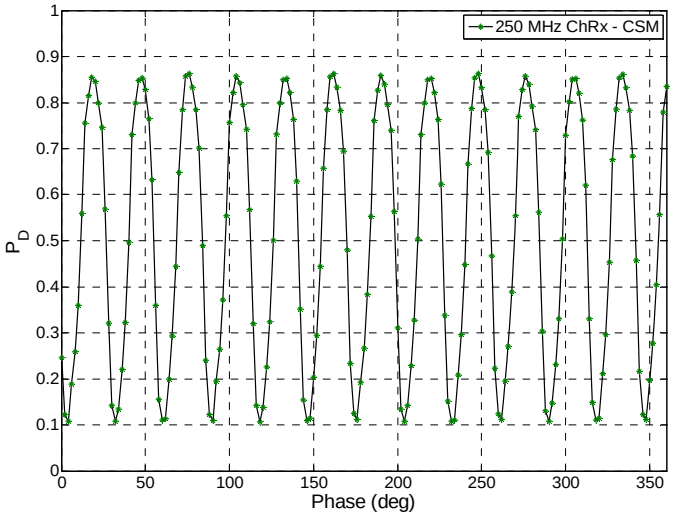

A.51 CSM detection performance versus mixer phase for a BPF-D/C channelized receiver using *SNR* = 0 dB and 250 MHz channels

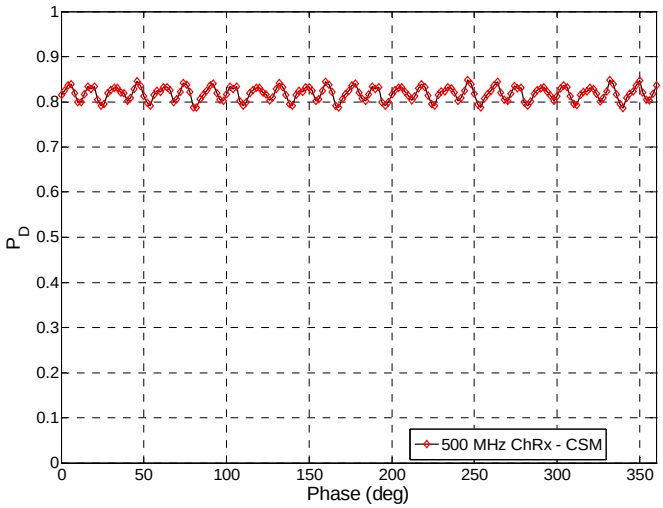

A.52 CSM detection performance versus mixer phase for a BPF-D/C channelized receiver using *SNR* = 0 dB and 500 MHz channels

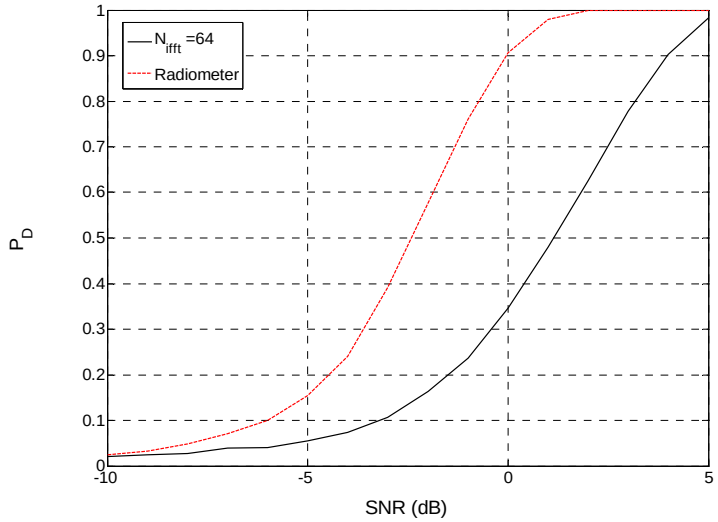

A.53 TTM detection performance for a BPF-D/C channelized receiver with $M = 20$, 250MHz channels (initial mixer phase at 18º)

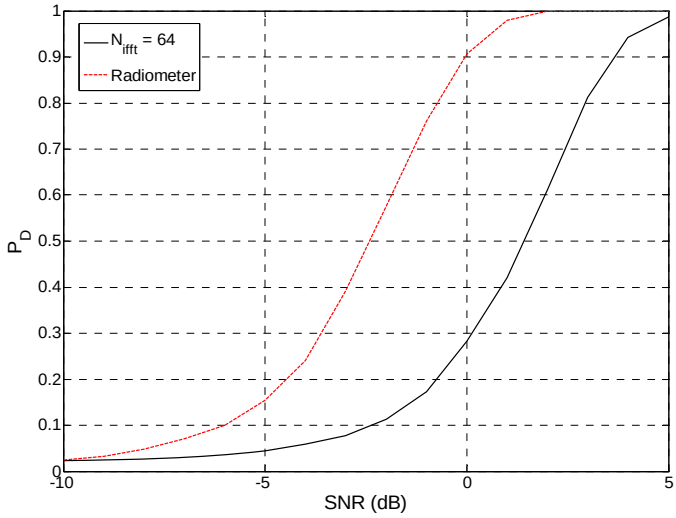

A.54 TTM detection performance for a BPF-D/C channelized receiver with $M = 10$, 500MHz channels (initial mixer phase at 18º)

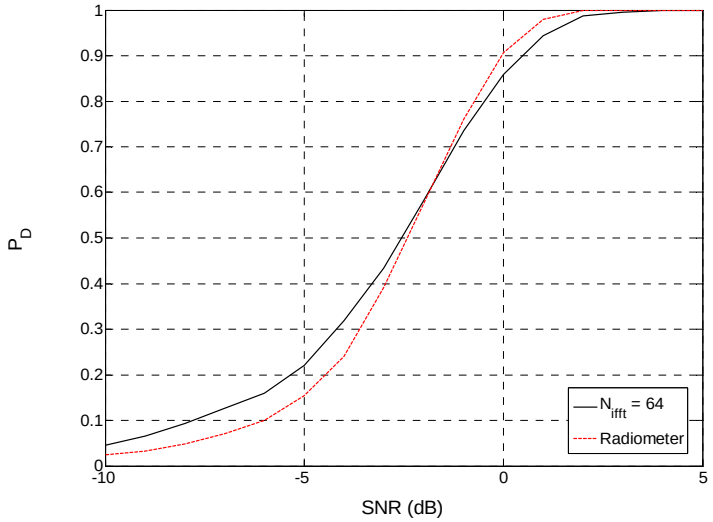

A.55 CTM detection performance for a BPF-D/C channelized receiver with $M = 20$, 250MHz channels (initial mixer phase at 16º)

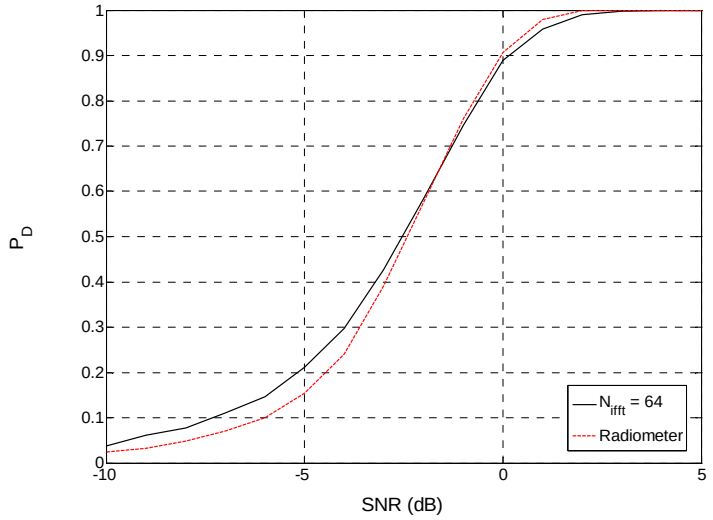

A.56 CTM detection performance for a BPF-D/C channelized receiver with $M = 10$, 500MHz channels (initial mixer phase at 16º)

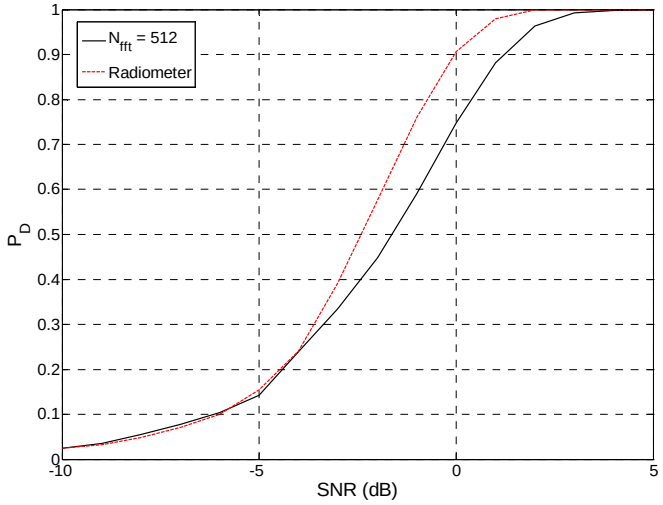

A.57 SSM detection performance for a BPF-D/C channelized receiver with $M = 20$, 250MHz channels (initial mixer phase at 16º)

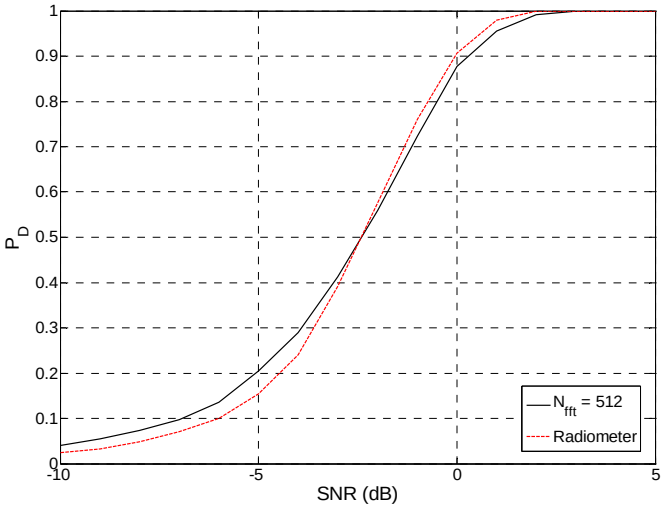

A.58 SSM detection performance for a BPF-D/C channelized receiver with $M = 10$, 500MHz channels (initial mixer phase at 16º)

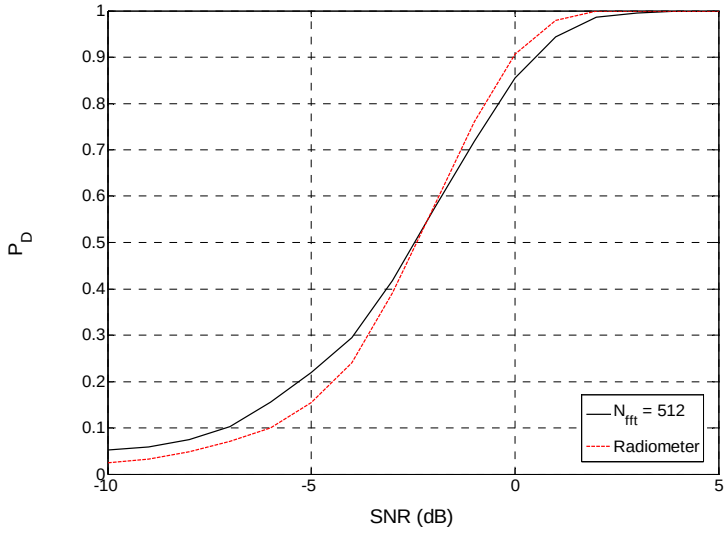

A.59 CSM detection performance for a BPF-D/C channelized receiver with $M = 20$, 250MHz channels (initial mixer phase at 18º)

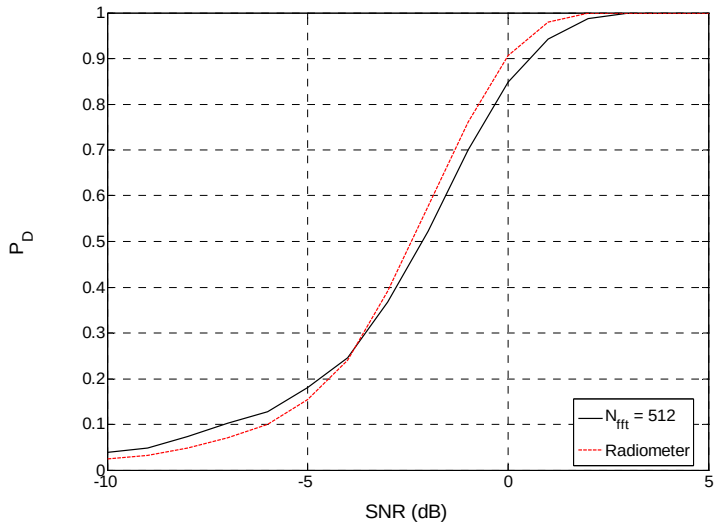

A.60 CSM detection performance for a BPF-D/C channelized receiver with $M = 10$, 500MHz channels (initial mixer phase at 18º)

Appendix B. MATLAB Code

B1. D/C ChRx – N_{fft} and N_{ifft}

```
% Brett D. Gronholz
% EENG 799 -- Summer/Fall 2004
%
% Updated and modified by:
% Willie H. Mims
% EENG 799 -- Fall 2005/Winter 2006
%
% UWB Detection Probability (Pd) - D/C ChRx
%   -- Varying Points in (I)FFT and SNR
%%%%%%%%%%%%%%%%%%%%%%%%%%%%%%%%%%%%%%%%%%%%
clear all, close all, clc, format compact
tic

%%%%%%%%%%%%%%%%%%%%%%%%%%
% Simulation Parameters
%%%%%%%%%%%%%%%%%%%%%%%%%%
Wrf = [250e6];              % channel bandwidth to simulate
Nz = [200];                 % zero-padding length for 'Wrf'
fl = 2.5e9;                 % lower ChRx frequency
fh = 7.5e9;                 % upper ChRx frequency
dc = 1;                     % downconvert? (1=yes,0=no)
ph = 0;                     % DC mixer starting phase
meth = 1;                   % processing method (1=TTM,2=SSM,3=CTM,4=CSM)
Nfft = [64,128,256];        % FFT lengths to simulate (TTM/CTM)
%Nfft = [512,1024,2048];    % FFT lengths to simulate (SSM/CSM)
SNR = [-10:1:5];            % SNR to simulate
Pfa = 10^-2;                % probability of false alarm
R = 10/Pfa;                 % number of realizations



%%%%%%%%%%%%%%%%%%%%%%%%%%
% UWB Signal Parameters
%%%%%%%%%%%%%%%%%%%%%%%%%%
fc = 5e9;       % center frequency
Tw = 2/fc;      % pulse duration
Ts = 2*Tw;      % symbol duration
To = Ts/2;      % symbol repetition interval
delt = 0.01e-9; % time resolution
fs = 1/delt;    % sample frequency
Ns = 1;         % number of symbols
P = 1;          % signal power
jtr = 0;        % jitter as percentage of Ts
method = 'uni'; % UWB modulation method
dly = 0;        % first pulse delay

%%%%%%%%%%%%%%%%%%%%%%
% Generate Signals
%%%%%%%%%%%%%%%%%%%%%%
x = uwb(Tw,To,delt,Ns,P,jtr,method,dly);    % UWB signal
x = [zeros(1,240) x zeros(1,240)];          % add zeros
Px = sum(x.^2)/length(x);                   % power in UWB signal
t = [0:delt:(length(x)*delt-delt)];         % time vector (length of 'x')
n1 = randn(1,length(x).*R);                 % matrix 'R' Noise realizations
```

```
for i = 1:R,
    n(i,:) = n1((length(x).*(i-1))+1:length(x).*i);
end

%%%%%%%%%%%%%%%%%%%%%%%%%%%%%%%%
% Filter Input Signals (Hrf)
%%%%%%%%%%%%%%%%%%%%%%%%%%%%%%%%
N = 4;              % order of Hrf BPF
NzRF = 200;         % one-sided zero padding length
[b,a] = butter(N,[fl/(fs/2) fh/(fs/2)]);% Hrf filter coeffs

xf = [zeros(1,NzRF) x zeros(1,NzRF)];   % zero-pad
xf = real(filtfilt(b,a,xf));            % filter
xf = xf(NzRF+1:end-NzRF);               % remove zeros
Pxf = sum(xf.^2)/length(xf);            % power in filtered UWB signal

nt = [zeros(R,NzRF) n zeros(R,NzRF)];   % zero-pad
for i = 1:R,
    nt(i,:) = filtfilt(b,a,nt(i,:));    % filter
    nf(i,:) = nt(i,NzRF+1:end-NzRF);    % remove zeros
end
nf = nf/sqrt(var(nf(:)'));              % normalize filtered noise power

%%%%%%%%%%%%%%%%%%
% ChRx Inputs
%%%%%%%%%%%%%%%%%%
s_in = xf;      % input signal
n_in = nf;      % input noise
Ps_in = sum(s_in.^2)/length(s_in);  % power in input signal

for c = 1:length(Nfft),                                          % Nfft loop

    %%%%%%%%%%%%%%%%%%%%%%%%%%
    % Channelized Receiver
    %%%%%%%%%%%%%%%%%%%%%%%%%%
    w = waitbar(0);             % create progress bar
    for q = 1:length(SNR),      % SNR loop
        nse = sqrt(Ps_in/10^(SNR(q)/10))*n_in;  % filtered noise matrix at
                                                % required SNR
        for k = 1:R,            % realizations loop
            waitbar(q/length(SNR),w,['ChRx Progress - ',num2str(c),'/'...
                ,num2str(length(Nfft)),'; ',num2str(q),'/'...
                ,num2str(length(SNR)),'; ',num2str(k),'/',num2str(R)]);
            inpn = nse(k,:);                    % input N
            inps = s_in;                        % input S
            inpsn = s_in + nse(k,:);             % input S+N
            outn = chrx(inpn,fs,Wrf,fl,fh,Nz,dc,ph); % output N
            outs = chrx(inps,fs,Wrf,fl,fh,Nz,dc,ph); % output S
            outsn = chrx(inpsn,fs,Wrf,fl,fh,Nz,dc,ph); % output S+N
                                                  % 1 of 4 'detection' methods
            if meth == 1,
                outxn = ifftshift(ifft(outn,Nfft(c),1),1);% Temp-Temp Matrix, N
                outxs = ifftshift(ifft(outs,Nfft(c),1),1);% Temp-Temp Matrix, S
                outxsn = ifftshift(ifft(outsn,Nfft(c),1),1);  % Temp-Temp
                                                              % Matrix, S+N
            elseif meth == 2,
                outxn = fftshift(fft(flipud(outn),Nfft(c),2),2);   % Spec-Spec
                                                                   %Matrix, N
                outxs = fftshift(fft(flipud(outs),Nfft(c),2),2);  % Spec-Spec
                                                                   % Matrix, S
                outxsn = fftshift(fft(flipud(outsn),Nfft(c),2),2);   % Spec-
```

```
                                                          % Spec Matrix, S+N
            elseif meth == 3,
                outxn = ctm(outn,Nfft(c),1,0); % Cross-Temporal Matrix, N
                outxs = ctm(outs,Nfft(c),1,0);  % Cross-Temporal Matrix, S
                outxsn = ctm(outsn,Nfft(c),1,0); % Cross-Temporal Matrix, S+N
            elseif meth == 4,
                outxn = fftshift(csm(outn,Nfft(c),1,0)); % Cross-Spectral
                                                          % Matrix, N
                outxs = fftshift(csm(outs,Nfft(c),1,0));  % Cross-Spectral
                                                          % Matrix, S
                outxsn = fftshift(csm(outsn,Nfft(c),1,0)); % Cross-Spectral
                                                          % Matrix, S+N
            else
                error('Invalid value (meth)')
            end
            Zn(k) = max(abs(outxn(:)));      % max 'outxn' test statistic
            Z(k) = max(abs(outxsn(:)));      % max 'outxsn' test statistic
        end                                 % next k...next noise realization
        Zs = fliplr(sort(Zn));              % sort 'outxn' test statistics
        T = Zs(floor(Pfa*R)+1);             % find/set threshold
        Pd(c,q) = length(find(Z > T))/R;    % probability of detection
    end                                                 % next q...SNR value
    close(w)

end                                                     % next c...Nfft
point

%save CTM_Nfft       % save all data from workspace

toc
```

B2. BPF-D/C ChRx – N_{fft} and N_{ifft}

```
% Brett D. Gronholz
% EENG 799 -- Summer/Fall 2004
%
% Updated and modified by:
% Willie H. Mims
% EENG 799 -- Fall 2005/Winter 2006
%
% UWB Detection Probability (Pd) - BPF-D/C ChRx
%   -- Varying Points in (I)FFT and SNR
%%%%%%%%%%%%%%%%%%%%%%%%%%%%%%%%%%%%%%%%%%%%%

clear; clc; close all hidden;
load 31GoldParams   % Coding parameters for DS-SS
tic



%%%%%%%%%%%%%%%%%%%%%%%%%%%
% Simulation Parameters
%%%%%%%%%%%%%%%%%%%%%%%%%%%
Wrf = [100e6];              % Channel bandwidth to simulate
Nz = [200];                 % Zero-padding length for 'Wrf'
fl = 2.5e9;                 % Lower ChRx frequency
fh = 7.5e9;                 % Upper ChRx frequency
ph = 0;                     % DC mixer starting phase
meth = 4;                   % Processing method (1=TTM,2=SSM,3=CTM,4=CSM)
Nfft = [64,128,256];        % FFT lengths to simulate (TTM/CTM)
%Nfft = [512,1024];         % FFT lengths to simulate (SSM/CSM)
SNR = [-10:1:5];            % SNR to simulate
Pfa = 10^-2;                % Probability of false alarm
R = 10/Pfa;                 % Number of realizations



%%%%%%%%%%%%%%%%%%%%%%%%%%%
% UWB Signal Parameters
%%%%%%%%%%%%%%%%%%%%%%%%%%%
fc = 5e9;               % Center frequency
Tw = 2/fc;              % Pulse duration
Ts = 2*Tw;              % Symbol duration
To = Ts/2;              % Symbol repetition interval
delt = 0.01e-9;         % Time resolution
fs = 1/delt;            % Sample frequency
Ns = 1;                 % Number of symbols
P = 1;                  % Signal power
jtr = 0;                % Jitter as percentage of Ts
method = 'uni';         % UWB modulation method
dly = 0;                % First pulse delay



%%%%%%%%%%%%%%%%%%%%%%%%%%%
% DS-SS Signal Parameters
%%%%%%%%%%%%%%%%%%%%%%%%%%%
fnot = 5e9;             % Center frequency (adjusted to 'snapshot' 5GHz)
delt = 0.01e-9;         % Time resolution
fsamp = 1/delt;         % Sampling frequency
rsym = 12500;           % Symbol rate
```

```
tsym = 1/rsym;          % Symbol period
rchip = rsym*31;        % Chip rate (adjusted to 'snapshot' 1GHz rate)

K = [1];                % K = 1 user case
rbits = 25;
nplus = 0;              % No noise parameter in subfunction


%%%%%%%%%%%%%%%%%%%%%%%%%%%%%%%%%%
% Generate Signals : UWB and DS-SS
%%%%%%%%%%%%%%%%%%%%%%%%%%%%%%%%%%
%% UWB %%
x = uwb(Tw,To,delt,Ns,P,jtr,method,dly);    % UWB signal
x = [zeros(1,240) x zeros(1,240)];          % Add zeros
Px = sum(x.^2)/length(x);                   % Power in UWB signal

%% DS-SS %%
c_wave(1,:) = FastSprdMod(GoldMatrix,3,nsamp,size(GoldMatrix,2),rbits);
[bitsin(1,:) sigvec(1,:) timvec(1,:)] = Fast_Bpsk_ModPrj2(datsel,indata,...
    rbits,ndelay,fnot,esym,nsamp,nplus,tsym);
TSW(1,:) =  c_wave.*sigvec;                 % Full vector over time
y(1,:) =    TSW(1,[1:length(x)]);           % Observation 'snapshot'

%% Noise %%
n1 = randn(1,length(x).*R);                 % Matrix 'R' noise realizations
for i = 1:R,
    n(i,:) = n1((length(x).*(i-1))+1:length(x).*i);
end

%%%%%%%%%%%%%%%%%%%%%%%%%%%%%%%%
% Filter Input Signals (Hrf)
%%%%%%%%%%%%%%%%%%%%%%%%%%%%%%%%
N = 4;                                      % Order of Hrf BPF
NzRF = 200;                                 % One-sided zero padding length
[b,a] = butter(N,[fl/(fs/2) fh/(fs/2)]);% Hrf filter coeffs

xf = [zeros(1,NzRF) x zeros(1,NzRF)];   % Zero-pad
xf = real(filtfilt(b,a,xf));            % Filter
xf = xf(NzRF+1:end-NzRF);               % Remove zeros
Pxf = sum(xf.^2)/length(xf);            % Power in filtered UWB signal

yf = [zeros(1,NzRF) y zeros(1,NzRF)];   % Zero-pad
yf = real(filtfilt(b,a,yf));            % Filter
yf = yf(NzRF+1:end-NzRF);               % Remove zeros
yf = sqrt(Pxf/var(yf))*yf;              % Scale (power equal to 'Pxf')

np = [zeros(R,NzRF) n zeros(R,NzRF)];   % Zero-pad
for i = 1:R,
    np1(i,:) = filtfilt(b,a,np(i,:));   % Filter
    nf(i,:) = np1(i,NzRF+1:end-NzRF);   % Remove zeros
end
nf = nf/sqrt(var(nf(:)'));              % Normalize filtered noise power


%%%%%%%%%%%%%%%%%%
% ChRx Inputs
%%%%%%%%%%%%%%%%%%
s_in = xf;                              % Input signal (UWB or DS-SS)
n_in = nf;                              % Input noise
```

```
Ps_in = sum(s_in.^2)/length(s_in);      % Power in input signal

figure(1), hold on, grid


%%%%%%%%%%%%%%%%%%%%%%%%%%%
% Radiometric Detection
%%%%%%%%%%%%%%%%%%%%%%%%%%%
w = waitbar(0);                         % Create progress bar
for i = 1:length(SNR),                  % SNR loop
    waitbar(i/length(SNR),w,['Radiometer Progress - ',...
        num2str(i),'/',num2str(length(SNR))]);
    nser = sqrt(Ps_in/10^(SNR(i)/10))*n_in; % Noise at required SNR
    Znr = sum(nser.^2,2);                   % Noise test statistic
    Zsr = flipud(sort(Znr));                % Sort Zn (descending)
    Tr = Zsr(floor(Pfa*R)+1);               % Find/set threshold
    for k = 1:R,
        Zr(k) = sum((s_in+nser(k,:)).^2);   % S+N test statistics
    end
    Pdr(i) = length(find(Zr > Tr))/R;       % Probability of detection
end
close(w)


for c = 1:length(Nfft),                                          % Nfft loop

    %%%%%%%%%%%%%%%%%%%%%%%%%%%
    % Channelized Receiver II
    %%%%%%%%%%%%%%%%%%%%%%%%%%%
    w = waitbar(0);             % Create progress bar
    for q = 1:length(SNR),                                       % SNR loop
        nse = sqrt(Ps_in/10^(SNR(q)/10))*n_in;  % Filtered noise matrix at
required SNR
        for k = 1:R,                                        % Realizations loop
            waitbar(q/length(SNR),w,['ChRx Progress - ',...
                num2str(q),'/',num2str(length(SNR)),'; ',...
                num2str(k),'/',num2str(R),'; ',num2str(c),'/',...
                num2str(length(Nfft))]);
            inpn = nse(k,:);                            % Input N
            inps = s_in;                                % Input S
            inpsn = s_in + nse(k,:);                    % Input S+N

            %%%%%%%%%%%%%%%%%%%
            % Forming CDM RF
            %%%%%%%%%%%%%%%%%%%
            CDM_RFn = chrx_RF(inpn,fs,Wrf,fl,fh,Nz); % Output N
            CDM_RFs = chrx_RF(inps,fs,Wrf,fl,fh,Nz); % Output S
            CDM_RFsn = chrx_RF(inpsn,fs,Wrf,fl,fh,Nz); % Output S+N

            %%%%%%%%%%%%%%%%%%%
            % Forming CDM BB
            %%%%%%%%%%%%%%%%%%%
            CDM_BBn = chrx_BB(CDM_RFn,fs,Wrf,fl,fh,Nz,ph);  % Output N
            CDM_BBs = chrx_BB(CDM_RFs,fs,Wrf,fl,fh,Nz,ph);  % Output S
            CDM_BBsn = chrx_BB(CDM_RFsn,fs,Wrf,fl,fh,Nz,ph); % Output S+N


            %%%%%%%%%%%%%%%%%%%%%%%%%%%%%%%%%%%%%%%%%%%%%%%%%%%%%%%%
            % Processing Techniques (with appropriate shifting)
            %%%%%%%%%%%%%%%%%%%%%%%%%%%%%%%%%%%%%%%%%%%%%%%%%%%%%%%%
```

```
            if meth == 1,
                outxn = ifftshift(ifft(CDM_BBn,Nfft(c),1),1);       % Temp-Temp
                                                                    % Matrix, N
                outxs = ifftshift(ifft(CDM_BBs,Nfft(c),1),1);       % Temp-Temp
                                                                    % Matrix, S
                outxsn = ifftshift(ifft(CDM_BBsn,Nfft(c),1),1);     % Temp-Temp
                                                                    % Matrix, S+N
            elseif meth == 2,
                outxn = fftshift(fft(flipud(CDM_BBn),Nfft(c),2),2);     % Spec-
                                                                    % Spec Matrix, N
                outxs = fftshift(fft(flipud(CDM_BBs),Nfft(c),2),2);     % Spec-
                                                                    % Spec Matrix, S
                outxsn = fftshift(fft(flipud(CDM_BBsn),Nfft(c),2),2);  % Spec-
                                                                    % Spec Matrix, S+N
            elseif meth == 3,
                outxn = ctm(CDM_BBn,Nfft(c),1,0);                  % Cross-Temporal
                                                                       % Matrix, N
                outxs = ctm(CDM_BBs,Nfft(c),1,0);                  % Cross-Temporal
                                                                       % Matrix, S
                outxsn = ctm(CDM_BBsn,Nfft(c),1,0);                % Cross-Temporal
                                                                       % Matrix, S+N
            elseif meth == 4,
                outxn = fftshift(csm(CDM_BBn,Nfft(c),1,0));     % Cross-Spectral
                                                                       % Matrix, N
                outxs = fftshift(csm(CDM_BBs,Nfft(c),1,0));     % Cross-Spectral
                                                                       % Matrix, S
                outxsn = fftshift(csm(CDM_BBsn,Nfft(c),1,0));  % Cross-Spectral
                                                                       % Matrix, S+N
            else
                error('Invalid value (meth)')
            end

            Zn(k) = max(abs(outxn(:)));      % Max 'outxn' test statistic
            Z(k) = max(abs(outxsn(:)));      % Max 'outxsn' test statistic
        end                                                    % Next k...next
noise realization
        Zs = fliplr(sort(Zn));              % Sort 'outxn' test statistics
        T = Zs(floor(Pfa*R)+1);             % Find/set threshold
        Pd(c,q) = length(find(Z > T))/R;    % Probability of detection
    end                                                  % Next q...SNR value
    close(w)
end                                                    % Next c...Nfft point

%save ChRx_Nfft       % save all data from workspace

toc
```

B3. BPF-D/C ChRx – Initial Phase

```
% Brett D. Gronholz
% EENG 799 -- Summer/Fall 2004
%
% Updated and modified by:
% Willie H. Mims
% EENG 799 -- Fall 2005/Winter 2006
%
% UWB Detection Probability (Pd) - BPF-D/C ChRx
%   -- Varying Initial Mixer Phase
%%%%%%%%%%%%%%%%%%%%%%%%%%%%%%%%%%%%%%%%%%%%%

clear; clc; close all hidden;
load 31GoldParams   % Coding parameters for DSSS
tic



%%%%%%%%%%%%%%%%%%%%%%%%%%%
% Simulation Parameters
%%%%%%%%%%%%%%%%%%%%%%%%%%%
Wrf = [250e6];              % Channel bandwidth to simulate
Nz = [200];                 % Zero-padding length for 'Wrf'
fl = 2.5e9;                 % Lower ChRx frequency
fh = 7.5e9;                 % Upper ChRx frequency
ph = [0:2:60];              % DC mixer starting phase to simulate
meth = 1;                   % Processing method (1=TTM,2=SSM,3=CTM,4=CSM)
Nfft = [64,128,256];        % FFT lengths to simulate (TTM/CTM)
%Nfft = [512,1024];         % FFT lengths to simulate (SSM/CSM)
SNR = [-10:1:5];            % SNR to simulate
Pfa = 10^-2;                % Probability of false alarm
R = 10/Pfa;                 % Number of realizations



%%%%%%%%%%%%%%%%%%%%%%%%%%%
% UWB Signal Parameters
%%%%%%%%%%%%%%%%%%%%%%%%%%%
fc = 5e9;               % Center frequency
Tw = 2/fc;              % Pulse duration
Ts = 2*Tw;              % Symbol duration
To = Ts/2;              % Symbol repetition interval
delt = 0.01e-9;         % Time resolution
fs = 1/delt;            % Sample frequency
Ns = 1;                 % Number of symbols
P = 1;                  % Signal power
jtr = 0;                % Jitter as percentage of Ts
method = 'uni';         % UWB modulation method
dly = 0;                % First pulse delay



%%%%%%%%%%%%%%%%%%%%%%%%%%%
% DS-SS Signal Parameters
%%%%%%%%%%%%%%%%%%%%%%%%%%%
fnot = 5e9;             % Center frequency (adjusted to 'snapshot' 5GHz)
delt = 0.01e-9;         % Time resolution
fsamp = 1/delt;         % Sampling frequency
rsym = 12500;           % Symbol rate
```

```
tsym = 1/rsym;          % Symbol period
rchip = rsym*31;        % Chip rate (adjusted to 'snapshot' 1GHz rate)

K = [1];                % K = 1 user case
rbits = 25;
nplus = 0;              % No noise parameter in subfunction


%%%%%%%%%%%%%%%%%%%%%%%%%%%%%%%%%%
% Generate Signals : UWB and DS-SS
%%%%%%%%%%%%%%%%%%%%%%%%%%%%%%%%%%
%% UWB %%
x = uwb(Tw,To,delt,Ns,P,jtr,method,dly);    % UWB signal
x = [zeros(1,240) x zeros(1,240)];          % Add zeros
Px = sum(x.^2)/length(x);                   % Power in UWB signal

%% DS-SS %%
c_wave(1,:) = FastSprdMod(GoldMatrix,3,nsamp,size(GoldMatrix,2),rbits);
[bitsin(1,:) sigvec(1,:) timvec(1,:)] = Fast_Bpsk_ModPrj2(datsel,indata,...
    rbits,ndelay,fnot,esym,nsamp,nplus,tsym);
TSW(1,:) =  c_wave.*sigvec;                 % Full vector over time
y(1,:) =    TSW(1,[1:length(x)]);           % Observation 'snapshot'

%% Noise %%
n1 = randn(1,length(x).*R);                 % Matrix 'R' Noise realizations
for i = 1:R,
    n(i,:) = n1((length(x).*(i-1))+1:length(x).*i);
end

%%%%%%%%%%%%%%%%%%%%%%%%%%%%%%%%
% Filter Input Signals (Hrf)
%%%%%%%%%%%%%%%%%%%%%%%%%%%%%%%%
N = 4;                                      % Order of Hrf BPF
NzRF = 200;                                 % One-sided zero padding length
[b,a] = butter(N,[fl/(fs/2) fh/(fs/2)]);% Hrf filter coeffs

xf = [zeros(1,NzRF) x zeros(1,NzRF)];   % Zero-pad
xf = real(filtfilt(b,a,xf));            % Filter
xf = xf(NzRF+1:end-NzRF);               % Remove zeros
Pxf = sum(xf.^2)/length(xf);            % Power in filtered UWB signal

yf = [zeros(1,NzRF) y zeros(1,NzRF)];   % Zero-pad
yf = real(filtfilt(b,a,yf));            % Filter
yf = yf(NzRF+1:end-NzRF);               % Remove zeros
yf = sqrt(Pxf/var(yf))*yf;              % Scale (power equal to 'Pxf')

np = [zeros(R,NzRF) n zeros(R,NzRF)];   % Zero-pad
for i = 1:R,
    np1(i,:) = filtfilt(b,a,np(i,:));   % Filter
    nf(i,:) = np1(i,NzRF+1:end-NzRF);   % Remove zeros
end
nf = nf/sqrt(var(nf(:)'));              % Normalize filtered noise power


%%%%%%%%%%%%%%%%%%
% ChRx Inputs
%%%%%%%%%%%%%%%%%%
s_in = xf;                              % Input signal (UWB or DS-SS)
n_in = nf;                              % Input noise
```

```
Ps_in = sum(s_in.^2)/length(s_in);      % Power in input signal

figure(1), hold on, grid


%%%%%%%%%%%%%%%%%%%%%%%%%%%
% Radiometric Detection
%%%%%%%%%%%%%%%%%%%%%%%%%%%
w = waitbar(0);                         % Create progress bar
for i = 1:length(SNR),                  % SNR loop
    waitbar(i/length(SNR),w,['Radiometer Progress - ',...
        num2str(i),'/',num2str(length(SNR))]);
    nser = sqrt(Ps_in/10^(SNR(i)/10))*n_in; % Noise at required SNR
    Znr = sum(nser.^2,2);                   % Noise test statistic
    Zsr = flipud(sort(Znr));                % Sort Zn (descending)
    Tr = Zsr(floor(Pfa*R)+1);               % Find/set threshold
    for k = 1:R,
        Zr(k) = sum((s_in+nser(k,:)).^2);   % S+N test statistics
    end
    Pdr(i) = length(find(Zr > Tr))/R;       % Probability of detection
end
close(w)


for c = 1:length(Wrf),                                          % ChBW loop

    %%%%%%%%%%%%%%%%%%%%%%%%%%%
    % Channelized Receiver II
    %%%%%%%%%%%%%%%%%%%%%%%%%%%
    w = waitbar(0);             % Create progress bar
    nse = sqrt(Ps_in/10^(SNR/10))*n_in;  % Filtered noise matrix at required
SNR
    for q = 1:length(ph),                                       % Phase loop
        for k = 1:R,                                    % Realizations loop
            waitbar(q/length(ph),w,['ChRx Progress - ',num2str(c),'/',...
                num2str(length(Wrf)),'; ',num2str(q),'/',...
                num2str(length(ph)),'; ',num2str(k),'/',num2str(R)]);
            inpn = nse(k,:);                            % Input N
            inps = s_in;                                % Input S
            inpsn = s_in + nse(k,:);                    % Input S+N

            %%%%%%%%%%%%%%%%%%%
            % Forming CDM RF
            %%%%%%%%%%%%%%%%%%%
            CDM_RFn = chrx_RF(inpn,fs,Wrf(c),fl,fh,Nz); % Output N
            CDM_RFs = chrx_RF(inps,fs,Wrf(c),fl,fh,Nz); % Output S
            CDM_RFsn = chrx_RF(inpsn,fs,Wrf(c),fl,fh,Nz); % Output S+N

            %%%%%%%%%%%%%%%%%%%
            % Forming CDM BB
            %%%%%%%%%%%%%%%%%%%
            CDM_BBn = chrx_BB(CDM_RFn,fs,Wrf(c),fl,fh,Nz,ph(q));  % Output N
            CDM_BBs = chrx_BB(CDM_RFs,fs,Wrf(c),fl,fh,Nz,ph(q));  % Output S
            CDM_BBsn = chrx_BB(CDM_RFsn,fs,Wrf(c),fl,fh,Nz,ph(q)); % Output S+N



            %%%%%%%%%%%%%%%%%%%%%%%%%%%%%%%%%%%%%%%%%%%%%%%%%%%%%%%%%%%
            % Processing Techniques (with appropriate shifting)
            %%%%%%%%%%%%%%%%%%%%%%%%%%%%%%%%%%%%%%%%%%%%%%%%%%%%%%%%%%%
```

```
            if meth == 1,
                outxn = ifftshift(ifft(CDM_BBn,Nfft,1),1);      % Temp-Temp
                                                                   % Matrix, N
                outxs = ifftshift(ifft(CDM_BBs,Nfft,1),1);      % Temp-Temp
                                                                   % Matrix, S
                outxsn = ifftshift(ifft(CDM_BBsn,Nfft,1),1);    % Temp-Temp
                                                                   % Matrix, S+N
            elseif meth == 2,
                outxn = fftshift(fft(flipud(CDM_BBn),Nfft,2),2);    % Spec-Spec
                                                                   % Matrix, N
                outxs = fftshift(fft(flipud(CDM_BBs),Nfft,2),2);    % Spec-Spec
                                                                   % Matrix, S
                outxsn = fftshift(fft(flipud(CDM_BBsn),Nfft,2),2); % Spec-Spec
                                                                   % Matrix, S+N
            elseif meth == 3,
                outxn = ctm(CDM_BBn,Nfft,1,0);              % Cross-Temporal
                                                            % Matrix, N
                outxs = ctm(CDM_BBs,Nfft,1,0);              % Cross-Temporal
                                                            % Matrix, S
                outxsn = ctm(CDM_BBsn,Nfft,1,0);            % Cross-Temporal
                                                            % Matrix, S+N
            elseif meth == 4,
                outxn = fftshift(csm(CDM_BBn,Nfft,1,0));    % Cross-Spectral
                                                            % Matrix, N
                 outxs = fftshift(csm(CDM_BBs,Nfft,1,0));   % Cross-Spectral
                                                            % Matrix, S
                outxsn = fftshift(csm(CDM_BBsn,Nfft,1,0));  % Cross-Spectral
                                                            % Matrix, S+N
            else
                error('Invalid value (meth)')
            end

            Zn(k) = max(abs(outxn(:)));      % Max 'outxn' test statistic
            Z(k) = max(abs(outxsn(:)));      % Max 'outxsn' test statistic
        end                                                 % Next k...next
                                                            noise realization
        Zs = fliplr(sort(Zn));              % Sort 'outxn' test statistics
        T = Zs(floor(Pfa*R)+1);             % Find/set threshold
        Pd(c,q) = length(find(Z > T))/R;    % Probability of detection

    powspec(q,:) = sum(CDM_BBs'.^2);
    powspec(q,:) = 10*log10(powspec(q,:)/max(powspec(q,:)));
    end                                                     % Next q...Phase
increment
    close(w)
end                                                          % Next c...ChBW

powspec_mean = mean(powspec,1);
powspec_std = std(powspec);

% save ChRx_ph       % save all data from workspace

toc
```

B4. Subroutines

```
function sig = uwb(Tw,To,delt,Ns,P,jtr,method,dly);

%   Brett D. Gronholz
%   EENG 799 -- Summer/Fall 2004
%
%   Updated and modified by:
%   Willie H. Mims
%   EENG 799 -- Fall 2005/Winter 2006
%


%   UWB  Ultra-Wideband Signal Generator
%   SIG = UWB(Tw,To,delt,Ns,P,jtr,method,dly)
%
%   INPUTS
%       Tw     - pulse duration
%       To     - symbol repetition interval
%       delt   - time resolution
%       Ns     - number of symbols
%       P      - signal power
%       jtr    - jitter as percentage of Ts = 2*Tw
%       method - 'uni', 'ppm', 'pam', or 'bppm'
%       dly    - first pulse delay
%
%   OUTPUT
%       sig    - UWB output signal

rand('state',sum(100*clock))

% Variables
Tm = 0.4*Tw;                    % pulse width parameter
t = 0:delt:(2*Tw-delt);         % time vector for UWB pulse generation
Nc = length(t);                 % number of samples/symbol
Nr = length(0:delt:To-delt);    % number of samples/repetition interval

% Generate UWB pulse (2nd derivative of Gaussian pulse)
w = (1-4*pi*((t-1.2*Tm)/Tm).^2).*exp(-2*pi*((t-1.2*Tm)/Tm).^2); % UWB pulse
Pw = (1/To)*sum(w.^2)*delt;         % power in w
s = sqrt(P/Pw)*w;                   % received UWB waveform

if strcmpi(method,'uni'),
    sig = zeros(1,Ns*Nr);
    r = round(2*(rand(1,Ns)-0.5)*jtr*Nc/2);
    r(1) = 0;
    for i = 1:Ns,
        sig(Nr*(i-1)+1+r(i):Nr*(i-1)+Nc/2+r(i)) = s(1:Nc/2);
    end

elseif strcmpi(method,'ppm'),
    ppm1 = s;
    ppm0 = fliplr(ppm1);
    sig = zeros(1,Ns*Nr);
    r = round(2*(rand(1,Ns)-0.5)*jtr*Nc);
    r(1) = 0;
    bits = randint(1,Ns);
    for i = 1:Ns,
        if bits(i) == 0,
            sig(Nr*(i-1)+1+r(i):Nr*(i-1)+Nc+r(i)) = ppm0;
        else
```

```
            sig(Nr*(i-1)+1+r(i):Nr*(i-1)+Nc+r(i)) = ppm1;
        end
    end

elseif strcmpi(method,'pam'),
    pam1 = sqrt(0.5)*s(1:Nc/2);
    pam0 = -pam1;
    sig = zeros(1,Ns*Nr);
    r = round(2*(rand(1,Ns)-0.5)*jtr*Nc/2);
    r(1) = 0;
    bits = randint(1,Ns);
    for i = 1:Ns,
        if bits(i) == 0,
            sig(Nr*(i-1)+1+r(i):Nr*(i-1)+Nc/2+r(i)) = pam0;
        else
            sig(Nr*(i-1)+1+r(i):Nr*(i-1)+Nc/2+r(i)) = pam1;
        end
    end

elseif strcmpi(method,'bppm'),
    bppm10 = s;
    bppm01 = -s;
    bppm00 = fliplr(bppm01);
    bppm11 = fliplr(bppm10);
    sig = zeros(1,Ns*Nr);
    r = round(2*(rand(1,Ns)-0.5)*jtr*Nc);
    r(1) = 0;
    bits = randint(1,2*Ns);
    for i = 1:Ns,
        switch bi2de([bits(2*i-1) bits(2*i)])
        case [0]
            sig(Nr*(i-1)+1+r(i):Nr*(i-1)+Nc+r(i)) = bppm00;
        case [1]
            sig(Nr*(i-1)+1+r(i):Nr*(i-1)+Nc+r(i)) = bppm01;
        case [2]
            sig(Nr*(i-1)+1+r(i):Nr*(i-1)+Nc+r(i)) = bppm10;
        case [3]
            sig(Nr*(i-1)+1+r(i):Nr*(i-1)+Nc+r(i)) = bppm11;
        end
    end

else
    error('Modulation type error.');
end

sig = [zeros(1,round(dly/delt)) sig];
```

```
function Cout = csm(x,Nfft,dim,clr)

%   Brett D. Gronholz
%   EENG 799 -- Summer/Fall 2004
%
%   Updated and modified by:
%   Willie H. Mims
%   EENG 799 -- Fall 2005/Winter 2006
%


%   CSM   Cross-Spectral Matrix
%   Cout = csm(x,Nfft,dim,clr)
%
%   INPUTS
%       x    - input matrix
%       Nfft - # of points in FFT (to form SSM)
%       dim  - dimension (1==col-by-col, 2==row-by-row)
%       clr  - set autocorrelation terms to zero if 1, normal if 0
%
%   OUTPUTS
%       Cout - Cross-Spectral Matrix (CSM)
%

X = fft(x,Nfft,2);          % FFT of rows of input matrix

ndim = size(X,mod(dim,2)+1);% input matrix length along specified dimension
noth = size(X,dim);         % input matrix length along other dimension

clear Cout

if dim == 1,
    % Column-by-Column Correlation
    Cout = zeros(ndim,ndim);    % initialize matrix
    Cout = X'*X/noth;           % C-by-C correlation
elseif dim == 2,
    % Row-by-Row Correlation
    Cout = zeros(ndim,ndim);    % initialize matrix
    Cout = X*X'/noth;           % R-by-R correlation
end

if clr == 1,
    % Set Diagonal (Autocorrelation) Elements to Zero
    for i = 1:ndim,
        Cout(i,i) = 0;
    end
end
```

```
function Cout = ctm(x,Nfft,dim,clr)

%   Brett D. Gronholz
%   EENG 799 -- Summer/Fall 2004
%
%   Updated and modified by:
%   Willie H. Mims
%   EENG 799 -- Fall 2005/Winter 2006
%


%   CTM   Cross-Temporal Matrix
%   Cout = ctm(x,Nfft,dim,clr)
%
%   INPUTS
%       x    - input matrix
%       Nfft - # of points in IFFT (to form TTM)
%       dim  - dimension (1==col-by-col, 2==row-by-row)
%       clr  - set autocorrelation terms to zero if 1, normal if 0
%
%   OUTPUTS
%       Cout - Cross-Temporal Matrix (CTM)
%

X = ifft(x,Nfft,1);         % IFFT of columns of input matrix

ndim = size(X,mod(dim,2)+1);% input matrix length along specified dimension
noth = size(X,dim);         % input matrix length along other dimension

clear Cout

if dim == 1,
    % Column-by-Column Correlation
    Cout = zeros(ndim,ndim);    % initialize matrix
    Cout = X'*X/noth;           % C-by-C correlation
elseif dim == 2,
    % Row-by-Row Correlation
    Cout = zeros(ndim,ndim);    % initialize matrix
    Cout = X*X'/noth;           % R-by-R correlation
end

if clr == 1,
    % Set Diagonal (Autocorrelation) Elements to Zero
    for i = 1:ndim,
        Cout(i,i) = 0;
    end
end
```

```
function out = chrx(inp,fs,Wrf,fl,fh,Nz,dc,ph)

%   Brett D. Gronholz
%   EENG 799 -- Summer/Fall 2004
%
%   Updated and modified by:
%   Willie H. Mims
%   for the following class:
%   EENG 673 Project -- Summer 2005

%   EENG 799 -- Fall 2005/Winter 2006

% CHRX Channelized Receiver
%   out = chrx(inp,fs,Wrf,fl,fh,Nz,dc,ph)
%
%   INPUTS
%       inp  - input signal - from RF filter output
%       fs   - sample frequency of input signal
%       Wrf  - channel bandwidth
%       fl   - lower ChRx frequency
%       fh   - upper ChRx frequency
%       Nz   - one-sided zero padding length (for 'filtfilt')
%       dc   - downconvert? (1==yes,0==no)
%       ph   - downconversion starting phase
%
%   OUTPUT
%       out  - channelized receiver output matrix
%

if nargin ~= 8,
    error('Not enough input arguments!')
end
if fs <= 0,
    error('Sample frequency (fs) must be positive and non-zero.')
end
if Wrf <= 0,
    error('Channel bandwidth (Wrf) must be positive and non-zero.')
end
if fl <= 0,
    error('Lower frequency (fl) must be positive and non-zero.')
end
if fh <= 0,
    error('Upper frequency (fh) must be positive and non-zero.')
end
if mod((fh-fl)/Wrf,1) ~= 0,
    error('"fh-fl" must be an integer multiple of "Wrf"')
end
if Nz < 0,
    error('Zero padding length (Nz) must be positive or zero.')
end
if (dc ~= 1 & dc ~= 0),
    error('Invalid parameter (dc)')
end

N = 4;              % filter order
Nc = (fh-fl)/Wrf;    % number of channels - integer values
delt = 1/fs;        % delta t

inp = [zeros(1,Nz) inp zeros(1,Nz)];    % zero-pad
tdc = [0:delt:(length(inp)*delt-delt)]; % time vector for downconversion
for i = 1:Nc,
```

```
    if dc == 1, % downconvert
        [b,a] = butter(N,Wrf/(fs/2));    % LPF coeffs
        inpx = real(inp.*exp(-j*2*pi*((fl+(i-1)*Wrf)*tdc+pi/180*ph)));
    elseif dc == 0, % don't downconvert
        [b,a] = butter(N,[(fl+(i-1)*Wrf)/(fs/2) (fl+i*Wrf)/(fs/2)]);  % BPF
                                                                       coeffs
        inpx = inp;
    end
    outt(i,:) = real(filtfilt(b,a,inpx));   % filter input sig
    out(i,:) = outt(i,Nz+1:end-Nz);         % remove zeros
end
```

```
function [bitsin,sigvec,timvec] =
Fast_Bpsk_ModPrj2(datsel,indata,rbits,ndelay,fnot...
    ,esym,nsamp,nplus,tsym)

%   Created: 16 May 2004
%   Capt Ray Nelson
%
%   Updated and modified by:
%   Willie H. Mims
%   for the following class:
%   EENG 673 Project -- Summer 2005

%   EENG 799 -- Fall 2005/Winter 2006

% ============================================================
% Fast_BPSK_MODPrj2 Function:  Binary Phase Shift Keying Modulator
% ============================================================
%   Fast BPSK Modulator for EENG 670 Project#2: A fast implementation of the
%   software modulator originally developed by Dr Michael A. Temple
%
%   INPUTS
%
%       datsel - Data control variable: 'user' --> User SUPPLIED Data
%                                        ("indata") for Modulation
%                                       'rand' --> Random Data GENERATED for
%                                        Modulation
%       indata - For "datsel" = 'user' ... User SUPPLIES "indata" vector for
%                Modulation
%       rbits - For "datsel" = 'rand' ... Number of "rbits" Randomly GENERATED
%               for Modulation
%       ndelay - Number of LEADING samples preceeding first valid sample of
%                first Complete Symbol
%       fnot - Modulator Output Frequency (Hertz)
%       snr - Input Signal-to-Noise Ratio in Decibels (dB)
%       tsym - SYMbol Time / Duration
%       esym - Energy per putput SYMbol
%       nsamp - Number of output waveform SAMPles per Symbol Period (tsym)
%       nplus - Add noise to output signal to achieve desired SNR?
%           nplus = 0 ... DO NOT add noise to output signal vector
%           nplus = 1 ... ADD noise to output signal vector
%
%   OUTPUTS
%
%       bitsin - Actual BITS INto the Modulator
%       sigvec - Modulated SIGnal VECtor
%       timvec - Sample TIMe VECtor for one symbol
%
% This modulator produces a sampled BPSK output waveform with symbols generated
% per Eq 4.31 of Sklar's Digital Communications text (2nd Ed.).
%
%       [1] => s1 => Phz = 180 Deg
%       [0] => s2 => Phz =  0 Deg
%


%
% tic % Start Subroutine Timer
%
wnot = 2*pi*fnot; % Radian frequency of Carrier
%snrat = 10^(snr/10);  % Calculate Ratio form of Input SNR
sigamp = sqrt(2*esym/tsym); % Signal Component Amplitude
%
```

```
% IF datsel = "user" use "indata" vector as "rdata" vector
%
rdata = []; % Initialize Data Vector
if datsel=='user'
    rdata = indata;
end
%
% IF datsel = "rand" generate a Random "rdata" vector of length "rbits"
%
if datsel=='rand'
    rdata=round(rand(1,rbits));
end
%
bitsin = rdata; % Actual BITS INto the Modulator
%
% Calculate Number of Symbol Periods (nsym) in RDATA
%
bitsym = 1; % Number of bits/symbol = 1 for BPSK
nsym = rbits/bitsym;
tstep = tsym/nsamp;
%tstep = 0.01e-9;



% Create time vector
timvec = tstep*(0:nsamp-1);

% Create time matrix, T, from timvec
T = repmat(timvec',1,nsym);

% Create phase matrix, Phi, from bitsin
Phi = repmat((pi*bitsin),nsamp,1);

% Create Symbol matrix using T and Phi
Arg = wnot*T + Phi;
Symbol = sigamp*cos(Arg);

% Create SIGnal VECtor
sigvec = reshape(Symbol,1,(nsym*nsamp));

% Fill "LEADING" samples of "sigvec" with last symbol data
%
if ndelay > 0
    sigvec=[sigvec((length(sigvec)-ndelay+1):length(sigvec)) sigvec];
end
%
% If desired (function of nplus), generate and add zero mean AWGN vector to
% signal output
% vector using noise amplitude (nosamp) calculated from inputs: snr, esym, tsym
%
% if nplus==1
%     randn('state',sum(100*clock)); % Reset Random # Generator
%     nosamp = sqrt(esym/(snrat*tsym));
%     noise = nosamp*randn(size(sigvec));
%     sigvec = sigvec + noise;
% end
%
% sub_time = toc % Stop Subroutine Timer
return
%
```

```
function [FastSprdMod] = FastSprdMod(SprdMatrix,SRow,nsamp,NChips,NSyms)

%
%   Created: 16 May 2004
%   Capt Ray Nelson
%
%   Updated and modified by:
%   Willie H. Mims
%   for the following class:
%   EENG 673 Project -- Summer 2005

%   EENG 799 -- Fall 2005/Winter 2006

% Create Spreading Modulation Waveform with:
%       - Total Duration = #Symbols X Tsym
%       - One Code Period per Tsym
%       - NChips = #Chips per Tsym (Input)
%       - NSyms = Total #Symbols
%       - nsamp = #Samples per Tsym (Input)
%       - SprdMatrix = Spreading Code Matrix (Input)
%         ... Rows of SprdMatrix are User Codes
%       - SRow = Row # of Desired Code / User
%
% Fast Spreading Modulation Function:  A fast implementation of the
% original SprdMod function developed by Dr Michael A. Temple

%tic % Start Function Timer
SprdSym=repmat(SprdMatrix(SRow,:),(nsamp/NChips),NSyms);
FastSprdMod=reshape(SprdSym,1,(NSyms*nsamp));

%toc % Stop Function Timer
return
% END FUNCTION
```

```
function CDM_BB = chrx_BB(CDM_RF,fs,Wrf,fl,fh,Nz,ph)

%   Brett D. Gronholz
%   EENG 799 -- Summer/Fall 2004
%
%   Updated and modified by:
%   Willie H. Mims
%   for the following class:
%   EENG 799 -- Fall 2005/Winter 2006
%

% CHRX Channelized Receiver II : Downconversion
%   CDM_BB = chrx_BB(CDM_RF,fs,Wrf,fl,fh,Nz,ph)
%
%   INPUTS
%       CDM_RF  - Input signal vector (CDM) - from RF to BPF output
%       fs      - Sample frequency of input signal
%       Wrf     - Channel bandwidth
%       fl      - Lower ChRx frequency
%       fh      - Upper ChRx frequency
%       Nz      - One-sided zero padding length (for 'filtfilt')
%       ph      - Downconversion starting phase
%
%   OUTPUT
%       CDM_BB  - Channelized receiver output matrix, downconverted (stage 2)
%

N = 4;                  % Filter order
Nc = (fh-fl)/Wrf;       % Number of channels - integer values
delt = 1/fs;            % Delta t

CDM_RF = [zeros(Nc,Nz) CDM_RF zeros(Nc,Nz)];    % Zero-pad
tdc = [0:delt:(length(CDM_RF(1,:))*delt-delt)]; % Time vector for
downconversion

for i = 1:Nc,
    [b,a] = butter(N,Wrf/(fs/2));    % LPF coeffs
    inpx(i,:) = real(CDM_RF(i,:).*exp(-j*2*pi*((fl+(i-1)*Wrf)*tdc+pi/180*ph)));
    outt(i,:) = real(filtfilt(b,a,inpx(i,:)));  % Filter input signal
    CDM_BB(i,:) = outt(i,Nz+1:end-Nz);          % Remove zeros
end
```

```
function CDM_RF = chrx_RF(inp,fs,Wrf,fl,fh,Nz)

%   Brett D. Gronholz
%   EENG 799 -- Summer/Fall 2004
%
%   Updated and modified by:
%   Willie H. Mims
%   for the following class:
%   EENG 799 -- Fall 2005/Winter 2006
%

% CHRX Channelized Receiver II : RF BPF
%   CDM_RF = chrx_RF(inp,fs,Wrf,fl,fh,Nz,ph)
%
%   INPUTS
%       inp  - Input signal - from RF filter output
%       fs   - Sample frequency of input signal
%       Wrf  - Channel bandwidth
%       fl   - Lower ChRx frequency
%       fh   - Upper ChRx frequency
%       Nz   - One-sided zero padding length (for 'filtfilt')
%
%   OUTPUT
%       CDM_RF  - Channelized receiver output matrix, BPF (stage 1)
%

N = 4;                  % Filter order
Nc = (fh-fl)/Wrf;       % Number of channels - integer values
delt = 1/fs;            % Delta t

inp = [zeros(1,Nz) inp zeros(1,Nz)];    % Zero-pad

for i = 1:Nc,   % Band pass filtering

    [b,a] = butter(N,[(fl+(i-1)*Wrf)/(fs/2) (fl+i*Wrf)/(fs/2)]);  % BPF coeffs
    inpx = inp;
    outt(i,:) = real(filtfilt(b,a,inpx));   % Filter input signal
    CDM_RF(i,:) = outt(i,Nz+1:end-Nz);      % Remove zeros
end
```

Bibliography

[1] "First report and order: revision of part 15 of the commission's rules regarding ultra-wideband transmission systems," No. ET Docket 98-153, (Washington), Federal Communications Commission, Government Printing Office, April 2002.

[2] B.D. Gronholz, M.A. Temple, R.F. Mills, W.H. Mims and T.D. Niedzwiecki, "Communication channel assessment: detection of uwb signals using a channelized receiver," in *International Conference on Wireless Networks, Communications, and Mobile Computing*, Vol. 2, pp. 1071-1076, June 2005.

[3] C.M. Canadeo, "Ultra wideband multiple access performance using th-ppm and ds-bpsk modulations," master's thesis, Air Force Institute of Technology, 2003.

[4] N. Lehmann and A.M. Haimovich, "New approach to control the power spectral density of a time hopping uwb signal," in *Proceedings of the Conference on information Sciences and Systems, CISS,* March 2003.

[5] ——, "The power spectral density of a time hopping uwb signal: A survey," in *IEEE Conference on UWB Systems and Technologies (UWBST 2003)*, November 2003.

[6] J. Romme and L. Piazzo, "On the power spectral density of time hopping impulse radio," in *IEEE conference on UWB Systems and technologies (UWBST 2002)*, 2002.

[7] K.S. Shanmugan, "Estimating the power spectral density of ultra wideband signals," in *International Conference on Personal Wireless Communications*, pp. 124-128, December 2002.

[8] B.D. Gronholz, "Non-cooperative detection of ultra wideband signals," Master's Thesis, Air Force Institute of Technology, 2004.

[9] R.L. Peterson, R.E. Ziemer and D.E. Borth, *Introduction to Spread-Spectrum Communications*. New Jersey: Prentice Hall, 1995.

[10] R.E. Ziemer and W.H. Tranter, *Principles of Communications: Systems, Modulation, and Noise, 4th ed*. Boston: Houghton Mifflin, 1995.

[11] J.K. Holmes, *Coherent Spread Spectrum Systems*. New York: Wiley-Inter-science, 1982.

[12] R.C. Titsworth and L.R. Welch, *Power Spectra of Signals Modulated by Random and Pseudorandom Sequences.* Tech. Rep. 32-140, Jet Propulsion Laboratory, Pasadena, California, October 1961.

[13] W.C. Lindsey and M.K. Simon, *Telecommunication Systems Engineering*. New Jersey: Prentice Hall, 1973.

[14] B. Sklar, *Digital Communications: Findamentals and Applications*. New Jersey: prentice Hall, 2001.

[15] H.L. Van Trees, *Detection, Estimation, and Modulation Theory (part 1)*. New York, NY: John Wiley and Sons, 2001.

[16] M.I. Skolnik, *Introduction to Radar Systems*. New York, NY: McGraw-Hill, 2002.

[17] R.F. Mills and G.E. Prescott, "A comparison of various radiometer detection models," in *IEEE Transactions on Aerospace and Electronic Systems*, Vol. 32, No. 1, pp. 467-473, 1996.

[18] J. Tsui, "Digital techniques for wideband receivers," Norwood, MA, Artech House, 2001.

[19] W.H. Mims, M.A. Temple, R.F. Mills and B.D. Gronholz, "Spectral sensing ultra wideband signals using a down-converting channelized receiver," in *First IEEE international symposium on New Frontiers in Dynamic Spectrum Access Networks*, pp. 706-709, November 2005.

[20] W. Namgoong, "Channelized digital receivers for impulse radio," in *IEEE international Conference on Communications (ICC 2003)*, May 2003.

[21] T.W. Parks and C.S. Burrus, *Digital Filter Design*. John Wiley and Sons, 1987.

REPORT DOCUMENTATION PAGE

Form Approved
OMB No. 074-0188

1. REPORT DATE *(DD-MM-YYYY)*	**2. REPORT TYPE**	**3. DATES COVERED** *(From – To)*
23-03-2006	Master's Thesis	Aug 2004 – Mar 2006

4. TITLE AND SUBTITLE

Wideband Signal Detection Using a Down-Converting Channelized Receiver

5a. CONTRACT NUMBER

5b. GRANT NUMBER

5c. PROGRAM ELEMENT NUMBER

6. AUTHOR(S)

Mims, Willie H., Second Lieutenant, USAF

5d. PROJECT NUMBER

5e. TASK NUMBER

5f. WORK UNIT NUMBER

7. PERFORMING ORGANIZATION NAMES(S) AND ADDRESS(S)
Air Force Institute of Technology
Graduate School of Engineering and Management (AFIT/EN)
2950 Hobson Way, Building 640
WPAFB OH 45433-7765

8. PERFORMING ORGANIZATION REPORT NUMBER

AFIT/GE/ENG/06-42

9. SPONSORING/MONITORING AGENCY NAME(S) AND ADDRESS(ES)
Air Force Research Laboratory, Sensors Directorate (AFMC)
Attn: Mr. Tom D. Niedzwiecki AFRL/SNRP
2241 Avionics Circle, Building 620
WPAFB OH 45433-7333 DSN: 785-4879 email: Tom.Niedzwiecki@wpafb.af.mil

10. SPONSOR/MONITOR'S ACRONYM(S)

11. SPONSOR/MONITOR'S REPORT NUMBER(S)

12. DISTRIBUTION/AVAILABILITY STATEMENT
APPROVED FOR PUBLIC RELEASE; DISTRIBUTION UNLIMITED.

13. SUPPLEMENTARY NOTES

14. ABSTRACT

Ultra wideband (UWB) signals typically occupy a very large spectral bandwidth resulting from extremely short duration pulses. Direct sequence spread spectrum (DSSS) signals typically occupy a large spectral bandwidth resulting from spreading methods. Both signals can be difficult to detect without having prior knowledge of their structure and/or existence.

This research develops and evaluates techniques for the non-cooperative (non-matched filter) detection of such signals. Impulse-like UWB and DSSS signals are received in an Additive White Gaussian Noise (AWGN) channel and are assessed using a bandpass filtered, down-converting (BPF-D/C) channelized receiver architecture.

Modeling and simulation is conducted to characterize BPF-D/C channelized receiver detection performance, which is compared with the performance of two other non-cooperative detection receivers: a previously-introduced down-converting (D/C) channelized receiver and a conventional radiometer.

The BPF-D/C channelized receiver detection performance for both signals of interest is shown to depend on the initial phase of the down-conversion mixers. There are usually some combinations of signal-to-noise ratio (SNR) and channel bandwidth where the BPF-D/C channelized receiver outperforms the radiometer and D/C channelized receiver for a UWB pulse. For a DSSS waveform, detection performance using the BPF-D/C channelized receiver is consistently poorer than radiometric detection.

15. SUBJECT TERMS
Bandwidth, Frequency, Spread Spectrum, Bandpass Filter, Signal Processing

16. SECURITY CLASSIFICATION OF:			**17. LIMITATION OF ABSTRACT**	**18. NUMBER OF PAGES**	**19a. NAME OF RESPONSIBLE PERSON**
REPORT	**ABSTRACT**	**c. THIS PAGE**			Michael A. Temple, PhD (ENG)
U	**U**	**U**	**UU**	143	**19b. TELEPHONE NUMBER** *(Include area code)* (937) 255-3636, ext 4279; e-mail: Michael.Temple@afit.edu